

An Empirical Analysis of the Interconnection Queue*

Sarah Johnston[†] Yifei Liu[‡] Chenyu Yang[§]
University of Calgary University of Wisconsin-Madison University of Maryland

June 10, 2026

Abstract

Electricity generation projects applying to connect to the U.S. power grid go through an interconnection queue. Most projects that begin the process do not complete it. Using new data, we find that a long queue delays the necessary engineering studies, and high interconnection costs cause projects to withdraw from the queue. We develop and estimate a dynamic model of the queue and quantify the effects of policy reforms. We find that speeding up the delivery of studies can significantly increase completed capacity, with about a fifth of the gain coming from projects re-optimizing their entry, waiting, and completion strategies. Imposing entry fees reduces entry into the queue but not average waiting time, because changes in queue composition and project strategies weaken the direct effect of having fewer entrants. Fee designs we consider mainly deter marginal entrants that contribute little to congestion, and completed capacity increases only modestly at best.

*We thank Joseph Aldy, Jim Bushnell, Steve Cicala, Jackson Dorsey, Ken Gillingham, Will Gorman, Charles Hodgson, Koichiro Ito, Ashley Langer, David Popp, Mar Reguant, Andrew Sweeting, Frank Wolak, and participants at many seminars and conferences for helpful comments and discussions. We also thank Christian McDewell and four industry experts for insight into the electricity market. We also thank the numerous undergraduate research assistants at UW-Madison and the University of Maryland who helped with data collection. We gratefully acknowledge financial support from the National Science Foundation (SES-2215063), the NBER-Sloan Economics of Innovation in the Energy Sector Initiative, the University of Maryland Grand Challenges Grant Program, and the University of Wisconsin - Madison Office of the Vice Chancellor for Research and Graduate Education with funding from the Wisconsin Alumni Research Foundation.

[†]Department of Economics, University of Calgary, Calgary, AB T2N 1N4; sarah.johnston2@ucalgary.ca.

[‡]Department of Agricultural and Applied Economics, University of Wisconsin-Madison, Madison, WI 53706; yifei.violet.liu@wisc.edu.

[§]Department of Economics, University of Maryland, College Park, MD 20740; cyang111@umd.edu.

1 Introduction

Electricity production accounts for over a quarter of both U.S. and global carbon emissions (EPA, 2026; IEA, 2026, 2025). Many countries’ climate goals center on transitioning to a low carbon grid while electrifying heating and transportation. Meeting these goals will require large-scale investment in wind and solar powered generators.

Yet, connecting an electricity generation project to the U.S. power grid is difficult. The process, known as interconnection, takes several years and must be completed before the developer can build the project. It can also be costly: connecting projects must often pay to upgrade the transmission system because the local grid is at capacity (Plumer, 2023). Renewable energy developers cite interconnection as the single biggest hurdle they face (Driscoll, 2022), and less than a quarter of the wind and solar projects that start the process complete it (Rand et al., 2025). We study the design of this interconnection process.

A project (a proposed generating facility at a specific site) seeking to connect to the transmission grid joins a waitlist known as the interconnection queue. The grid operator then conducts a series of engineering studies to determine the project’s “interconnection cost.” This cost includes both the equipment required to connect the project to the grid and the transmission system upgrades (if any) needed to accommodate it on the broader network. The date the project joined the queue determines priority for these studies. Projects must pay for the studies to remain in the queue and can drop out at any time. A project usually needs three studies to arrive at a final cost, after which it either pays this cost and connects, or leaves.

Each additional project in the queue can delay the studies of those behind it. The cost of being in the queue is low, however, and may be insufficient to offset this congestion externality. Grid operators devote substantial resources to processing requests that ultimately withdraw. These concerns have motivated reforms such as FERC Order 2023, which raises study deposits and introduces penalties for withdrawing from the queue.

To study this process, we hand collect novel data from PJM, the largest of the U.S. regional grid operators. PJM serves 67 million people in parts of the Mid-Atlantic, Midwest, and Southern United States (PJM, 2026). Our data cover all generator interconnection requests from 2008 through 2020: 4,174 requests and the 7,492 engineering studies for these requests.

Project developer complaints about delayed studies and high interconnection costs are borne out in the data. We find that the studies often take far longer than PJM’s official timeline, with the later studies being the most delayed. For example, PJM expects the third and final interconnection

study to take 6 months, but the median wait in the data is 15 months, and the 90th percentile is 36 months. While the median interconnection costs are \$0.05 million/megawatt (MW), the 90th percentile is \$0.40 million/MW, roughly a quarter of the installation cost for wind and solar projects. We also find that observably similar projects can have very different interconnection costs, a finding consistent with developers' complaints that these costs are unpredictable (Caspary et al., 2021).

We also show that high interconnection costs cause projects to withdraw from the queue. For example, the 34 percent of projects with a second study interconnection cost above \$0.1 million/MW are 33 percent more likely to withdraw before the third study than those below this threshold. We find a similar pattern for the first and third studies. Instrumenting for cost with the change in cost across studies, which is unpredictable, yields similar estimates.

We next quantify three potential externalities in the queue. The first is a congestion externality: are the necessary engineering studies returned more slowly when more projects are ahead in the queue? The second is a geographic cost externality: do contemporaneous projects in the queue or completed interconnections affect the interconnection costs of other nearby projects? The third is a local output externality: do completed interconnections reduce local wholesale electricity prices and thus the expected profits of nearby projects in the queue?

We find the congestion externality is quantitatively important. We estimate how the probability that a project receives a study in a given quarter declines with the number of higher-priority projects ahead of it. This effect is identified because PJM, not the project, controls when studies arrive. A 10 percent increase in the number of higher-priority projects reduces a project's probability of receiving the third and final study by 12.7 percent, on average.

Conversely, we do not find that the other two externalities are quantitatively important in our setting. We test for cost externalities via two channels: whether a project's cost is affected by others still in the queue — through nearby capacity ahead of it or withdrawals from its cost-share group — and whether its cost is lowered by spare transmission capacity left by costly past interconnections. In both cases, the estimates are small and mostly statistically insignificant. This finding is likely due to PJM's cost-sharing rules: cost-sharing is extensive but confined to small groups, so most projects do not affect one another's costs. Even within a cost-share group, a withdrawal does not systematically raise or lower remaining projects' costs. Similarly, using a staggered difference-in-differences, we find that a new project beginning operation does not reduce wholesale prices in its location relative to other locations in PJM. The likely explanation is PJM's deliverability requirement, under which connecting projects must upgrade the transmission system to mitigate local grid congestion. These findings motivate our focus on the congestion externality and policies that target waiting times.

We then develop a structural model of the queue to quantify how policy reforms affect completed capacity and welfare. We model withdrawal decisions as an optimal stopping problem. A project waits in the queue for studies and forms beliefs about when the next study will arrive and what its interconnection cost estimate will be. The continuation value of a project depends on its characteristics and the status of the queue, which we measure both PJM-wide and at the level of the local transmission owner, whose engineering input the studies rely on.

To handle the non-stationarity in the data, we develop a tractable queuing equilibrium concept. In this equilibrium, the composition and size of the queue are jointly determined by optimal project strategies and the PJM study process. Project beliefs are consistent with the state transitions implied by the queue in equilibrium. We prove that such an equilibrium exists.

We estimate the model in three steps. First, we estimate models of new study arrival rates, interconnection costs, and additional information revealed by each study. These estimates allow us to construct project beliefs. Second, we embed these beliefs in the project’s optimal stopping problem. We then use the observed withdrawal and completion decisions to recover the waiting cost and payoff for completing interconnection. We prove that project preference heterogeneity and waiting costs are nonparametrically identified by variation in interconnection costs across studies. Intuitively, because these cost changes are difficult to predict, the cost a project learns at each study acts as a shock to its continuation value, and how its withdrawal and completion decisions respond to these shocks across successive studies pins down preference heterogeneity and the cost of waiting. Third, we use the implied value of entering the queue to estimate the entry cost.

We use the estimated project preferences and the equilibrium model to simulate the effects of policy reforms: speeding up study delivery and imposing fees to enter or stay in the queue. Faster study delivery is the goal of recent efforts to deploy AI for engineering studies, such as PJM’s 2025 partnership with Google’s Tapestry (PJM Interconnection, 2025*b*). FERC Order 2023 takes both approaches: it penalizes transmission providers for study delays, and it raises study deposits and introduces withdrawal penalties (FERC, 2023). The withdrawal penalties function like fees collected at study stages and refunded upon completion, one of the fee designs we evaluate.

We find that faster engineering studies substantially increase completed capacity. For 2012–2020 queue entrants, speeding up study delivery by 50% increases completed capacity by about 30%, or 18.4 GW, and shortens average wait times by 20%. Of the added capacity, 71% (13.1 GW) is renewable. Given a social cost of carbon of \$185 per ton, this increase in renewable capacity would create \$2.8 billion in annual benefits. About a fifth of this gain comes from projects re-optimizing entry, waiting, and completion strategies in anticipation of the faster queue, a response that a

partial-equilibrium calculation holding strategies fixed would miss.

The benefits of fees are modest for all designs we consider. Our main counterfactual exercise evaluates three per-megawatt fees to enter the queue: a nonrefundable fee, a deposit refunded only if the project completes, and a budget-neutral design, in which all collected fees are rebated to completers. Under a \$20,000/MW entry fee, comparable to new fee schedules PJM currently considers (PJM Interconnection, 2026), nonrefundable fees reduce entry, but mainly deter projects that wait less, shifting the composition of the queue. The total completed capacity falls by 0.3% and average wait times slightly increase in equilibrium. Deposits reduce entry less, but entering projects wait longer, also increasing the overall waiting time. The completed capacity increases by 0.5%. Even under the budget-neutral design — a benchmark rather than a feasible policy — completed capacity rises only 3.2%.

The key intuition for the small effects is that the projects creating the most congestion are also the most valuable. Higher-value projects stay longer in the queue, slowing studies for others; these projects are the most likely to complete. Most of the gain in the deposit or budget-neutral design comes from the completion subsidy, in the form of rebated fees, rather than from reduced congestion, because the fee deters marginal entrants who contribute little to congestion in the first place. For a similar reason, charging a flat entry fee or increasing fees to advance to the next study after a project’s entry does not meaningfully increase completed capacity.

Related Literature

The interconnection queue is a critical but understudied bottleneck in electricity market entry. While it has received attention in the energy policy literature (Gergen, Cannon Jr and Torgerson, 2008; Alagappan, Orans and Woo, 2011; Gorman et al., 2024), it has been largely absent from formal economic analysis, primarily due to data constraints. This paper fills that gap using novel data from PJM, the largest U.S. transmission organization by customers served. The most closely related paper is Gonzales, Ito and Reguant (2023), who study how transmission grid expansion enables renewable entry; our paper instead focuses on the interconnection queue as the primary barrier to entry. We also contribute to a broader literature on how transmission constraints affect competition, emissions, and investment (Wolak, 2015; Ryan, 2021; Davis and Hausman, 2016; Fell, Kaffine and Novan, 2021; LaRiviere and Lyu, 2022; Doshi, 2026), as well as on the institutional barriers to expanding transmission infrastructure (Davis, Hausman and Rose, 2023; Hausman, 2025).

Our structural approach contributes to the energy and environmental economics literature studying investment and industry dynamics (Ryan, 2012; Gowrisankaran, Reynolds and Samano, 2016;

Fowle, Reguant and Ryan, 2016; Blundell, Gowrisankaran and Langer, 2020; Butters, Dorsey and Gowrisankaran, 2021; Elliott, 2021; Gowrisankaran, Langer and Zhang, 2022; Leisten and Vreugdenhil, 2023). By quantifying how interconnection queue policy reforms can improve renewable entry, we also contribute to the literature on public policy and renewable energy investment (Metcalfe, 2010; Hitaj, 2013; Johnston, 2019; Aldy, Gerarden and Sweeney, 2023; Deschenes, Malloy and McDonald, 2023).

We also contribute to the empirical literature on dynamic assignment mechanisms (Agarwal et al., 2021; Waldinger, 2021; Verdier and Reeling, 2022; Liu, Wan and Yang, 2024; Huitfeldt, Marone and Waldinger, 2024) by studying a queuing problem in a novel and consequential market. Our central methodological contribution is a tractable equilibrium concept for a non-stationary queue with time-varying unobserved heterogeneity. The size and composition of the queue shifted substantially over our sample period, making standard oblivious equilibrium (Weintraub, Benkard and Van Roy, 2008) inapplicable. We build on the nonstationary oblivious equilibrium of Weintraub et al. (2010). The non-stationarity in the data is driven by factors that projects may reasonably foresee, such as the continued decrease in wind, solar, and battery costs and the increase in queue congestion. We adopt a finite-horizon assumption, as in Igami (2017) and Yang (2020), where agent beliefs in equilibrium are consistent with the trend of non-stationarity. We provide theoretical results on both the existence of the equilibrium and identification of agent preferences in this environment.

2 PJM Interconnection Process

The grid operator, PJM, runs the interconnection process, which involves two other parties: developers and transmission owners (TOs). Developers (e.g., NextEra Energy) enter their projects (e.g., 2.5 MW Front Royal Solar Field) in the queue and pay the interconnection cost identified in the studies. These developers can be either independent power producers (more common for renewables) or regulated utilities (more common for natural gas). PJM conducts the interconnection studies in conjunction with the local TO, which supplies the design standards and engineering input and constructs the upgrades (PJM Interconnection, L.L.C., 2020). We assume the cost developers pay reflects the competitive cost of these upgrades. PJM is a nonprofit grid operator, and TOs are regulated utilities with no incentive to inflate cost since, over our sample period, interconnection-funded upgrades did not enter their rate base.

PJM also plans transmission separately from the interconnection process, through the Regional Transmission Expansion Plan (RTEP). RTEP investment is driven by reliability needs and funded

by consumers through transmission rates. Over our sample period, the process did not consider projects waiting in the queue or anticipate their entry (PJM, 2020). We therefore treat RTEP as exogenous to the interconnection process and hold it fixed in our counterfactuals.

2.1 Queuing Rules

To enter a project in the interconnection process, a developer must secure land sufficient to build it (PJM, 2023*b*). Developers usually meet this requirement by acquiring exclusive options to lease the land. Developers must also pay a deposit to enter the queue or move on to the next stage. The deposit amount depends on the request size and stage, with larger requests typically requiring higher deposits. For the median request size of 20 MW, the three deposits would be \$12,000, \$10,000, and \$50,000 during our sample period. Projects that withdraw have their deposit returned, less a 10 percent non-refundable portion and any study costs already incurred (PJM, 2023*a*).

Projects can enter the queue at any time, but each year is typically divided into two windows. Projects that enter in the same 6-month window are put in the same cohort and will receive up to three studies (feasibility, system impact, and facility study) sequentially. Through these studies, projects learn increasingly accurate information about the cost of interconnection. To receive the next study, a project must incur a cost, but it can freely leave the queue at any time. PJM may require just one or two studies if it determines that a project is required neither to make significant network upgrades nor to share costs with other projects. After the last study is issued, the project chooses to leave the queue or sign an interconnection service agreement in which it agrees to pay the final interconnection cost, thus completing the interconnection process.

The official timeline for the interconnection process is rigid. For projects that apply within the same time window, PJM starts conducting the first studies (feasibility studies) one month after the closing of the window. Within three months, projects are supposed to receive their first studies. At this point, projects have another month to decide whether to advance to the second study (system impact study). The second study then takes four months, at which point projects have one month to decide whether to request the third and final study (facility study). The third study takes six months. Finally, projects and PJM agree on final details and sign the interconnection service agreement, over a 6.5-month period (PJM, 2021).¹

Despite this timeline, significant delays in delivering studies can occur due to the number of backlogged interconnection requests and a lack of staff capacity (Shoemaker, 2021; Petersen, Siegner

¹This agreement also sets a commercial operation date. After signing the interconnection service agreement, the project may suspend the process for up to 3 years (up to 1 year if the suspension has a negative impact on subsequent requests) (PJM, 2025), though these suspensions are rare.

and Coequyt, 2026). Upon receiving a study, a project has approximately one month to decide whether to pay the deposit to request the next study, but it has little control over when PJM delivers the study. These delays have been the subject of formal developer complaints; for example, a solar developer in PJM filed a complaint with the Federal Energy Regulatory Commission (FERC) after waiting more than two years for a second study (Hale, 2021).

2.2 Study Information

Each study reports an interconnection cost estimate along with engineering information. The interconnection cost has two components: the direct cost to connect the project to the grid, and the cost of network upgrades to relieve overloads the new project triggers.² PJM expressly states in studies that the interconnection costs do not consider permitting costs or rights of way, which can be significant hurdles (Liu, 2025). The first study reports preliminary direct interconnection costs and flags whether the project may share network upgrade costs with others. The second study reports the network upgrade costs, including the project’s share, and updates the direct costs. The third study finalizes engineering specifications and costs.

The engineering tests reported in each study determine which network upgrades the project is responsible for and whether it shares that responsibility with other projects. Three tests—generator deliverability, multiple facility contingency, and short circuit analysis—jointly quantify how much the project will overload the grid; they are conducted in either the first or the second study, depending on project characteristics and local transmission network conditions. Two additional tests—short circuit dynamic analysis and system protection analysis—identify whether the project triggers the same network violation as other projects in the queue, in which case PJM assigns it to a cost-share group jointly responsible for the upgrade. Group assignments are typically first reported in the second study, alongside the network upgrade cost. We include indicators for whether the engineering tests have been conducted and for whether a project is in a cost-share group as state variables in the structural model. These variables summarize the test information that informs project beliefs about study arrival and final cost.

Studies report additional information that affects a developer’s assessment of the project. They specify the locations and types of equipment required to connect the project and to upgrade the grid, which can affect the costs of permitting and right-of-way access. Studies may also flag costly requirements even when no interconnection cost is assessed, like bringing facilities up to the trans-

²We combine the two components into a single cost measure for our analysis; see Johnston, Liu and Yang (2025) for more detail and descriptive statistics on each.

mission owner’s published standards.³ Studies further report an estimated construction timeline for work related to interconnection, which could delay in-service dates. In the structural model, we capture this additional information as unobserved payoff heterogeneity, realized when the relevant study arrives.

2.3 Timing of Interconnection within Project Development

Projects apply for interconnection early in project development. The permitting and interconnection processes occur simultaneously, and developers perceive interconnection as the primary bottleneck (Nilson, Hoen and Rand, 2024). Projects signing long-term contracts to sell their power—nearly all renewable projects—do so while in the queue or after receiving the terminal study. After signing the interconnection service agreement, the project and all required interconnection infrastructure are constructed, typically in less than a year, far shorter than the time spent in the queue.⁴

The slow, unpredictable interconnection process can disrupt other steps in project development. Power buyers are willing to sign long-term contracts a few years before a project begins operation, but developers must apply for interconnection much earlier. Developers are thus left trying to forecast demand a few years in advance and enter projects into the queue accordingly. A long wait may also cause signed long-term contracts or a developer’s land lease option to expire, prompting the developer to renegotiate the lease or abandon the project.

Projects also face risks unrelated to interconnection that can cause cancellation. A project may not be selected in a competitive solicitation for a power purchase agreement, fail to secure a necessary permit, or encounter local opposition that blocks siting. Each additional quarter in the queue is another quarter of exposure to these shocks, so a slower interconnection process increases cancellations from these channels.

2.4 Queue Design Reforms

Recent regulatory reforms aim to address the growing interconnection backlog. In 2023, FERC, the federal regulator overseeing U.S. transmission policy, approved Order No. 2023, which aimed to shift queue priority from “first-come, first-served” to “first-ready, first-served” (Hale and Christian, 2023).

³For example, the impact study of a gas power plant (AA2-030) does not assess an interconnection cost because the project is an expansion of an existing plant, but the project “is required to construct all connection facilities in accordance with the TO published standards. ComEd would review and approve all customer relay protection design drawings and relay settings.”

⁴For wind projects, construction typically takes six months to a year (AWEA, 2019); solar projects follow similar timelines. Network upgrades can take longer, but projects can sometimes begin operating before all upgrades are completed.

The Order has four main components: (a) raising the cost to enter and remain in the queue, (b) imposing penalties for withdrawing from the queue, (c) imposing penalties for delays in completing studies, and (d) transitioning from studying each request serially to cluster studies, under which requests are grouped into large clusters and receive a single study per cluster. The study-delay penalties in (c) fall on the transmission provider, which in PJM’s case is PJM itself rather than the transmission owners; the penalties cannot be recovered through transmission rates, though PJM may seek FERC approval to recover a penalty from a transmission owner at fault (FERC, 2023). Implementation is ongoing: PJM, for example, opened its first reformed cluster cycle in 2026, with applications due April 27 (PJM Interconnection, 2025*a*).

3 Interconnection Request Data and Descriptive Evidence

3.1 Data Sources and Construction

Our main data cover the 4,174 interconnection requests to PJM from 2008 to 2020. Each request corresponds to a single proposed project at a specific location. Requests are submitted by project developers, and each request is for connection to the network of one transmission owner. A request can be either a new plant or a proposal to increase maximum capacity at an existing plant; the study process is the same for both types of requests.

Our data come from PDFs of 7,492 engineering studies, which we hand-collected. From each study PDF we record the interconnection cost estimate, which engineering tests were performed and their results, and cost-sharing information—whether the request is sharing costs and which requests it shares them with. We begin collection in 2008 because earlier studies have irregular formats that make it difficult to identify the relevant costs. We also collect the study issue date, and, from PJM, we observe the queue entry date, the entry cohort, and the withdrawal or operation date. This information lets us reconstruct, for each quarter, the set of requests waiting for each study and each request’s priority relative to others, both PJM-wide and within its TO. Table 1 presents summary statistics for these data.

3.2 Queue Composition and Growth

The PJM queue is dominated by requests for solar, natural gas, and wind projects. These three fuels accounted for 85 percent of interconnection requests from 2008 to 2020. Natural gas projects tend to be much larger than wind and solar projects; they accounted for 17 percent of requests but 42 percent of requested capacity. The composition of requests shifted over our sample, with solar

Table 1: Summary Statistics

	1 st Study		2 nd Study		3 rd Study	
	Mean	Std. Dev.	Mean	Std. Dev.	Mean	Std. Dev.
Cost per MW of capacity	0.12	0.40	0.17	0.47	0.11	0.21
Wait time (mos.)	4.9	1.5	11.3	8.1	15.1	9.8
Size in MW	97	196	105	190	157	257
Capacity increase at existing plant	0.21	0.41	0.23	0.42	0.15	0.36
Solar	0.59	0.49	0.60	0.49	0.61	0.49
Natural Gas	0.17	0.37	0.16	0.36	0.19	0.39
Wind	0.09	0.29	0.10	0.30	0.12	0.33
Battery	0.10	0.30	0.10	0.29	0.05	0.21
Coal, oil, diesel	0.02	0.14	0.02	0.12	0.01	0.08
Other	0.03	0.18	0.03	0.17	0.02	0.15
Cost sharing	0.04	0.20	0.59	0.49	0.62	0.48
Receive engr. tests	0.81	0.39	0.88	0.32	0.04	0.19
Distance to substation (km)	5.13	7.00	5.26	7.64	5.70	8.54
Ordinance	0.28	0.45	0.31	0.46	0.32	0.47
Observations	4,168		2,495		829	

Projects entering the queue in 2008-2020. 6 projects are missing the 1st study in the data. Cost per megawatt (MW) capacity is interconnection cost estimate, in millions of 2020 dollars, divided by the project’s size in MW. Wait time for the 1st Study is wait in months for the first study after joining the queue. Wait time for the 2nd Study is wait in months for second study after receiving the first study. Wait time for the 3rd Study is wait in months for third study after receiving the second study. Reported wait times are capped at the 90th percentile (36 mos. for the second and third studies) to limit the influence of outliers. The corresponding uncapped means are 5.3, 14.9 and 18.0. Capacity increase at existing plant is an indicator for a request to increase maximum generating capacity at an existing power plant; the size for these requests is the incremental capacity, not the total plant capacity. Cost sharing is an indicator for if a project shares network upgrade costs with other projects; network upgrade costs are typically first reported in the 2nd study. Receive engr. tests is an indicator for receiving any of three engineering tests: generator deliverability, multiple facility contingency, and short circuit analysis. Distance to substation is the distance to the nearest connected substation in km. Ordinance is an indicator for a local ordinance restricting renewable energy development.

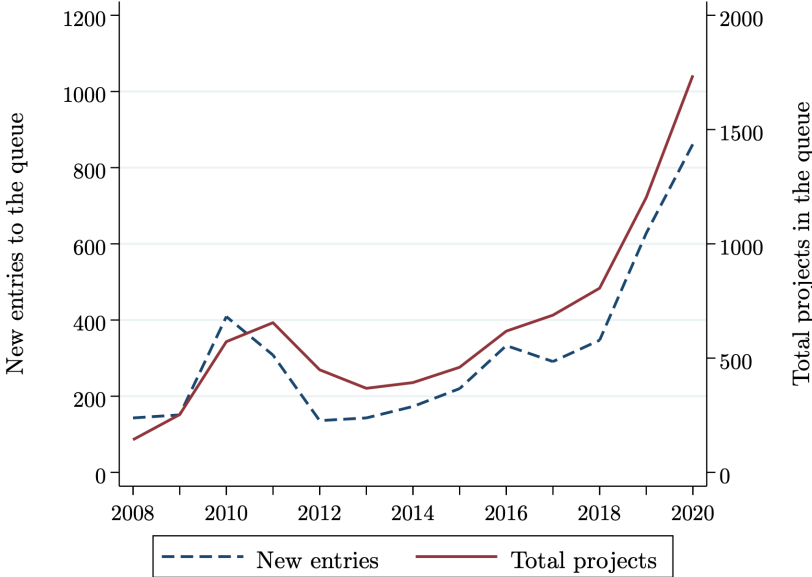
accounting for a growing share of requests after 2015 and batteries a growing share after 2017. In the rest of the paper, we refer to wind, solar, and battery projects as “renewable”, and all others as “non-renewable”.

The number of interconnection requests has increased dramatically over time, driven by the falling cost of renewables. Figure 1 plots new interconnection requests each year (dotted line) and the average number of projects in the queue by year (solid line). The increase began around 2015 and was concentrated in renewable projects.⁵ Because renewables are smaller on average, the rise

⁵The spike around 2010 was due to a temporary federal program that gave solar and wind developers the option to claim a cash grant in lieu of the non-refundable investment tax credit (see Aldy, Gerarden and Sweeney (2023) for program details).

in requested capacity was less pronounced: 42 GW of new requests in 2008 compared to 69 GW in 2020. This pattern reflects falling installation costs for wind and, especially, solar projects (Seel et al., 2024; Wiser et al., 2024). Consistent with a technology-driven explanation, similar increases in renewable interconnection requests occurred across all U.S. regional grid operators (Gorman et al., 2024).

Figure 1: Queue Size Over Time



The figure plots the size of the PJM interconnection queue from 2008 to 2020, based on projects that entered from 1997 to 2020. The solid red line is the annual average number of projects in the queue, counting each project from its entry until withdrawal or final study receipt (or, for entries before 2008, its operation date). The dotted blue line is the total number of new entries each year.

3.3 Developers and Transmission Owners

Developers. We can identify the developer for only a subset of projects. Starting with the second study, PJM lists the interconnection customer name for each request. This name is often the limited liability company holding the project, not the developer that controls it. We match these names to developers using news articles, regulatory documents, and developer websites, matching 43.3% of projects overall, 80.9% of those that reached the second study, and 37.0% of those that reached the third.

The developer data suggest that treating requests as independent, as we do in the model, is a reasonable approximation. Developer concentration is low: the 1,809 matched projects map to 389

unique developers, the largest of which (Invenergy) accounts for 4.5% of matched projects, and the fifteen largest together account for less than 33% (Appendix Table E.3). Developers also do not appear to manage projects as a portfolio: when a developer had more than one project in an entry cohort, either all or none were completed 64% of the time, consistent with developers advancing every individually profitable project. Projects can be sold to other developers, so a profitable one need not be withdrawn even when its original developer is capacity-constrained. Repeated entry is also rare: only 9.2% of requests enter at a site that already hosted an earlier request by the same developer, and just 1.4% follow that developer’s earlier withdrawal at the same site.

Transmission owners. PJM has 22 transmission owners whose engineering input the studies rely on.⁶ Appendix Table E.4 shows that the average TO has 190 projects and 18.5 GW of queued capacity in our sample, with a standard deviation of 22.7 GW.

Projects are individually small relative to their TO. The average project is about 0.5% of its TO in our sample, by both project count and capacity, and under 3% even at a 25th-percentile TO. Developer concentration is also low within TOs: the average TO contains projects from 31 distinct developers.

3.4 Waiting Times

The first study arrives quickly and with little variation, but the later studies arrive much later and with far more. Projects receive the first study after a mean of 5 months, with a standard deviation of just 1.5. The second and third studies take far longer: against PJM’s official targets of 4 and 6 months, the second arrives after a mean of 11 months (SD 8) and the third after 15 months (SD 10).

While priority is by entry cohort, study arrival is stochastic. Cohorts that entered the queue earlier are more likely to receive a study than projects in later cohorts that are waiting for the same study, but this is not guaranteed. For example, among projects entering in 2012, the average second study arrival date was 2013Q2 for projects entering in the first half of the year and 2014Q4 for projects entering in the second half. Thus, the earlier cohort received their second study substantially earlier on average. However, 3.5% of projects that entered in the first-half 2012 cohort had still not received their second study by 2014Q4, the average arrival date for the later cohort.⁷

⁶TOs can own incumbent generation and, less commonly, projects in the queue, but we find no evidence this ownership correlates with interconnection wait times or costs.

⁷One reason wait times are variable is that these studies sometimes need to be revised. For example, 22 percent of projects in our sample had their second study revised. We will model the arrival of the final version of each study, not the intervening versions which are not always posted by PJM.

Time spent in the queue increased over our sample, though not as dramatically as the number of projects. On average, projects that reach the terminal study receive it 27 months after entering the queue. This duration rose from 22 months for projects entering in 2008-2012 to 29 months for those entering in 2013-2017 (see Appendix Figure E.3 for wait time statistics by entry quarter).

3.5 Interconnection Costs

Interconnection costs are low for most projects but very high for some. We use cost per MW as our measure of cost.⁸ For the second study, 29 percent of projects have interconnection costs less than 0.01 million per MW. The 75th percentile of the cost distribution is 0.14 million per MW and the 90th percentile is 0.40 million per MW. For comparison, installation costs for wind and solar projects are roughly 1.5 million per MW.

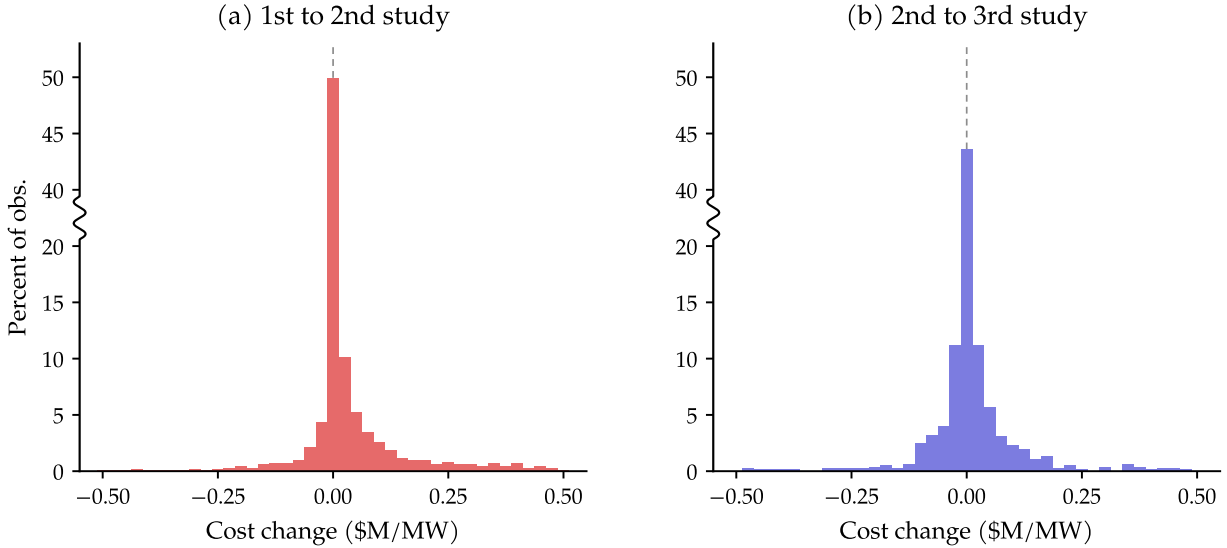
Developers face substantial uncertainty about what their interconnection costs will be. First, although a developer may be able to use engineering models to identify whether an interconnection will overload the grid, it is hard to predict what remedies a transmission owner will require and the cost of these remedies, according to our interview with an industry expert. Second, the withdrawal of other projects sharing the cost of a network upgrade changes a project's cost. After withdrawals, PJM may still require the upgrade, so the remaining projects' share of its cost increases. If PJM no longer requires the upgrade, the cost for the remaining projects will decrease. Consistent with these sources of uncertainty, observable project characteristics explain less than half the variation in interconnection costs, and projects in the same geographic area can have very different costs (Appendix Figure E.2, Johnston, Liu and Yang (2025)).

Changes in costs across studies within a project are also hard to predict. Figure 2 shows that interconnection costs for the same project do not systematically decrease across studies.⁹ This pattern suggests that cost changes are not anticipated. If developers were able to predict how a project's interconnection cost would evolve across studies, we would expect selection on this difference, i.e., projects that predicted their cost to fall would be more likely to stay, and the distribution would have more mass below zero.

⁸There do not appear to be economies of scale in interconnection costs for moderately sized projects. For projects from the 10th to 90th percentile in size, a 1 standard deviation increase in capacity is associated with 0.05 standard deviation decrease in the second study interconnection cost.

⁹Costs on average increase from the first to the second study because the second study includes the contribution to shared network upgrade costs, while the first study does not. For projects that do not share costs, the distribution of this cost difference is symmetric around zero.

Figure 2: Within-Project Changes in Interconnection Cost Estimates across Studies



Panel (a) shows a histogram of the difference in the first and second study interconnection cost estimates for projects that received study 2. $N = 2,495$; 151 projects with cost differences outside the plotted range are excluded (126 above and 25 below), as are 4 without a first study. Panel (b) shows a histogram of the difference in the second and third study interconnection cost estimates for projects that received study 3. $N = 829$; 19 projects with cost differences outside the plotted range are excluded (10 above and 9 below), as are 51 without a second study. The sample is projects queuing from 2008–2020. Y-axis is the percent of observations in each bin. Costs are in millions of 2020 dollars per MW.

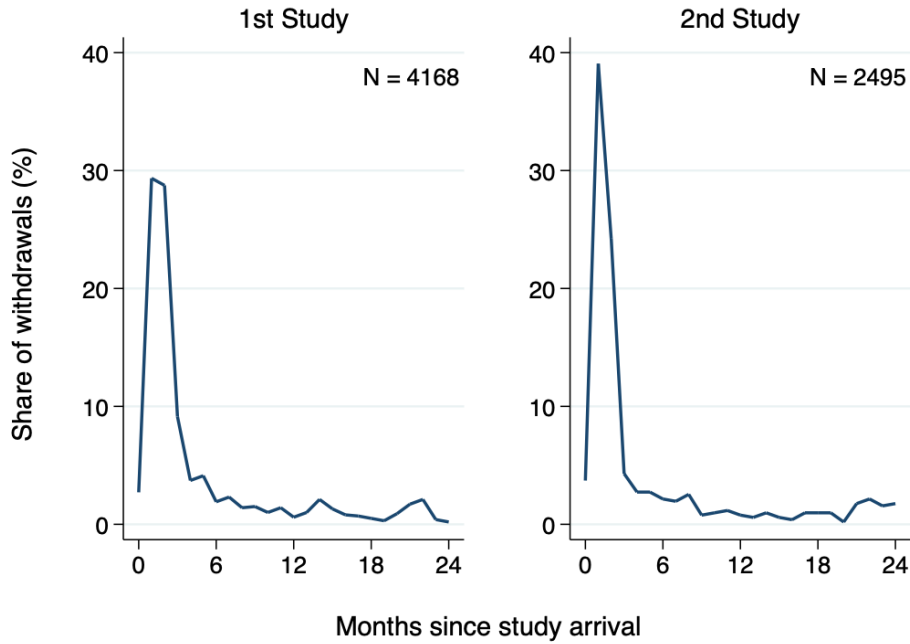
3.6 Withdrawals

Withdrawals concentrate sharply in the months immediately following each study. Figure 3 plots the share of projects withdrawing from the queue in each month relative to the arrival of their most recent study. The largest spike, reaching nearly 40 percent, occurs in the first two months after the second study, with a smaller but still pronounced spike of about 30 percent after the first study. The post-study spikes are consistent with developers making withdrawal decisions when new project information arrives in the form of cost estimates as well as engineering details that inform broader assessments of project viability.

We next test whether high interconnection costs explain these withdrawals. Specifically, we regress an indicator for withdrawing from the queue on an indicator for having a high (above 0.1 million per MW) interconnection cost. We define withdrawing as leaving the queue before the next study arrives, or before beginning operation for projects that have received their final study.

Across all three studies, we find that projects with a high interconnection cost estimate are more likely to withdraw from the queue (Table 2). For the first study, the OLS estimates in the

Figure 3: Withdrawals Relative to Study Arrival



Share of withdrawals by month relative to the arrival of each project’s most recent study, shown separately for projects whose most recent study was the 1st study (left panel) and the 2nd (right panel). The zero point on each x-axis marks the arrival of the corresponding study. Excludes projects that withdrew two or more years after the arrival of their most recent study. N denotes the total number of projects that received the 1st study and the 2nd, respectively.

first column imply that having a high interconnection cost is associated with an increase in the probability of withdrawal of 12 percentage points, or 38% at the mean withdrawal rate. For the second and third studies, the corresponding effects are an increase in the probability of withdrawal of 17 and 17 percentage points (36 and 33% at the mean withdrawal rate).¹⁰

The OLS estimates may be biased if developers can predict their interconnection costs and select into the queue based on this knowledge. If developers only plan projects in expensive locations when those projects are otherwise especially profitable, the resulting positive selection would attenuate the OLS estimates. To address this concern, we instrument for current interconnection costs with the change in costs across studies. This instrument relies on the finding that cost changes across studies are difficult to predict (Section 3.5).

¹⁰These results are robust to including additional controls for permitting difficulties—distance from project to grid connection point, an indicator for local solar and wind ordinances—that might be correlated with high interconnection costs.

Table 2: Effect of Interconnection Costs on the Probability of Withdrawing from the Queue

	1 st Study	2 nd Study		3 rd Study	
	OLS	OLS	IV	OLS	IV
High cost estimate (>0.1M/MW)	0.116*** (0.019)	0.169*** (0.028)	0.231*** (0.044)	0.170*** (0.060)	0.083 (0.116)
Mean of dependent var.	0.30	0.47	0.47	0.52	0.52
F-statistic (instrument)			1,433		256
Observations	3,983	1,974	1,974	517	517

Projects queuing from 2008-2020; projects still active excluded. SEs in parentheses; clustered by substation. The dependent variables are indicators for projects withdrawing from the queue before receiving the next study or before beginning operation for projects with their final study. High cost estimate indicates if that study’s interconnection cost estimate is above >0.1M/MW. All specifications control for project size (three bins), fuel type, if the project is a capacity increase at an existing plant, whether the 1st study mentions shared network upgrade costs, the log of the total costs to be shared listed in the 1st study for projects with cost sharing, transmission owner FE, and FE for the year of queue entry. IV results instrument for having a high cost using the change in having a high cost across studies. *** $p < 0.01$, ** $p < 0.05$, * $p < 0.1$.

The IV estimates for the second study are similar to the OLS estimates and statistically significant, suggesting that selection does not substantially bias the OLS results. The IV estimate for the effect of third study costs is positive and similar in magnitude to the OLS estimate, though it is not precisely estimated.

Between studies, withdrawals occur at a low and roughly constant rate. As discussed in Section 2.3, projects face exit risks from outside the queue. These risks can interact with queue delays: each additional quarter spent waiting for the next study exposes a project to another period in which risks such as local opposition may materialize.

4 Externalities in the Queue

Projects in the queue interact with one another through three channels: PJM’s finite capacity to process engineering studies (congestion externality), the physical transmission infrastructure shared across interconnections (cost externality), and the wholesale electricity market (output externality). We find that the congestion externality is quantitatively important, while the geographic cost and local output externalities are indistinguishable from zero.

4.1 Congestion Externality

We first investigate how queue length affects how long projects wait for studies. The congestion externality is mechanical under strict first-come, first-served queuing with a fixed processing rate. PJM’s study arrival is probabilistic rather than strictly ordered, so the strength with which arrival probability responds to queue position is an empirical question. As noted in Section 3.4, the first study arrives soon after entry, but the arrival times of later studies are more variable.

We estimate a discrete-time hazard model, where the conditional probability that the second or third study arrives in a quarter is given by a probit model. The effect of interest is that of an increase in the natural log of the number of higher-priority projects (those with the same or earlier entry dates) on the conditional arrival probability.¹¹ Throughout, we condition flexibly on time already spent in the queue, thus comparing projects with the same waiting time. These controls separate the queue-position effect from pure duration dependence in study processing, i.e., a study becoming more or less likely to arrive simply because a project has already waited longer. We allow the effect of higher-priority projects to vary with whether a project is waiting for the second or third study.

Identification. The queue-position coefficients identify the congestion externality because PJM, not the project, determines study arrival. Selection affects which projects occupy a given queue position: those with high profits or low waiting costs (reflecting unobservables such as power purchase agreements or land costs) are more likely to survive to the front. Yet, as the PJM manual and industry interviews confirm, study priority depends solely on queue position rather than on the profitability driving this selection, and projects cannot act to expedite their studies. The selection that places high-profit projects at the front therefore does not bias the position effect. The remaining threat is that project characteristics affect both how long PJM takes to complete a study and queue position. We control directly for the main characteristics affecting how long a study takes: project size, fuel type, and the prior study’s information (cost estimate, engineering tests, and whether it shares costs). Together, these arguments imply that the number of higher-priority projects is independent of the error term in the probit model.

Results. We find a significant congestion externality, which is largest for the third study. Table 3 reports the implied average marginal effects of higher priority projects on own study arrival. Our

¹¹We choose a log functional form because we expect the same increase in the number of higher-priority projects to have a larger effect on arrival probability near the front of the queue, where arrival probabilities are high, than near the back of the queue.

preferred specification, column (4), implies that a 10% increase in higher-priority projects reduces the second-study arrival probability by 2.7% on average.¹² For the third study, the effect is larger: a 10% increase in the number of higher-priority projects reduces the probability of study arrival by 12.7%. In support of our claim that PJM’s study delivery does not respond to expected project profitability, we re-estimate the arrival model including two proxies for project profitability: the average local wholesale electricity price and an indicator for binding local wind or solar ordinances. The effects of these variables on study arrival are small, indistinguishable from zero at $\alpha=0.05$, and have signs that vary across specifications. The queue-position effects remain similar (Appendix Table E.5).

Withdrawals by nearby projects can trigger study revisions, slowing delivery of the final version and thus imposing a further congestion externality. Column (5) adds a control for recent withdrawals in the same TO along with the total queue number in the same TO, so that the withdrawal coefficient reflects withdrawals conditional on queue size. The estimated coefficient is consistent with withdrawals reducing study arrival probability, but is small and statistically insignificant.

These estimates are robust to flexible time controls, addressing the concern that PJM’s study process may have evolved over this period. PJM did not make major changes to its process, but TOs may have learned to process studies more efficiently or hired more engineers in response to rising demand. To account for these effects, we re-estimate our preferred specification (column 4 of Table 3) controlling for a linear time trend and its interaction with an indicator for renewable generation. This interaction accounts for how learning may be technology specific. We do the same for a quadratic time trend and its interaction. Finally, we estimate a model with year fixed effects, a specification that highlights how the effect of queue position can be identified solely from cross-sectional differences in arrival probability for projects at different queue positions. Appendix Table E.6 shows that we consistently find a negative and statistically significant effect of the number of higher priority projects on study arrival for both the second and third studies. The estimates imply that a 10% increase in higher priority projects reduces study arrival probability by 2.1 to 2.7% for the second study and 10.5 to 12.7% for the third study.

A second concern is that the effect is driven by the end of the sample, when the queue was most congested. Restricting to projects that queued before 2019, which excludes 40% of the projects in our sample, we still find statistically significant and negative effects of queue position on study

¹²To calculate this effect, we assume that both the overall queue size and the TO queue size have the same percent increase and sum the average marginal effects for the queue size measures ($-0.028 - 0.015 = -0.043$) and multiply by 0.10 to find the effect of a 10% increase in queue size, yielding a change in probability of -0.0043. Dividing by the mean arrival rate (0.16 for the second study) implies a 2.7% reduction in arrival probability.

Table 3: Effect of Queue Position on Study Arrival

	(1)	(2)	(3)	(4)	(5)	(6)
	Probit	Probit	Probit	Probit	Probit	Probit
ln(# Higher priority)	-0.054*** (0.003)	-0.043*** (0.004)	-0.031*** (0.004)	-0.028*** (0.004)	-0.019*** (0.004)	-0.018** (0.008)
ln(# Higher priority) X Waiting for third study)		-0.026*** (0.005)	-0.017*** (0.006)	-0.020*** (0.006)	-0.018*** (0.006)	-0.014** (0.006)
ln(# Higher priority in TO)			-0.016*** (0.003)	-0.015*** (0.003)	-0.042*** (0.005)	-0.017*** (0.004)
ln(# Higher priority in TO) X Waiting for third study			-0.013*** (0.005)	-0.013*** (0.005)	-0.011** (0.005)	-0.013*** (0.005)
Waiting for third study	-0.295*** (0.020)	-0.209*** (0.017)	-0.218*** (0.017)	-0.218*** (0.017)	-0.234*** (0.018)	-0.246*** (0.018)
ln(# Withdrawals in TO)					-0.002 (0.001)	
ln(# in Queue in TO)					0.033*** (0.005)	
Prior Study Controls				X	X	X
Transmission Owner FE						X
Year FE						X
Observations	28,917	28,917	28,917	28,917	28,917	28,917
Pseudo R2	0.163	0.166	0.173	0.177	0.180	0.197

The sample includes projects queued from 2008-2020, observed over time at the quarterly level as they wait in the queue for study arrival. Marginal effects from probit regressions are reported. Standard errors in parentheses, clustered by substation. The dependent variable is an indicator for study arrival (overall mean = 0.11; mean for second study is 0.16 and for third study is 0.06). All specifications control for project size (three bins), fuel type (wind, solar, storage), if the project is a capacity increase at an existing plant, and time spent in the queue (measured in quarters). Specifications (4)-(6) additionally include controls from the immediately prior study, including the project's own cost estimate (three bins) from the prior study (e.g., the first study costs for projects awaiting the second study), indicators for whether the project receives engineering tests and whether it is part of a cost-share group. Specification (5) further controls for the log size of withdrawn projects waiting for the same or a later study within the same transmission owner over the past two quarters, and the log number of projects in the queue within the same transmission owner. *** p<0.01, ** p<0.05, * p<0.10.

arrival: 3.5% for the second study, 7.8% for the third (Appendix Table E.6, column 5).

4.2 Cost Externality

Projects connecting in the same location can affect one another's interconnection costs through the network infrastructure they share. Those queued ahead of a given project may consume available local capacity, leaving the project responsible for an upgrade. When several projects trigger a common upgrade, PJM assigns them to share its cost; if one member of a cost-share group withdraws, the others' costs can rise or fall. A completed project that paid for a costly network upgrade can also lower later projects' costs, because that upgrade may leave spare capacity behind.

4.2.1 Spillovers from Other Projects in the Queue

Higher-priority Local Capacity. PJM models higher-priority projects as in service when conducting engineering studies, so these projects can consume available local capacity. More higher-priority local capacity could therefore increase the probability a project triggers costly network upgrades, raising its interconnection cost.

We relate the probability of a high interconnection cost (above \$0.1 million per MW) to the amount of higher-priority capacity in a project’s local area when its study is issued. We repeat the analysis for the network-upgrade component of cost. We define the local area four ways: within 10 km, within 20 km, within the same transmission owner, and within the same k-means cluster, where we group substations into 50 regions by location and similarity in locational marginal prices.¹³ We include geographic-region and queue-year fixed effects and control for recent transmission investment by the grid operator. The resulting estimates are nonetheless suggestive rather than causal, since the entry and withdrawal decisions that determine higher-priority capacity are themselves affected by the state of the network.

We find that more higher-priority capacity does not raise a project’s cost under any of the four definitions, whether we measure total cost or its network-upgrade component alone. The point estimates in Appendix Table E.7 are uniformly small: even the largest in absolute value implies that a doubling of higher-priority capacity changes the probability of a high cost by about 2.4 percentage points, or roughly 6% of its sample mean of 0.37. This result is robust to an alternative definition of a high interconnection cost and to using the total capacity of active waiting projects rather than higher-priority capacity (available upon request).

Withdrawals Within Cost-Share Groups. When multiple projects trigger the same network upgrade or overlapping system violations, PJM assigns them to a cost-share group and allocates the cost in proportion to each project’s contribution to the reliability violation. More than half of projects (59%) share costs as of the second study. We observe complete group membership for only 29% of cost-sharing projects (153 groups), and conditional on belonging to a fully observed group, 37% of projects see at least one member withdraw before the focal project reaches a terminal study.

We test whether these withdrawals systematically affect costs for remaining projects. Because the group cost and its allocation change when membership changes, the withdrawal of one member has a theoretically ambiguous effect on the others: if PJM still requires the upgrade, the remaining members bear a larger share of its cost; if the withdrawal removes the need for it, their cost falls. We also test whether member withdrawals predict a focal project’s own withdrawal, since selective exit by projects facing high costs could mask a cost effect. These estimates are likewise suggestive rather than causal, since a member’s decision to withdraw may itself be driven by realizations of the shared cost.

We find the estimated effects of member withdrawals on cost are small and statistically insignif-

¹³For details, see Johnston, Liu and Yang (2025).

icant (Table 4, columns 1 and 2). A one-standard-deviation increase in the withdrawn share (0.22) implies a \$0.02–\$0.03 million per MW reduction in cost between studies, about a tenth of a standard deviation. The 95% confidence intervals rule out cost increases above about a tenth of a standard deviation of cost changes, but they are wider on the cost-decreasing side, where reductions of up to about a quarter of a standard deviation cannot be ruled out. Member withdrawals also have no significant effect on a project’s own decision to withdraw (column 3).

Table 4: Effects of Cost-Share Group Member Withdrawal on Own Cost and Withdrawal

	Change in cost per MW		Own withdrawal
	Total (1)	Network upgrade (2)	(3)
Share of group MW withdrawn	-0.132 (0.093)	-0.100 (0.089)	-0.009 (0.010)
Transmission Owner FE	X	X	X
Queue Year FE	X	X	X
Mean of dep. var [SD]	-0.017 [0.289]	-0.042 [0.274]	0.023 [0.149]
Mean of indep. var. [SD]	0.077 [0.224]	0.077 [0.224]	0.068 [0.197]
Observations	206	206	8,928

Projects queuing from 2008–2020, in a cost-share group whose full membership we observe. Standard errors are in parentheses and clustered by cost-share group. Columns (1)–(2) restrict the sample to projects that have received the third study, since projects typically begin to observe their cost-share group in second study; the dependent variable is the change in cost per MW from the second to the third study. Column (1) uses total interconnection cost per MW, and column (2) uses network upgrade cost per MW. Column (3) reports linear-probability estimates from a project-quarter discrete-time hazard panel; the dependent variable is an indicator for project withdrawal in the current quarter. The independent variable, Share of group MW withdrawn, is the share of cost-share group peers withdrawn during the relevant exposure window (the inter-study window for columns 1-2; since the focal’s most recent study for column 3). The mean of the independent variable in columns (1)–(3) is 0.077, 0.077, and 0.068, respectively. All specifications control for project size (three bins), fuel type (wind, solar, storage), whether the project is a capacity increase at an existing plant, and the log of total cost-share group size in MW. *** $p < 0.01$, ** $p < 0.05$, * $p < 0.10$.

4.2.2 Spillovers from Completed Interconnections

A completed interconnection can lower a later project’s cost by leaving spare transmission capacity, but cost-sharing and the project-specific nature of upgrades limit this spillover.¹⁴ We test for the spillover by regressing an indicator for a high cost estimate (above \$0.1 million per MW) on

¹⁴In FERC Order 2023, the Commission states that “absent cost sharing provisions among clusters, interconnection customers may significantly benefit from earlier-in-time network upgrades but not share in the cost of those network upgrades in a manner that is roughly commensurate with benefits” (p. 320), suggesting that this externality is more relevant in systems without cost sharing (FERC, 2023).

whether the most recently completed interconnection in the same area was costly, defined as a total interconnection cost above \$1 million; 22% of completed interconnections meet this threshold. We exclude prior interconnections that share costs with the focal project, so the regressor captures only the cross-cohort channel.

The estimated effects on a project's subsequent total cost are statistically insignificant and generally small across all four area definitions (Table 5, Panel A). The pattern is robust across 16 alternative definitions of costly prior interconnection and local area once region and year fixed effects are included (Table E.8). For the network-upgrade component, the effects are also insignificant for three of the four area definitions, but at the transmission-owner level a costly prior interconnection is associated with a 4.2-percentage-point reduction in the probability of a high network-upgrade cost, a 32% reduction relative to its sample mean (Panel B). The corresponding effect on total cost, however, is small and statistically insignificant (Panel A).

Discussion. Across these three channels, the evidence points to limited cost externalities. More higher-priority capacity does not detectably raise a project's cost; member withdrawals within cost-share groups produce no detectable effect on remaining projects' costs or on their own-withdrawal decisions; and the cross-cohort spillover from completed interconnections is mostly null, with a significant negative effect only at the transmission-owner level for the network-upgrade component. The common institutional explanation is PJM's cost-sharing rules, which spread the cost of an upgrade across the projects that jointly trigger it. Consistent with this explanation, queue capacity is empirically associated with a higher probability of cost-share group assignment, and group assignment is itself associated with lower subsequent costs (Appendix Tables E.9 and E.10). More broadly, where upgrades are triggered, the null is also consistent with upgrade costs being approximately linear in capacity at the binding margin; per-MW costs are then constant in queue size, even before cost-sharing dampens any residual spillover. Overall, our results are consistent with PJM's policy of extensive cost-sharing across small groups of projects muting what could otherwise be substantial externalities.

4.3 Local Output Externality

By lowering local wholesale prices, a completed interconnection could reduce the expected revenues, and hence the entry and completion incentives, of nearby projects. This channel is most likely to be present at locations with binding transmission constraints, where a new project's output cannot flow freely across the grid and instead depresses prices locally.

We test for the effect of a new project beginning operation on local prices. We first construct a monthly panel with an observation for each substation, which is a potential grid connection point. Our measure of monthly wholesale prices is the average peak-hour locational marginal price at that substation. We use the event-study Difference-in-Differences estimator from Callaway and Sant’Anna (2021) to estimate the effect of a new project beginning operation on these prices. The comparison group is substation-months where no new projects above the size threshold begin operation; we use thresholds of 20 and 100 MW.

We find little effect of a new project beginning operation on local prices. Figure 4 shows that the estimated price decrease is small and statistically indistinguishable from zero in each post-period month. The point estimates are consistently negative for the first seven to eight months of operation before turning positive, suggesting a small and transitory negative effect of roughly \$2 per MWh.

Local Price Effect at Locations of Transmission Constraints. To directly address the concern that the output externality may operate only at locations where projects face binding transmission constraints, we re-estimate the event study restricting the treatment group to substations where the new project was responsible for paying transmission network upgrade costs. These are precisely the projects connecting to an already-congested local grid, so any local market power over energy prices should be most detectable in this subsample. We continue to find a null effect (Appendix Figure E.4).

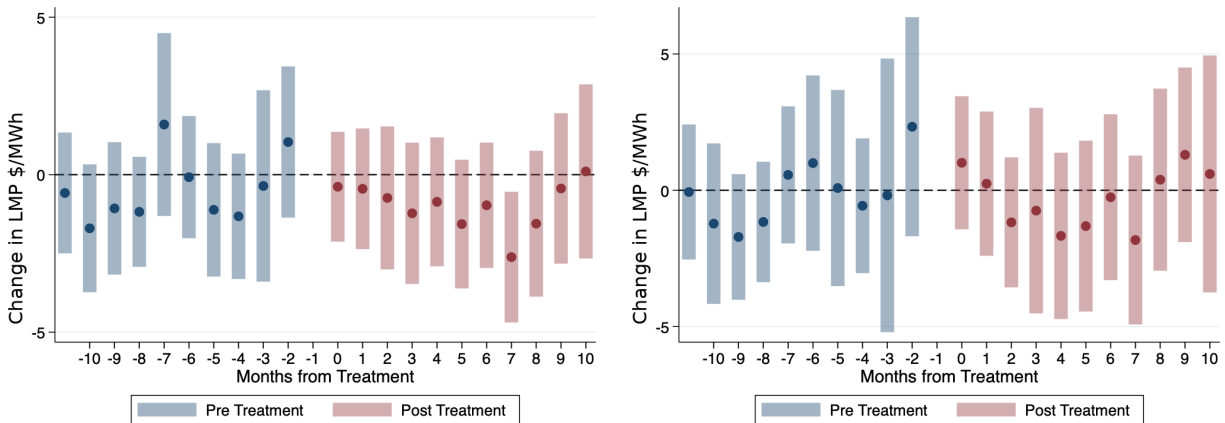
Discussion. This null result is consistent with the institutional details of the interconnection process. PJM’s deliverability requirement obligates most new projects to upgrade the transmission infrastructure to the point that they can deliver their power to load during peak demand. These upgrades relieve local congestion, allowing output to flow freely across the grid rather than depressing prices locally. A completed interconnection’s effect on the expected profits of future projects in the same location is therefore likely small, even where the grid was constrained prior to the upgrade.

As more projects complete and add to supply, PJM wholesale prices should fall. We incorporate this aggregate effect in the model by constructing project revenues from the wholesale-market equilibrium.

Figure 4: Effects of Interconnections on Local Wholesale Prices

(a) Adding 20 MW New Capacity

(b) Adding 100 MW New Capacity



Panel (a) plots event-study estimates of the effect of a new project with capacity of at least 20 MW beginning operation at a substation on local wholesale electricity prices. Panel (b) uses a 100 MW threshold. Treated observations are substation-months in which a project above the corresponding capacity threshold begins operation; control observations are substation-months without such entry. The dependent variable is the monthly average peak-hour locational marginal price at the substation level (mean = \$34.89/MWh), constructed from PJM locational marginal price data over 2008-2020. Estimates are obtained using the Callaway and Sant’Anna (2021) difference-in-differences estimator with doubly robust inverse probability weighting. Standard errors are clustered at the substation level.

Table 5: Effect of Prior Costly Interconnection on Probability of High Interconnection Cost

	10km (1)	20km (2)	Transmission owner (3)	K-means cluster (4)
Panel A: High Total Cost Estimate (mean = 0.37)				
Costly Prior Interconnection	0.056 (0.049)	-0.005 (0.043)	-0.012 (0.023)	-0.020 (0.026)
High Transmission Investment	-0.054* (0.031)	-0.054* (0.031)	-0.065*** (0.023)	-0.053* (0.031)
Geographic Region FE	X	X	X	X
Queue Year FE	X	X	X	X
Observations	2,328	2,328	2,328	2,328
R^2	0.525	0.523	0.239	0.525
Panel B: High Network Upgrade Cost Estimate (mean = 0.13)				
Costly Prior Interconnection	0.010 (0.034)	-0.029 (0.032)	-0.042*** (0.015)	0.011 (0.016)
High Transmission Investment	-0.026 (0.024)	-0.023 (0.023)	-0.040** (0.017)	-0.024 (0.024)
Geographic Region FE	X	X	X	X
Queue Year FE	X	X	X	X
Observations	2,328	2,328	2,328	2,328
R^2	0.475	0.481	0.181	0.480

Projects queuing from 2009–2020. Standard errors in parentheses, clustered by substation. In Panel A, the dependent variable is an indicator for whether the Study 2 or Study 3 total cost estimate is high, defined as exceeding \$0.1 million per MW. In Panel B, the dependent variable is an indicator for whether the Study 2 or Study 3 network upgrade cost estimate is high, defined as exceeding \$0.1 million per MW. The regressor of interest Costly Prior Interconnection is an indicator for a prior completed interconnection with total costs exceeding \$1 million within the same geographic region, varying across columns (10km radius, 20km radius, Transmission owner, or K-means cluster). High Transmission Investment is an indicator for PJM Regional Transmission Expansion Plan (RTEP) investment above the 75th percentile of the RTEP distribution within the same Transmission Owner, measured over a four-year window spanning three years before and one year after the study issue date. All specifications control for project size (three bins), fuel type (wind, solar, storage), whether the project expands an existing project, and the number of projects entering within three years prior to the study issue date within the same Transmission Owner. Column (4) additionally include controls from the immediately prior study, including the project's own cost estimate (three bins) from that study (e.g., first study costs for projects awaiting the second study), indicators for whether the project receives engineering tests and whether it is part of a cost-share group. * $p < 0.1$, ** $p < 0.05$, *** $p < 0.01$.

5 Model

Each project solves a finite-horizon optimal stopping problem. Time is discrete, indexed by $t = 1, 2, \dots$ in quarters. Potential projects arrive at the beginning of a period and decide whether to pay an entry cost to join the queue or leave immediately. Projects that join receive up to three studies. Between studies, projects incur waiting costs and can withdraw at any time. Each project also faces a per-period probability of exogenous exit due to events outside the interconnection process. After the final study, a project decides whether to complete interconnection or withdraw.

Projects do not directly interact with each other. They respond to a vector of variables called the *queue status*, which determines each project's study-arrival probabilities, distributions of interconnection costs, and operating revenues. We define the queue status in Section 5.3. The transitions of the queue status are deterministic and consistent with project strategies in the equilibrium. The queue status has both PJM-wide and TO-specific components, since TOs generally conduct the studies within their territories.

Below, we first specify the project decision problem. Then we provide an equilibrium concept where project strategies are functions of their beliefs about the equilibrium path of the queue statuses, and their strategies generate the path consistent with their beliefs.

5.1 Decision Problem

We describe a project's decision problem recursively, beginning with the completion decision and working backwards. PJM may require fewer than three studies if the project needs no significant network upgrades and does not share costs. A project's last required study is its *terminal study*, after which it decides whether to complete or withdraw. The first or second study can be terminal, while the third study always is. After a non-terminal first study, the project enters *Stage 1*, waiting for its second study; after a non-terminal second study, it advances to *Stage 2*, waiting for its third study. A project waits at most $T = 32$ quarters; one that reaches T without a terminal study exits with zero payoff.

Terminal study decision. Upon receiving its terminal study in period t , project i chooses to *complete* or *withdraw* at zero payoff. The net payoff from completing, on a per-megawatt basis, is

$$\pi_{it} = r_{it} - \omega_{it} - c_{it} + \xi_{it} \tag{1}$$

$$= \tilde{r}_{it} + \chi_t(x_i)\theta - \omega_{it} - c_{it} + \xi_i^{S1} + \xi_i^{S2} \tag{2}$$

where r_{it} is the present value of expected operating profit, ω_{it} is the expected cost of construction, and c_{it} is the interconnection cost in the terminal study. We decompose r_{it} into \tilde{r}_{it} , the present value of revenue from power production for the next 25 years discounted at 5% (Appendix B), and $\chi_t(x_i)\theta$, which captures other contributions to profit through a vector $\chi_t(x_i)$ that varies with project characteristics x_i and completion time t , e.g., operating costs, technology-specific subsidies, and capacity market revenues. This decomposition lets revenues from power production \tilde{r}_{it} respond endogenously to capacity changes in our counterfactual simulations. The term $\xi_{it} = \xi_i^{S1} + \xi_i^{S2}$ captures payoff information unobserved to the researcher, which a project observes from studies 1 and 2. Section 2.2 details the additional information provided in studies.¹⁵

The project also learns a final payoff shock ξ_{it}^f at the terminal study and completes if $\pi_{it} + \xi_{it}^f > 0$. We assume ξ_{it}^f is normally distributed with mean 0 and standard deviation $(t - e_i)^\kappa \cdot \sigma$, which varies with the waiting time $t - e_i$, where e_i is the project's time of entry. The dependence accommodates larger payoff dispersion among projects that have waited longer. Integrating over ξ_{it}^f , the expected completion value given the interconnection cost c is

$$\bar{V}_{it}(c, \xi_{it}) = E_{\xi_{it}^f} \left[\max\{\pi_{it} + \xi_{it}^f, 0\} \right]. \quad (3)$$

Stage-2 continuation. After receiving a non-terminal second study, project i decides each period to stay or withdraw. The project's state consists of the current time t , the study 2 cost c , study information z , and the accumulated unobserved heterogeneity $\xi = \xi^{S1} + \xi^{S2}$. The variables (c, z, ξ) are specific to each project i , but for notational simplicity, we suppress their i subscript. The continuation value satisfies

$$W_{it}^{S2}(c, z, \xi) = \max \left\{ 0, -\gamma^{S2} + \beta \delta_i^{S2} \left[\sum_{c'} q_i^{S2}(c'|t, c, z) \bar{V}_{it}(c', \xi) + (1 - Q_i^{S2}(t, c, z)) W_{i,t+1}^{S2}(c, z, \xi) \right] \right\}, \quad (4)$$

where γ^{S2} is the per-megawatt waiting cost, reflecting the cost of site control and study management,¹⁶ $1 - \delta_i^{S2} = 1 - \delta^{S2}(x_i)$ is the per-period probability of exogenous exit, capturing events outside the queue process such as failed permitting or expired land leases and varying with project characteristics x_i , $q_i^{S2}(c'|t, c, z)$ is the belief that the terminal study arrives with cost c' , $Q_i^{S2} = \sum_{c'} q_i^{S2}(\cdot)$ is the total study-arrival probability, and z consists of two indicators: whether engineering tests have been performed, and whether the project is in a cost-share group, as motivated in Section 2.2.

¹⁵More broadly, ξ^{S1} and ξ^{S2} can be interpreted as capturing payoff-relevant heterogeneity that accumulates over the waiting period.

¹⁶We add each study cost to the waiting cost of the period in which the study is received, with costs based on the PJM manual (PJM, 2023b).

Information Assumptions. A project has perfect foresight over the probabilities $q_i^{(\cdot)}$ and $Q_i^{(\cdot)}$ in each period t . In the equilibrium defined in Section 5.3, the deterministic transitions of queue status imply these probabilities. At the same time, projects do not know the realization of cost c' in the new study or whether a new study will arrive in the next period. We maintain these assumptions in the stage-1 decisions below.

Stage-1 continuation. After receiving a non-terminal first study, project i decides each period to stay or withdraw. The state consists of time t , the study 1 cost c , study information z , and the unobserved heterogeneity ξ^{S1} from stage 1. The second study arrival leads to either Stage 2 or the terminal study decision. The continuation value satisfies

$$\begin{aligned}
W_{it}^{\text{S1}}(c, z, \xi^{\text{S1}}) = \max\left\{0, -\gamma^{\text{S1}} + \beta \delta_i^{\text{S1}} \left[\sum_{c'} q_i^{\text{S1},f}(c'|t, c, z) \bar{V}_{it}(c', \xi^{\text{S1}}) \right. \right. \\
+ \sum_{c', z'} q_i^{\text{S1}}(c', z'|t, c, z) E_{\xi^{\text{S2}}} [W_{it}^{\text{S2}}(c', z', \xi^{\text{S1}} + \xi^{\text{S2}}) | t] \quad (5) \\
\left. \left. + (1 - Q_i^{\text{S1}}(t, c, z)) W_{i,t+1}^{\text{S1}}(c, z, \xi^{\text{S1}}) \right] \right\},
\end{aligned}$$

where γ^{S1} is the per-megawatt waiting cost, $1 - \delta_i^{\text{S1}}$ is the per-period probability of exogenous exit, $q_i^{\text{S1},f}(c'|t, c, z)$ is the probability that a terminal second study arrives with cost c' ; $q_i^{\text{S1}}(c', z'|t, c, z)$ is the probability that a non-terminal second study arrives with updated state (c', z') , and $Q_i^{\text{S1}} = \sum_{c'} q_i^{\text{S1},f}(\cdot) + \sum_{c', z'} q_i^{\text{S1}}(\cdot)$ is the total arrival probability. We assume that ξ^{S2} is normally distributed with mean 0 and standard deviation that also varies with waiting time $\sigma^{\text{S2}} \cdot (t - e_i)^{\kappa^{\text{S2}}}$, and that it is conditionally independent of ξ^{S1} given project characteristics, current interconnection cost, and study information.

Entry. The expected value from entering the queue in period t is

$$\text{EV}_i = E_{\xi^{\text{S1}}, c, z} \left[q_i^f \bar{V}_{i,t+1}(c, \xi^{\text{S1}}) + (1 - q_i^f) W_{i,t+1}^{\text{S1}}(c, z, \xi^{\text{S1}}) \right], \quad (6)$$

where q_i^f is the probability that the first study is terminal, and the integration is over the joint distribution of ξ^{S1}, c, z realized at the first study. The entry value is evaluated at the moment of first-study receipt, abstracting from variation in waiting time up to that point; the variation in first-study arrival is small relative to later studies. We assume that ξ^{S1} is normally distributed with mean 0 and standard deviation σ^{S1} , and that it is conditionally independent of c and z given project characteristics. Project i enters the queue if $\text{EV}_i \geq C_i$, where the entry cost C_i follows a

beta distribution on $[0, \bar{C}]$ with mean $\exp(x_i^{\text{ent}}\gamma)$, where x_i^{ent} is a vector of project characteristics. We discuss the specification of the distribution in more detail in Section 6.3.

5.2 State Transitions and Initial State Distribution

We parameterize the state-transition process that governs how PJM manages the queue using probit and ordered-probit models. These models describe, given a project’s queue status and characteristics, the probability of new study arrival and the joint distribution of cost, study information, and unobserved heterogeneity at each new study. We also specify the distribution of a project’s states after study 1. The details are in Appendix D.

5.3 Equilibrium

We assume that in each period t , an exogenous mass of projects $N_t(x)$ decide whether to enter the queue. A portion of the mass enters the queue based on the entry decisions consistent with (6), and the mass gradually decreases because of endogenous withdrawals, exogenous exits, and completions.

Queue status. Each project’s state-transition probabilities depend on a queue-status vector $\mathcal{K}_t(e, x)$, where e is the project’s entry quarter and x collects its time-invariant characteristics including fuel type, capacity, and TO location. In the empirical model, $\mathcal{K}_t(e, x)$ consists of four components: (1) the number of queued projects with weakly higher priority, i.e., those that entered in quarter $\tilde{e} \leq e$, which determines the project’s position in the PJM-wide queue; (2) the number of such higher-priority projects located in the same TO; (3) the total capacity of queued projects in the same TO; and (4) the accumulated completed capacity of each fuel type up to period t . The first two components affect study-arrival rates, the third affects the distribution of interconnection costs through the likelihood of cost-share group assignment (Section 4.2), and the fourth affects the present value of revenue through wholesale electricity prices. Projects take the path of $\mathcal{K}_t(e, x)$ as given when solving their decision problems.

Equilibrium definition. We define a queuing equilibrium as a path of queue statuses $\{\mathcal{K}_t(e, x)\}_{t,e,x}$, together with entry probabilities and project strategies, satisfying three conditions: (i) project entry, waiting, and completion strategies are optimal given beliefs, as defined in Section 5.1; (ii) project beliefs about study-arrival probabilities and the distribution of costs and study information are consistent with those implied by the queue statuses and the prior study’s information (Section 5.2);

and (iii) the path of queue statuses is generated by the entry, exit, and completion decisions of projects.

In the last condition, we model projects as a continuum of masses, and the project entry, withdrawal and completion decisions move their masses deterministically. These masses in turn imply the path of \mathcal{K}_t that projects take as given. The equilibrium is therefore a fixed point where the queue status is consistent with the individual decisions it induces. In Appendix A, we formalize this definition, characterize the optimal strategies as cutoff rules, and prove equilibrium existence.

In this appendix, we also provide conditions under which endogenous withdrawals occur immediately after projects receive a study. Furthermore, projects do not endogenously withdraw between studies, and only exogenous exits occur with probability $1 - \delta^s$ in these intervening periods. This behavior is consistent with Section 3.6, where we document that the withdrawals cluster in a short period after a study arrives. This characterization separates the endogenous withdrawals from exogenous exits and simplifies the estimation of the model.

This equilibrium definition emphasizes the congestion externality, which we find to be quantitatively important in Section 4. Project strategies are, in equilibrium, functions of their beliefs about the queue positions, which reflect queue congestion and affect study arrival, and their beliefs about whether they are in a cost-share group, which affects the next study's costs. However, given the empirically small effect of withdrawals by other projects within a group and the weak correlation between study costs and local queue congestion, we do not model projects tracking the decisions of individual projects.

Relationship to similar equilibrium concepts. This equilibrium concept is a large-market rational-expectations equilibrium for a non-stationary environment. Section 3.3 shows that, even at the TO level, an individual project is small relative to the total capacity of projects from a TO in the queue. The equilibrium concept is related to dynamic industry and search models in which agents know equilibrium aggregate objects but still face idiosyncratic uncertainty. For example, firms in Hopenhayn (1992) know the stationary industry environment but not their future productivity shocks, and workers and firms in search models know market tightness and matching rates but not the date of a match. Relative to Markov-perfect industry dynamics, such as Ericson and Pakes (1995), our projects do not track the full individual state vector of all other projects. Instead, as in oblivious equilibrium (Weintraub, Benkard and Van Roy, 2008) and nonstationary oblivious equilibrium (Weintraub et al., 2010), each projects's strategy conditions on its own state and on

the equilibrium path of industry-wide states.¹⁷

6 Estimation

We estimate the model in three steps. First, we estimate state transition and exogenous exit probabilities directly from the data; these serve as beliefs in the project’s decision problem. Second, taking these beliefs as given, we use simulated maximum likelihood to recover payoffs, waiting costs, and shock distributions from observed withdrawal and completion decisions. Third, we construct a pool of potential entrants, compute their model-implied entry values, and estimate the distribution of entry costs from observed entry decisions. Our estimation sample is projects entering the queue from 2012–2020, with pre-2012 entrants’ actions held fixed; the 2012 start avoids the entry spike from a temporary federal program (Section 3). We use project actions through the second quarter of 2023,¹⁸ before PJM began transitioning from serial to cluster studies.

6.1 Estimation of Transition and Exogenous Exit Probabilities

We estimate the study arrival process using a hazard model with a probit link. Identification, discussed in Section 4.1, comes from the structure of PJM’s process, where priority for studies is based only on entry date.

We similarly estimate the cost and study-information transitions. We use an ordered probit for the cost transition across the four cost bins and probit models for changes in the two binary indicators in z . The identifying assumption is that the error terms in these models are independent of the regressors in the estimation sample. This assumption could fail in two ways. First, PJM’s process might respond to factors not in our specification that correlate with these regressors, such as detailed network characteristics. Our specification includes whether a project is in a cost-share group, the only network characteristic for which we find predictable effects on cost (Section 4.2). Second, developers might selectively withdraw based on private information about future cost changes, biasing the survivor sample. Both empirical and anecdotal evidence suggest these cost changes are

¹⁷A feature of our model is that agents correctly anticipate the non-stationary changes in equilibrium objects that affect payoffs and state-transition probabilities. In particular, we assume that projects have rational expectations over both technology costs, i.e., the time variation in ω , and interconnection-queue congestion. This assumption is reasonable in our empirical context. The anticipation of falling renewable costs is consistent with contemporaneous policy and industry forecasts, such as the DOE’s 2012 SunShot scenario and IRENA’s 2016 cost-reduction projections (DOE, 2012; International Renewable Energy Agency, 2016). At the same time, projects also understood that increasing renewable development would congest the queue and slow queue processing, as described in AWEA’s petition to FERC and in FERC’s subsequent interconnection-reform Notice of Proposed Rulemaking (NOPR) (AWEA, 2015; FERC, 2016).

¹⁸We supplement the data with the completion decisions observed until the third quarter of 2024 for those who had received a terminal study in 2023.

difficult to predict (Section 3.5). We further assume independence across transition components.¹⁹ Full estimates are in Appendix D. We find that completed engineering tests are associated with slower study arrival, which captures the idea that PJM selectively applies the tests to projects more likely to affect transmission, warranting more detailed studies. Being in a cost-share group is associated with a lower cost in the next study, consistent with the findings in Section 4.2.

For the distribution of first-study states (c, z) , we take a nonparametric approach. We group projects by observable characteristics, estimate the within-group marginals of c and z , and combine them, assuming that c and z are independent (see Appendix D.4 for details).

Because endogenous withdrawals occur immediately after a study (Section 5.3), we treat all between-period withdrawals as exogenous and estimate the probability of withdrawal using a hazard model with a probit link. These exits are a minority of withdrawals, under 10% before the second study and under 30% before the third. Because they are distributed fairly evenly over the wait window (Section 3.6), we model the per-period exit probability as constant within a stage, predicting it from project characteristics—fuel type, an indicator for expansion of existing plant, and the log of capacity—and an indicator for study stage. This specification predicts average per-period exogenous exit probabilities of 0.029 with little difference between the two stages; details are in Appendix D.6.

6.2 Project Payoffs and Waiting Costs

Payoff inputs. Estimation takes the revenue from power production \tilde{r}_{it} and construction cost ω_{it} as known inputs to the project’s payoff. We construct \tilde{r}_{it} from observed PJM wholesale electricity prices over the sample period, summed over a 25-year operating horizon and discounted at 5% (Appendix B). For ω_{it} , we use EIA installation costs adjusted for relevant tax credits and subsidies, multiplying by 0.65 for solar (investment tax credit) and 0.55 for storage (Appendix Table E.11). In counterfactual simulations, \tilde{r}_{it} is recomputed under each candidate equilibrium by reconstructing the supply curve with the updated capacity mix.

6.2.1 Identification

Taking the transition probabilities, present value of operational revenues \tilde{r}_{it} , and construction cost ω_{it} as given, we use the projects’ withdrawal and completion decisions to identify the following parameters: (1) the payoff parameter θ ; (2) the standard deviations of the unobserved heterogeneity ξ_i^{S1} , ξ_i^{S2} , and ξ_i^f ; and (3) the waiting cost γ^{S1} and γ^{S2} .

¹⁹We also estimated an alternative specification in which the normal shocks in the study arrival probit model are correlated with those in the ordered probit model for costs; the correlation is small (−0.17) and not statistically significant.

First, we formally prove the nonparametric identification of (1)–(3) in Appendix C. The proof proceeds backwards from the terminal study. At that point, projects that have reached study 3 are selected: they previously chose to remain in the queue, and their continuation values may be correlated with earlier study costs. The identifying variation is therefore not the level of the study-3 cost in isolation. Rather, conditional on the state at study 2 and the elapsed waiting time, the realized study-3 cost provides exogenous variation in the completion probability,²⁰ conditional on the information available at the prior decision node.

The proof in the appendix shows how the study 3 interconnection cost traces out the distribution of ξ^f . The key step compares two derivatives: the derivative of the probability of withdrawing immediately after study 2 with respect to the study-2 cost, and the derivative of the joint probability of continuing after study 2, receiving a study-3 cost, and withdrawing at study 3 with respect to the same study-2 cost. Taking their ratio nets out the density of $\xi^{S1} + \xi^{S2}$ and leaves the CDF of the terminal shock ξ^f . The same ratio-of-derivatives argument then identifies the distributions of ξ^{S2} and ξ^{S1} . Given these distributions, the payoff parameters and waiting costs are identified from the waiting and withdrawal probabilities conditional on interconnection costs.²¹ Because the waiting costs are identified from withdrawal behavior, they measure the full per-period opportunity cost of remaining an active project, not only out-of-pocket spending.

6.2.2 Estimation

Given the estimates of transition and exogenous exit probabilities in Section 6.1, we use simulated maximum likelihood to estimate the payoff parameters, the scale parameters in the parametric distributions of the shocks, and the waiting costs. For the latent $(\xi_{it}^{S1}, \xi_{it}^{S2})$ in each project’s state space, we discretize the support of unobserved heterogeneity to a 30-point grid.²² We then solve the project’s optimal decision problem for each combination of a grid value and observed characteristics,

²⁰Some projects may expect a high study-2 cost to be revised downward, but those beliefs are still conditional on the information available from studies 1 and 2. The realized change in the interconnection costs of study 3 is still conditionally independent of the selection on ξ s given the information from prior studies.

²¹Another potential source of heterogeneity is waiting costs. We find that it is not possible to separately identify unobserved heterogeneities in both waiting costs and the payoff heterogeneities whose variances change over time. For example, a researcher may observe that projects that wait more are more likely to advance to the next study and more likely to complete. This data pattern can be rationalized with waiting cost heterogeneity and ξ^f whose variance increases in waiting time. Yet, the same data pattern can also be rationalized with just the payoff heterogeneities $\xi^{S1}, \xi^{S2}, \xi^f$.

²²In the dynamic program, beliefs about future latent values are represented as probability distributions over these grid points. For a project after a non-terminal study 1, the belief is over $\xi^{S1} + \xi^{S2}$. Thus, when a project has not yet received a later study realization, its continuation value integrates over the possible future realizations by summing the value function over the grid, weighted by the corresponding probabilities. The grid spans $[-10, 10]$, which is wide relative to the sum of estimated scales of $\xi^{S1} + \xi^{S2}$ in Table 6 even when waiting time is long. The large support makes the approximation insensitive to boundary points in practice.

allowing beliefs about state transitions and payoffs to vary across these combinations. For each observed project that enters the queue, we integrate over the unobserved heterogeneity to compute the likelihood of its observed waiting and completion decisions. In the baseline specification, we set $\xi_i^{S2} = 0$ for projects receiving a terminal first study; an alternative specification allowing ξ_i^{S2} to realize in this case has a small impact on the results.

Table 6 reports the simulated maximum likelihood estimates. All units are in million dollars per megawatt. In panel A, we find that project payoffs vary systematically with technology and size. The omitted group is new natural gas generation. In the payoff function, we include the present value of wholesale revenue over the service life for all fuel types except batteries, whose operation involves buying and selling power. We also include construction costs. Therefore, the fuel-type specific coefficients should be interpreted as the payoff of a fuel type relative to gas after netting out these two components. We estimate higher payoffs for solar and battery, which is not surprising given gas projects' higher marginal costs of production.²³ We also estimate higher payoffs for expansions of existing plants, which, in our sample, are all gas interconnection requests that require a lower construction cost than new gas plants. Larger projects are also more profitable, especially among renewable projects.

Panel B shows substantial waiting costs: \$3,400/MW per quarter while a project waits for the second study and \$1,400/MW per quarter while it waits for the third. We interpret these as the carrying cost of keeping a project active and on schedule. The equivalent annual cost while waiting for the third study, \$5,600/MW per year, is consistent with a project holding its position: maintaining site control and a minimal development team.²⁴ The higher cost while waiting for the second study, \$13,600/MW per year, is consistent with the spending of a project in active development, when developers advance permitting, engineering, and the agreements required for the next study; an itemized estimate of development spending for a utility-scale solar project in PJM implies roughly \$8,000/MW per year excluding posted security and study deposits (Leyline Renewable Capital, 2022), with the financing cost of posted security (\$110,000/MW in the same itemization) adding \$5,500–\$8,800/MW per year at costs of capital between 5 and 8%.

Panel C shows that unobserved payoff heterogeneity is substantial and that its dispersion grows the longer a project waits. A one-standard deviation of ξ^{S1} is \$1.39 million/MW, similar to the

²³We set batteries' present value of wholesale revenues (\tilde{r}_{it}) to 0. Therefore, the coefficients for wind and solar capture additional profit relative to gas after accounting for both the wholesale revenues and construction costs, but the battery coefficient captures battery profit relative to gas, after accounting for only the construction cost.

²⁴Developers typically hold land under option during development, converting to a lease once the project proceeds; industry estimates of development-period site-control spending for a utility-scale solar project in PJM are roughly \$4,000/MW per year (Leyline Renewable Capital, 2022).

construction cost of a new project. The estimates on the scales of the shocks and their rate of increase in waiting time are both precisely estimated. The standard deviation of the heterogeneity after the second study is smaller than that after the first study for projects that have waited less than 2 years (8 quarters).

6.3 Entry Costs

Next, we construct a set of potential entrants and estimate the entry costs. For potential entrants, we group observed projects by their fuel types, sizes, whether they expand existing plant, time of entry and their locations, and we then sample, with replacement, from each group of observed projects. We provide details in Appendix D.5. Sampling based on observed characteristics does not introduce selection issues in our model, because entrants are ex-ante identical up to the observed characteristics. Their unobserved heterogeneity realizes after entry.

To ensure that the equilibrium simulation remains tractable, we include 514 non-entrants in the sample, which implies an average entry probability of 85%.²⁵

Identification. To identify entry costs, we compute the entry value in Equation (6) for both observed entrants and potential entrants that do not enter the queue, using the payoff parameters and continuation values identified above. Entry costs are identified from the response of entry decisions to variation in these entry values. The key source of variation is the decline in renewable construction costs ω over time (Equation (2)), which raises the value of entering the queue. The resulting variation in the entry value, which increases over time, appears in the equilibrium, because a project that enters early would also receive studies early, and it may be forced to complete before lower construction costs are realized. Early potential projects therefore would still have less incentive to enter than later entrants. As a result, the increase in renewable entry relative to the increase in the corresponding equilibrium entry values identifies the distribution of entry costs.

Estimates. Table 7 reports the estimated entry costs based on maximum likelihood. We assume that the entry cost C is supported on $[0, \bar{C}]$, and C/\bar{C} has a beta distribution (with support on the unit interval) with a mean of $\exp(x^{\text{ent}}\gamma)$, where x^{ent} is the vector of project characteristics reported in the table. The implied distribution is $\text{Beta}(\exp(x^{\text{ent}}\gamma)/\bar{C}\psi, (1 - \exp(x^{\text{ent}}\gamma)/\bar{C})\psi)$, determined by the mean $\exp(x^{\text{ent}}\gamma)$ and another free parameter ψ . The corresponding variance of the distribution is $\frac{\exp(x^{\text{ent}}\gamma)(\bar{C} - \exp(x^{\text{ent}}\gamma))}{\psi + 1}$. We choose \bar{C} to be \$1.2 million/MW, higher than the maximum entry

²⁵Doubling the number of non-entrants does not change our counterfactual results.

value \$1.03 million/MW implied by the previous model estimates.

The estimates show that the renewables and capacity increase at an existing plant have lower costs, but capacity's effect is not distinguishable from 0. These patterns are consistent with entry costs being driven mainly by site-control requirements. Renewable projects may face lower site-control costs because developers often secure land through leases or options, allowing farmers to continue using the land during the option or development period before construction. Expansion of existing plants is also less costly because they expand existing facilities rather than require new site development. Entry costs are nearly 0 at the median, and low up to the 85th percentile (\$0.27 million/MW) relative to a median entry value of \$0.37 million/MW (\$0.35 million/MW for renewables), consistent with queue entry not requiring physical construction.

Table 6: Structural Estimates

<i>Panel A. Payoff Estimates</i>	
Wind	-0.087* (0.048)
Solar	0.476*** (0.014)
Battery	1.030*** (0.033)
Capacity increase at existing plant	0.827*** (0.033)
Renewables \times ln(size)	0.198*** (0.011)
ln(size)	0.070*** (0.012)
After 2018	-0.198*** (0.025)
Renewables \times after 2018	0.360*** (0.030)
Intercept	-1.960*** (0.041)
<i>Panel B. Waiting Costs</i>	
Waiting for third study	-0.002*** (0.000)
Intercept	0.003*** (0.000)
<i>Panel C. Unobservables: Baseline Scale σ and Waiting Time Effect κs</i>	
Study 1: σ^{S1}	1.390*** (0.050)
Study 2: σ^{S2}	0.553*** (0.013)
Study 2: κ^{S2}	0.363*** (0.013)
Terminal Study: κ	0.221*** (0.006)
Terminal Study: σ	0.618*** (0.009)

Parameters in panels (A)–(C) are in units of \$ million per MW. The κ parameters are unitless. Standard errors in parentheses. * $p < 0.1$, ** $p < 0.05$, *** $p < 0.01$.

Table 7: Entry Cost Distribution Estimates

<i>Panel A. Entry Cost Distribution Parameters</i>	
Renewables	-0.227** (0.106)
Capacity increase at existing plant	-0.660*** (0.196)
ln(size)	0.054 (0.034)
Intercept	-1.965*** (0.245)
ψ	0.575** (0.236)
<i>Panel B. Implied Entry Cost Quantiles (\$M/MW)</i>	
50th percentile	<0.001
75th percentile	0.039
80th percentile	0.108
85th percentile	0.270
90th percentile	0.580
95th percentile	0.985

The entry cost distribution is estimated as a beta distribution on $[0, \bar{C}]$. Let $\mu_i = \exp(x_i^{ent}\gamma)$ and let ψ denote the precision parameter. Then $C_i/\bar{C} \sim \text{Beta}(\alpha_i, \beta_i)$ with $\alpha_i = (\mu_i/\bar{C})\psi$ and $\beta_i = (1 - \mu_i/\bar{C})\psi$. Quantile rows report the implied quantiles of the entry cost distribution in \$M/MW, based on the estimated mixture over observed entry covariates. Standard errors are in parentheses. * $p < 0.1$, ** $p < 0.05$, *** $p < 0.01$.

7 Simulations

We apply the estimated project preferences in the equilibrium model defined in Section 5.3. We first show that the model fits the data well. We then evaluate two reforms: speeding up engineering studies and raising the cost of entering or remaining in the queue. The counterfactuals allow for equilibrium responses in entry, waiting, completion and wholesale prices.

7.1 Equilibrium Simulation

To simulate the equilibrium, we start from the observed queue and iteratively update project strategies, queue statuses, project beliefs, and wholesale prices until convergence.²⁶ We use this procedure for the model-fit analysis below and for all counterfactual simulations.

We assume that, in the no policy (as-is) equilibrium, projects expect the wholesale prices after 2020 to stay at a constant level of \$32.9/MWh, which is the price in the last quarter of 2020. This assumption reflects the relatively stable prices in PJM over the past decade, but ignores the surge in demand and high prices in later years driven by unexpected events such as demand from data centers and growth of AI. We think this is a reasonable assumption, because the projects entering

²⁶We cannot rule out the presence of multiple equilibria, but starting from queue statuses perturbed around the observed values yields highly similar equilibrium outcomes.

in 2020 and earlier would not have predicted these events.

Wholesale prices adjust endogenously in the counterfactuals. The stable price assumption above implies demand growth, because more projects complete over time and add to PJM supply. We therefore compute the implied demand for 2021-2028 that is consistent with the stable price assumption in the as-is equilibrium, where 2028 corresponds with the last quarter of action by projects who entered in 2020 and wait a maximum of 32 quarters. In policy counterfactuals where we change the queuing environment, we use observed demand from 2012-2020 (Appendix B) and the implied demand from 2021-2028 calculated from the as-is equilibrium as well as the counterfactual completions to re-compute the wholesale prices. These prices would then change the wholesale revenues of projects' payoff functions. The new equilibrium is achieved when project strategies, queue statuses, the wholesale prices (and the implied project revenues), and project beliefs are consistent with each other. We assume that wholesale prices after 2028 will stay constant at the 2028 equilibrium level.

7.2 Model Fit

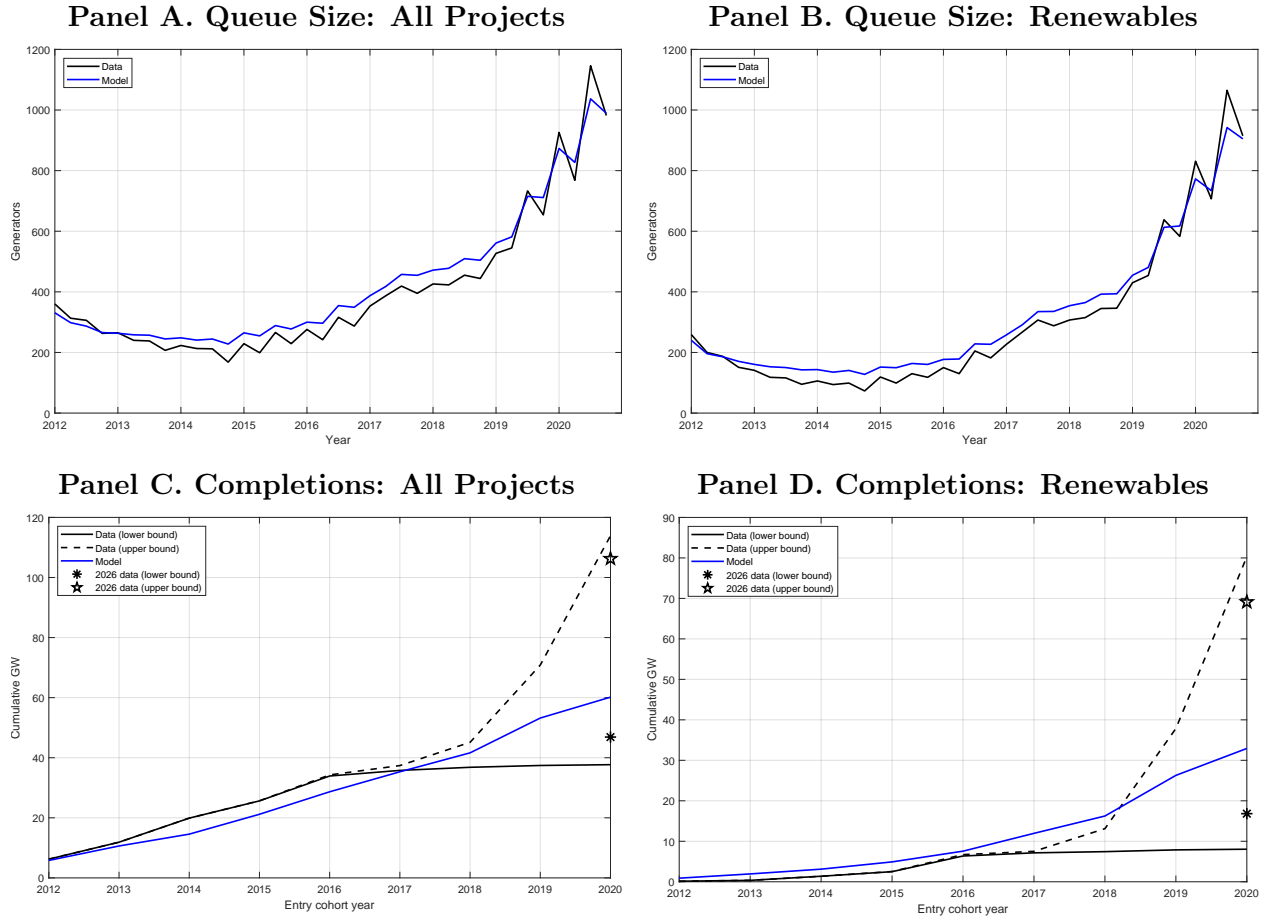
The model fits the data well in the estimation sample (Figure 5). Panels A and B plot predicted and observed queue sizes, which are the numbers of waiting projects at a given time, for all projects and renewables; both predictions track the data closely, slightly under-predicting congestion at the end of the sample. Panels C and D plot cumulative eventual completion by entry time, defined as the sum of eventually completed capacity by projects entering in or before a given quarter. The blue line is the model's prediction; the solid black line shows capacity completed by 2023 (a lower bound on eventual completion), and the dotted black line above it adds capacity still waiting in 2023 (an upper bound). The model prediction is close to the data in early years and stays within the bounds in later years, for both total and renewable capacity. Our model predicts that about 60 GW will eventually be in service in PJM from those entering between 2012 and 2020.

The model prediction is also consistent with the completions observed after the estimation sample. We collected 2026 data on the 2012-2020 entry cohorts; by then, more projects had received terminal studies, and more had completed. Our prediction falls within the implied tighter bounds (indicated by stars).

7.3 Study Speedup

We next consider counterfactuals with accelerated study arrivals. Specifically, we uniformly scale up each component of study arrival probabilities, Q_i^{S1} and Q_i^{S2} in Equations (5) and (4), by 10, 20 and 50%, subject to the constraint that each probability is capped at one. Table 8 reports levels

Figure 5: Model Fit: Queue Size and Completions



Panels A–B plot queue counts by calendar quarter (2012–2020) for all projects and renewable projects, respectively. Panels C–D plot cumulative eventual completed capacity by entry quarter. The solid black line is observed completed capacity by end of sample; the dotted line adds projects still unresolved at the cutoff; the dashed blue line is model-predicted eventual completions. The solid star shows observed completions of those entering between 2012 and 2020 as of 2026; the hollow star adds projects still in queue as of 2026.

under the as-is equilibrium and changes under each speedup for completion, waiting time, entry, entry surplus, and the long-run wholesale price.

Speedup substantially increases completed capacity. A 50% speedup increases total completion by 31%. This speedup also reduces waiting time, measured from entry to withdrawal or completion, by 20%.²⁷ Furthermore, entry surplus, defined as the sum of $E \max\{EV_i - C_i, 0\}$ across all potential projects, increases steadily, though less than proportionally at the largest speedup. The long-run wholesale electricity price decreases by 6.4% as a result. These surplus figures cover only queue entrants. The lower wholesale price also benefits consumers, though with inelastic demand this is largely a transfer from incumbent generators rather than an additional welfare gain.

Table 8: Study-Speedup Counterfactuals

	(1)	(2)	(3)	(4)	(5)	(6)	(7)
	As-is	10%		20%		50%	
		Level	Δ	Level	Δ	Level	Δ
Completed (GW)	60.2	64.8	+4.6	69.1	+8.9	78.6	+18.4
Renewable	32.9	36.0	+3.1	39.1	+6.1	46.0	+13.1
Non-renewable	27.2	28.8	+1.5	30.0	+2.8	32.6	+5.3
Time in queue (quarters)	10.0	9.5	-0.4	9.1	-0.8	8.0	-2.0
Renewable	11.0	10.6	-0.4	10.2	-0.9	8.9	-2.1
Non-renewable	6.5	6.2	-0.3	5.9	-0.6	5.0	-1.5
Entry (GW)	263.5	264.8	+1.3	265.9	+2.3	267.8	+4.2
Renewable	151.4	152.2	+0.9	153.0	+1.6	154.3	+3.0
Non-renewable	112.2	112.6	+0.4	112.9	+0.7	113.4	+1.3
Entry surplus (\$Bn)	75.2	79.6	+4.4	83.5	+8.2	90.8	+15.6
Renewable	44.5	47.7	+3.2	50.7	+6.2	56.5	+12.0
Non-renewable	30.8	31.9	+1.2	32.8	+2.0	34.3	+3.5
Wholesale price (\$/MWh)							
Long run	32.9	32.4	-0.4	31.9	-1.0	30.7	-2.1

Entries and completions are in GW. Time in queue is in quarters. Surplus rows are entry surplus defined as $E \max\{EV_i - C_i\}$ in \$Bn. Long run price indicates the predicted 2028 price. We compute the implied demand in 2021-2028 that would justify a wholesale price of \$32.9/MWh. The Long run price is the 2028 equilibrium price given the observed demand from 2012-2020 and the calculated demand from 2021-2028.

Option Value of Waiting. The increased completed capacity comes almost entirely from higher completion among projects that choose to enter the queue, rather than from increased entry into the queue. The change in entry is a result of two countervailing forces. On the one hand, given

²⁷The reduction in waiting time is proportionally lower than the increase in study arrival probabilities for several reasons. First, our waiting-time measure includes both withdrawals and completions. Speedup increases the incentive to wait in the queue, which can lengthen waiting time for projects that eventually withdraw. Second, about 15% of projects receive a terminal first study and therefore are not affected by post-entry speedups in later study stages.

that the standard deviations of ξ^{S2} and ξ^f increase with waiting time, a faster queue reduces the option value of remaining in the queue. On the other hand, faster study arrivals reduce accumulated waiting costs, discounting, and exposure to exogenous exits, thereby increasing the value of entering the queue.

Columns (1)-(5) of Table 9 decompose these channels, using 50% speedup as an example. Columns (1)-(3) report the effects under the as-is equilibrium and under the 50% speedup. In Columns (4) and (5), we isolate the option-value channel. We hold the as-is equilibrium queue statuses fixed, but reduce the standard deviations of ξ^{S2} and ξ^f to reflect the shorter waiting time induced by the 50% speedup. Specifically, for each waiting time τ , we replace the standard deviation of ξ^f , $\tau^\kappa \sigma$, with $(\max\{0, \tau - \Delta t\})^\kappa \sigma$, where $\Delta t = 2.0$ quarters is the average reduction in waiting time under the speedup. We also do the same for ξ^{S2} . We then allow projects to re-optimize once given these smaller standard deviations. Column (4) reports the resulting levels, and column (5) reports the changes relative to the as-is equilibrium.

The results show that the reduction in the option value would lower completion, entry and surpluses. Projects also withdraw faster, leading to a slight reduction in waiting time.²⁸ This decomposition provides an additional explanation, beyond entry costs, for why the entry response to a 50% speedup is smaller than the completion response. The reduction in option value would decrease total entry by 2.1 GW. However, the increase in entry value from lower waiting costs and avoided exogenous exits under faster study arrivals is three times as large, implying that the offsetting increase in entry value increases entry by 6.3 GW. The net effect is therefore a smaller increase in entry of 4.2 GW.

Effects of Dynamic Strategies. In columns (6)-(7) of Table 9, we illustrate the importance of accounting for adjustment in equilibrium beliefs and strategies. In this decomposition, we hold project strategies fixed as in the as-is equilibrium, increase the study arrival probability, and simulate new queue statuses starting from the as-is equilibrium queue. We then compute completion, waiting time, and the entry surplus under the higher study arrival probability and the updated equilibrium queue statuses, while keeping project strategies fixed. Column (6) reports the resulting levels, and column (7) reports the changes relative to the as-is equilibrium. Comparing these changes with the full 50% speedup counterfactual shows how much of the policy effect is missed when we do not account for projects adjusting their strategies.

At the 50% speedup, ignoring the equilibrium strategy adjustments understates the gains in total

²⁸Note that we are holding the queue status fixed, and this reduction in waiting time is entirely from faster withdrawals.

completion by 21% (14.5 GW rather than 18.4 GW). Because entry is mechanically unchanged, the difference in completions comes entirely from projects waiting more and receiving more terminal studies. The gains in project surpluses are understated by 21%.

Environmental Benefits. The additional renewable capacity under the 50% speedup avoids 15.1 million metric tons of CO₂ annually, worth \$2.8 billion per year at a social cost of carbon of \$185 per metric ton. We compute these benefits using EPA’s Avoided Emissions and geneRation Tool (AVERT v4.3, April 2024), which estimates region-specific marginal displacement rates for emissions avoided when new renewable generation displaces fossil generation. For PJM, AVERT’s capacity factors imply that the counterfactual’s additional 5.03 GW of wind and 6.82 GW of solar generate 13.0 and 13.3 TWh of power per year, respectively; applying AVERT’s 2023 PJM marginal CO₂ displacement rates gives the 15.1 million metric tons.²⁹

Table 9: Decomposition of 50% Speed Up Effects

	(1)	(2)	(3)	(4)	(5)	(6)	(7)
	As-is	50% speedup		Option value		Strategies fixed	
		Level	Δ	Level	Δ	Level	Δ
Completed (GW)	60.2	78.6	+18.4	58.7	-1.5	74.7	+14.5
Renewable	32.9	46.0	+13.1	32.3	-0.6	42.5	+9.6
Non-renewable	27.2	32.6	+5.3	26.3	-0.9	32.1	+4.9
Time in queue (quarters)	10.0	8.0	-2.0	9.8	-0.2	8.5	-1.5
Renewable	11.0	8.9	-2.1	10.9	-0.1	9.5	-1.6
Non-renewable	6.5	5.0	-1.5	6.3	-0.2	5.4	-1.1
Entry (GW)	263.5	267.8	+4.2	261.5	-2.1	263.5	+0.0
Renewable	151.4	154.3	+3.0	150.5	-0.9	151.4	+0.0
Non-renewable	112.2	113.4	+1.3	111.0	-1.2	112.2	+0.0
Entry surplus (\$Bn)	75.2	90.8	+15.6	69.0	-6.2	87.7	+12.4
Renewable	44.5	56.5	+12.0	41.3	-3.1	53.1	+8.6
Non-renewable	30.8	34.3	+3.5	27.6	-3.1	34.6	+3.8

Entries and completions are in GW. Time in queue is in quarters. Surplus rows are entry surplus defined as $E \max\{0, EV_i - C_i\}$ in \$Bn. Δ is the change relative to as-is. The Option value columns take the as-is equilibrium queue statuses and rescale the standard deviations of ξ^f to $\max(0, t - \Delta t)^\kappa$ (and similarly for ξ^{S2}) for each value of waiting time τ , where $\Delta t = 2.0$ quarters is the average reduction in waiting time from the speedup. We then allow the generators to re-optimize once, responding to the as-is equilibrium queue statuses but ξ^{S2} and ξ^f shocks with smaller standard deviations. In Strategies fixed columns, we take both the as-is equilibrium queue statuses as well as the generator strategies, increase the study arrival probability and simulate new queue statuses. The completion, waiting time and the entry surplus are computed given the increased study arrival probability, the new equilibrium queue statuses and the as-is strategies.

²⁹The avoided air pollutants, such as PM2.5, would increase the benefits, while the 5.3 GW increase in gas capacity has an ambiguous effect, since its emissions may be offset by displacing coal-fired generation.

7.4 Imposing Fees to Reduce Congestion

Another key component of the ongoing interconnection queue reforms is the use of fees to raise entry barriers and reduce congestion. We focus on the effects of a per-megawatt entry fee and discuss two alternative forms of fees in Section 7.4.1.

There are three different ways the fee can be assessed: (1) as a nonrefundable fee, which the project pays upon entry and does not recover regardless of its outcome; (2) as a deposit, which is returned only if the project completes interconnection, so projects that withdraw forfeit the deposit; and (3) as a fee that PJM collects from all entrants and redistributes, on a per-megawatt basis, to projects that complete interconnection. We refer to these three designs as the nonrefundable fee, deposit, and fee with budget-neutral rebate designs, respectively. Although the third design may be hard to implement in real time, since the rebate depends on future withdrawals and completions, it provides a useful benchmark for a fee design that fully recycles entrant payments to completers.

We compute new equilibria under fees ranging from \$1,000/MW to \$50,000/MW. At a fee level x , a project receives no rebates under design (1), receives x upon completion under design (2), and receives an amount greater than x in design (3), where the actual amount is determined by the total entering and completed capacity in the equilibrium.³⁰

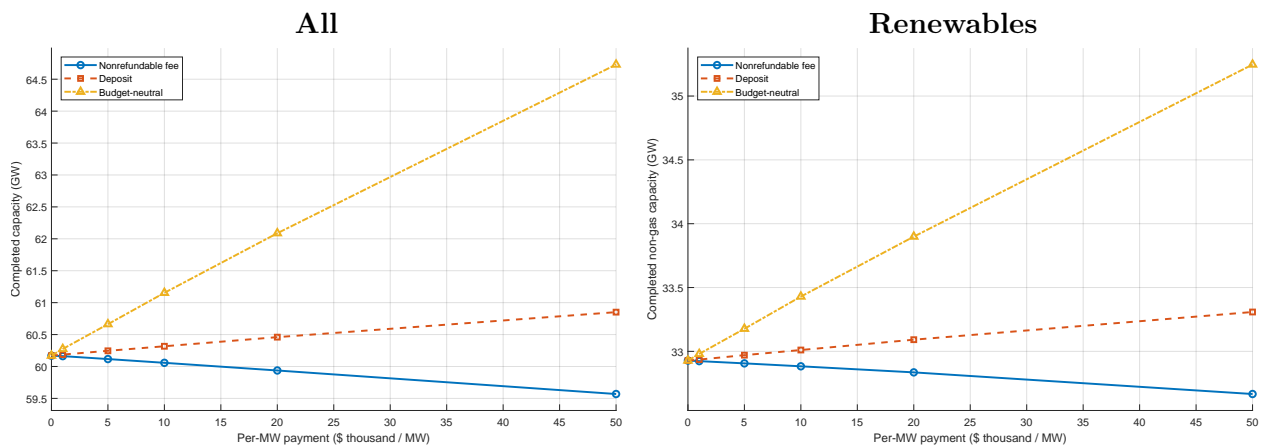


Figure 6: Completed GW vs. Per-MW Entry Fee Level

Each point is an equilibrium simulation. Three series: nonrefundable fee (solid), deposit (dashed), fee with budget-neutral rebate (dotted). The as-is equilibrium is when fees are 0.

Figure 6 plots the impact of fees on completed capacity. We find that, for all projects and renewables specifically, nonrefundable fees reduce completion, deposits increase completion, and the

³⁰More specifically, suppose a total of A megawatts of projects enter the queue in our sample (2012-2020), and the completed capacity is B , then completing projects would receive xA/B per megawatt in the fee with budget-neutral rebate design.

fee with budget-neutral rebate increases the completion six times as much as the deposit design. At the highest fee level of \$50,000/MW, the deposit design increases the total and renewable completion by 1.2%, relative to the levels (60.2 GW and 32.9 GW) in the as-is equilibrium. The budget-neutral design increases the total completion by 7.5% and renewables by 7.0%.

Table 10: Per-MW Entry Fee Counterfactuals: \$20,000/MW

	(1)	(2)	(3)	(4)	(5)	(6)	(7)
	As-is	Nonrefundable Fee		Deposit		Budget-neutral	
		Level	Δ	Level	Δ	Level	Δ
Completed (GW)	60.2	59.9	-0.2	60.5	+0.3	62.1	+1.9
Renewable	32.9	32.8	-0.1	33.1	+0.2	33.9	+1.0
Non-renewable	27.2	27.1	-0.1	27.4	+0.1	28.2	+0.9
Time in queue (quarters)	10.0	10.0	+0.0	10.0	+0.0	10.1	+0.2
Renewable	11.0	11.0	+0.0	11.1	+0.1	11.2	+0.2
Non-renewable	6.5	6.5	-0.0	6.5	+0.0	6.6	+0.1
Entry (GW)	263.5	261.7	-1.9	262.0	-1.6	262.9	-0.6
Renewable	151.4	150.4	-1.0	150.5	-0.8	151.0	-0.4
Non-renewable	112.2	111.3	-0.9	111.4	-0.7	111.9	-0.3
Entry surplus (\$Bn)	75.2	70.1	-5.1	71.1	-4.1	74.2	-1.1
Renewable	44.5	41.5	-2.9	42.1	-2.4	43.8	-0.7
Non-renewable	30.8	28.6	-2.2	29.0	-1.7	30.4	-0.4
Payments collected (\$Bn)		5.2		5.2		5.3	
Renewable		3.0		3.0		3.0	
Non-renewable		2.2		2.2		2.2	
Deposits returned (\$Bn)				1.2		5.3	
Renewable				0.7		2.9	
Non-renewable				0.5		2.4	
Wholesale price (\$/MWh)							
Long run	32.9	32.9	+0.0	32.8	-0.0	32.7	-0.2

Fee level: \$20,000 per MW of nameplate capacity, charged at study entry. Entries and completions are in GW. Time in queue is in quarters. Surplus and fee rows are in \$Bn. Surplus rows are entry surplus defined as $E \max\{0, EV_i - C_i\}$ in \$Bn. Δ is the change relative to as-is. Zero values in the fees section are left blank.

Table 10 reports more detailed results at a fee level of \$20,000/MW, comparable to new fee schedules that PJM is currently considering (PJM Interconnection, 2026). The nonrefundable fee, deposit and the budget-neutral design change the total completion by -0.3%, 0.5% and 3.2%.

We note that none of the fee designs reduces waiting time for entering projects. Under the nonrefundable fee design, this result is mostly driven by the change in the composition of projects in the queue. To see this, we first group projects by fuel types, location, entry time and sizes and plot the change in waiting time within each group after imposing an entry fee of \$20,000/MW. Appendix Figure F.5 shows that for most groups, the average waiting time falls within the group.

Yet, the fees also change the number of entrants in each group, and the average waiting time among entrants is almost unchanged after the fee. As Table F.15 shows, the fees reduce the entry of small projects more, which often need fewer than 3 studies. Their reduced entry increases the proportion of longer-waiting projects in the queue.

In contrast, waiting time under the deposit and budget-neutral designs is more influenced by equilibrium changes of project strategies. Under the deposit design, 41% of projects that enter the queue wait longer, and all projects that enter the queue under the budget-neutral design wait longer, incentivized by the expectation of a completion subsidy in the form of rebated fees.

Taken together, these results suggest that these fees have a modest effect on completion and do not significantly reduce congestion. The key intuition is that the projects that create the most congestion, because they are the most willing to wait, are also those with the highest payoffs and the greatest likelihood of completion, so fees do not deter them. The projects the fees do deter are small and marginal: they exit quickly or need fewer than three studies, so they spend little time ahead of others in the queue, and the queue remains essentially as congested as before. The completion gains under the deposit and budget-neutral designs must therefore operate through the completion subsidy embedded in the rebates rather than through a faster queue.

7.4.1 Flat Fees and Study Fees

One alternative fee is a flat fee at queue entry, with the same dollar amount charged regardless of project size. We find that such a fee would have a more limited, but still positive effect on total completion. Appendix Figure F.6 plots the effects up to 500,000 dollars per project. At this level, total and renewable completion would increase by 0.5% relative to as-is. A flat fee also reduces entry by smaller and renewable projects, as the per-megawatt fee does, but its effects are larger for these groups (Table F.16). Nonrefundable flat fees and deposits have similar effects, because flat fees select on larger projects that are less sensitive to whether a flat fee, which is small on a per-megawatt basis, is charged or rebated.

We also consider higher per-megawatt study fees for projects advancing to the second and third studies. Appendix Figure F.7 shows that these fees slightly increase completion at low levels (\$5,000/MW) but reduce completion at higher levels, regardless of whether they are refundable. The intuition is that study fees are imposed after projects have entered and learned some of their payoff-relevant unobserved heterogeneity. A study fee thus screens continuing projects with high ξ s. In contrast, an entry fee is imposed before the realizations of unobserved heterogeneity and does not select on them.

8 Conclusion

We use novel data from PJM, the largest U.S. regional grid operator, to study the interconnection queue. We find a congestion externality: if a project has more projects ahead of it in the queue, the probability of study arrival in a given quarter falls. We also find that interconnection costs are a key factor in projects' decisions to withdraw from the queue.

We next study policy reforms using a dynamic model that accounts for equilibrium effects. We find that speeding up study delivery can significantly reduce waiting time and increase completion. Projects of all fuel types and sizes benefit, even when entering projects adjust their strategies and wait longer. Speeding up study delivery by 50% adds more renewables to the grid, yielding \$2.8 billion per year in environmental benefits from avoided carbon emissions.

In contrast, imposing fees at levels comparable to current interconnection queue reforms has more limited effects on completion and does not reduce waiting time. This result reflects a positive correlation between a project's payoff and its impact on congestion: the highest-value projects are the most willing to wait and create the most congestion. A potential implication is that screening projects by their value may not relieve queue congestion.

The reforms underway across the U.S. bundle the two instruments we analyze: AI-assisted automation and penalties on transmission providers for delayed studies target study speed, while stricter deposits and readiness milestones screen entry. Our analysis suggests that returns to accelerating studies are large, and that, unlike entry screening, the gains are shared by developers of small and large projects alike.

References

- Agarwal, Nikhil, Itai Ashlagi, Michael A Rees, Paulo Somaini, and Daniel Waldinger.** 2021. "Equilibrium allocations under alternative waitlist designs: Evidence from deceased donor kidneys." *Econometrica*, 89(1): 37–76.
- Alagappan, Lakshmi, Ren Orans, and Chi-Keung Woo.** 2011. "What drives renewable energy development?" *Energy policy*, 39(9): 5099–5104.
- Aldy, Joe, Todd Gerarden, and Richard Sweeney.** 2023. "Investment versus Output Subsidies: Implications of Alternative Incentives for Wind Energy." *Journal of the Association of Environmental and Resource Economists*, 10(4): 981–1018.
- AWEA.** 2015. "Petition for Rulemaking of the American Wind Energy Association to Revise Generator Interconnection Rules and Procedures." *Federal Energy Regulatory Commission, Docket No. RM15-21-000*, States that developers submitted numerous interconnection applications, interconnection queues grew larger, and queue processing became slower.

- AWEA.** 2019. “Wind Powers America Annual Report 2019.” <https://www.awea.org/resources/publications-and-reports/market-reports>.
- Blundell, Wesley, Gautam Gowrisankaran, and Ashley Langer.** 2020. “Escalation of scrutiny: The gains from dynamic enforcement of environmental regulations.” *American Economic Review*, 110(8): 2558–2585.
- Butters, R. Andrew, Jackson Dorsey, and Gautam Gowrisankaran.** 2021. “Soaking up the sun: Battery investment, renewable energy, and market equilibrium.” NBER Working Paper 29133.
- Callaway, Brantly, and Pedro H.C. Sant’Anna.** 2021. “Difference-in-Differences with multiple time periods.” *Journal of Econometrics*, 225(2): 200–230.
- Caspary, Jay, Michael Goggin, Rob Gramlich, and Jesse Schneider.** 2021. “Disconnected: The Need for a New Generator Interconnection Policy.” Americans for a Clean Energy Grid Report.
- Cicala, Steve.** 2022. “Imperfect markets versus imperfect regulation in US electricity generation.” *American Economic Review*, 112(2): 409–441.
- Davis, Lucas, and Catherine Hausman.** 2016. “Market Impacts of a Nuclear Power Plant Closure.” *American Economic Journal: Applied Economics*, 8(2): 92–122.
- Davis, Lucas W., Catherine Hausman, and Nancy L. Rose.** 2023. “Transmission Impossible? Prospects for Decarbonizing the US Grid.” NBER Working Paper 31377.
- Deschenes, Oliver, Christopher Malloy, and Gavin McDonald.** 2023. “Causal effects of Renewable Portfolio Standards on renewable investments and generation: The role of heterogeneity and dynamics.” *Resource and Energy Economics*, 75(101393).
- DOE.** 2012. “SunShot Vision Study: A Comprehensive Analysis of the Potential for U.S. Solar Electricity Generation.” U.S. Department of Energy DOE/GO-102012-3037; NREL/BK-5200-47927. Models a SunShot scenario in which solar technology costs decline by about 75 percent between 2010 and 2020.
- Doshi, Gaurav.** 2026. “Chicken and Egg: Electricity Transmission and Investment in Renewable Energy.” *Journal of Public Economics*, 256(105598).
- Driscoll, William.** 2022. “Interconnection delays and costs are the biggest barrier for utility-scale renewables, say developers.” <https://pv-magazine-usa.com/2022/02/14/interconnection-delays-and-costs-are-the-biggest-barrier-for-utility-scale-renewables-say-dev>
- Elliott, Jonathan T.** 2021. “Investment, Emissions, and Reliability in Electricity Markets.”
- EPA.** 2026. “Electric Power Sector Emissions.” <https://www.epa.gov/ghgemissions/electric-power-sector-emissions>.
- Ericson, Richard, and Ariel Pakes.** 1995. “Markov-perfect industry dynamics: A framework for empirical work.” *The Review of economic studies*, 62(1): 53–82.
- Fell, Harrison, Daniel Kaffine, and Kevin Novan.** 2021. “Emissions, Transmission, and the Environmental Value of Renewable Energy.” *American Economic Journal: Economic Policy*, 13(2): 241–272.

- FERC.** 2016. “Reform of Generator Interconnection Procedures and Agreements: Notice of Proposed Rulemaking.” *157 FERC ¶ 61,212, Docket No. RM17-8-000*, Proposes reforms to improve certainty and transparency and to reduce withdrawals, restudies, delays, and multiple interconnection requests.
- FERC.** 2023. “Docket No. RM22-14-000; Order No. 2023: Improvements to Generator Interconnection Procedures and Agreements.” <https://www.ferc.gov/media/e-1-order-2023-rm22-14-000>.
- Fowle, Meredith, Mar Reguant, and Stephen P Ryan.** 2016. “Market-based emissions regulation and industry dynamics.” *Journal of Political Economy*, 124(1): 249–302.
- Gergen, Michael J, George D Cannon Jr, and Shannon D Torgerson.** 2008. “A modest proposal: A market-based approach to generation interconnection process reform.” *The Electricity Journal*, 21(9): 8–18.
- Gonzales, Luis E., Koichiro Ito, and Mar Reguant.** 2023. “The Investment Effects of Market Integration: Evidence from Renewable Energy Expansion in Chile.” *Econometrica*, 91(5): 1659–1693.
- Gorman, Will, Julie Mulvaney Kemp, Joseph Rand, Joachim Seel, Ryan Wisser, Nick Manderlink, Fredrich Kahrl, Kevin Porter, and Will Cotton.** 2024. “Grid connection barriers to renewable energy deployment in the United States.” *Joule*.
- Gowrisankaran, Gautam, Ashley Langer, and Wendan Zhang.** 2022. “Policy Uncertainty in the Market for Coal Electricity: The Case of Air Toxics Standards.” NBER Working Paper 30297.
- Gowrisankaran, Gautam, Stanley S Reynolds, and Mario Samano.** 2016. “Intermittency and the value of renewable energy.” *Journal of Political Economy*, 124(4): 1187–1234.
- Hale, Zach.** 2021. “Solar developer adds to pile of complaints targeting PJM study delays.”
- Hale, Zach, and Molly Christian.** 2023. “FERC approves ‘historic’ rule to clear backlog of US generation projects.”
- Hausman, Catherine.** 2025. “Power flows: transmission lines, allocative efficiency, and corporate profits.” *American Economic Review*, 115(8): 2574–2615.
- Hitaj, Claudia.** 2013. “Wind power development in the United States.” *Journal of Environmental Economics and Management*, 65: 394–410.
- Hopenhayn, Hugo A.** 1992. “Entry, exit, and firm dynamics in long run equilibrium.” *Econometrica: Journal of the Econometric Society*, 1127–1150.
- Huitfeldt, Ingrid, Victoria Marone, and Daniel C Waldinger.** 2024. “Designing dynamic reassignment mechanisms: Evidence from GP allocation.” National Bureau of Economic Research.
- IEA.** 2025. “CO2 Emissions – Global Energy Review 2025 – Analysis.” <https://www.iea.org/reports/global-energy-review-2025/co2-emissions>.
- IEA.** 2026. “Electricity 2026.” <https://www.iea.org/reports/electricity-2026>.

- Igami, Mitsuru.** 2017. “Estimating the innovator’s dilemma: Structural analysis of creative destruction in the hard disk drive industry, 1981–1998.” *Journal of Political Economy*, 125(3): 798–847.
- International Renewable Energy Agency.** 2016. “The Power to Change: Solar and Wind Cost Reduction Potential to 2025.” International Renewable Energy Agency, Abu Dhabi. Projects 2015–2025 LCOE reductions of 26 percent for onshore wind, 35 percent for offshore wind, at least 37 percent for CSP, and 59 percent for solar PV.
- Johnston, Sarah.** 2019. “Nonrefundable Tax Credits versus Grants: The Impact of Subsidy Form on the Effectiveness of Subsidies for Renewable Energy.” *Journal of the Association of Environmental and Resource Economists*, 6(3): 433–460.
- Johnston, Sarah, Yifei Liu, and Chenyu Yang.** 2025. “Grid connection costs as a barrier to new generation: Evidence from PJM and implications for transmission policy.”
- LaRiviere, Jacob, and Xueying Lyu.** 2022. “Transmission constraints, intermittent renewables and welfare.” *Journal of Environmental Economics and Management*, 112(102618).
- Leisten, Matthew, and Nicholas Vreugdenhil.** 2023. “Dynamic Regulation with Firm Linkages: Evidence from Texas.” Working Paper.
- Leyline Renewable Capital.** 2022. “The Growing Impact of Delays on Solar Development Costs across Different Regions.” <https://www.leylinecapital.com/news/the-growing-impact-of-delays-on-solar-development-costs-across-different-regions>, Reports an itemized development-cost estimate for a 100 MW utility-scale solar project in PJM over a 25-month timeline, including \$804,900 of site-control costs and \$11 million of posted upgrade security. Accessed June 10, 2026.
- Liu, Tracy, Zhixi Wan, and Chenyu Yang.** 2024. “Dynamic matching on a commuter carpooling platform.” Working Paper.
- Liu, Yifei.** 2025. “Permitting, Litigation Risk, and Energy Infrastructure Investment.”
- Metcalf, Gilbert.** 2010. “Investment in energy infrastructure and the tax code.” In *Tax policy and the economy, Vol. 24.*, ed. Jeffrey Brown. Chicago:University of Chicago Press.
- Nilson, Robi, Ben Hoen, and Joseph Rand.** 2024. “Survey of Utility-Scale Wind and Solar Developers Report [Slides].” Lawrence Berkeley National Laboratory (LBNL), Berkeley, CA (United States).
- Petersen, Alisa, Katie Siegner, and John Coequyt.** 2026. “The interconnection queue continues to be a barrier to American economic competitiveness.” *RMI*. <https://rmi.org/interconnection-reform-ai-data-centers-generator-queues/>.
- PJM.** 2020. “PJM Manual 14B: PJM Region Transmission Planning Process.” 48 ed., <https://www.pjm.com/-/media/DotCom/documents/manuals/archive/m14b/m14bv48-pjm-regional-transmission-planning-process-10-01-2020.pdf>.
- PJM.** 2021. “Connecting to the Grid FAQs: How long does the interconnection process take?” <https://learn.pjm.com/three-priorities/planning-for-the-future/connecting-grid/how-long-does-the-interconnection-process-take>.

- PJM.** 2023*a*. “PJM Manual 14A: New Services Request Process.” 30 ed., <https://www.pjm.com/-/media/DotCom/documents/manuals/m14a.ashx>.
- PJM.** 2023*b*. “PJM Manual 14G: Generation Interconnection Requests.” 8 ed., <https://www.pjm.com/-/media/DotCom/documents/manuals/m14g.pdf>.
- PJM.** 2025. “PJM Manual 14C: Generation and Transmission Interconnection Facility Construction.” 17 ed.
- PJM.** 2026. “State of the Market Report for PJM 2025.” https://www.monitoringanalytics.com/reports/PJM_State_of_the_Market/2025/2025-som-pjm-vol1.pdf.
- PJM Interconnection.** 2025*a*. “PJM Announces Application Deadline for First Cycle of New Interconnection Process.” *PJM Inside Lines*.
- PJM Interconnection.** 2025*b*. “PJM, Google & Tapestry Join Forces to Apply AI to Enhance Regional Planning, Generation Interconnection.” *Press release, April 10, 2025*.
- PJM Interconnection.** 2026. “Expedited Interconnection Track Tariff Sheets.” <https://www.pjm.com/-/media/DotCom/committees-groups/cifp-lla/2026/20260203/20260203-expedited-interconnection-track-tariff-sheets.pdf>, Tariff, Part X [NEW]. Accessed May 13, 2026.
- PJM Interconnection, L.L.C.** 2020. “Open Access Transmission Tariff, Part VI (Administration and Study of New Service Requests), Attachment P (Interconnection Construction Service Agreement), Appendix 2.” *Version effective April 1, 2020 (FERC Docket No. ER19-1958)*, PJM designated as Transmission Provider; interconnected Transmission Owner builds the Transmission Owner Interconnection Facilities under the Standard Option, sec. 3.2. Available at <https://agreements.pjm.com/eTariff/>.
- Plumer, Brad.** 2023. “The U.S. Has Billions for Wind and Solar Projects. Good Luck Plugging Them In.” *The New York Times*. <https://www.nytimes.com/2023/02/23/climate/renewable-energy-us-electrical-grid.html>.
- Rand, Joseph, Nick Manderlink, Steven Zhang, Chris Talley, Will Gorman, Ryan H. Wisner, Joachim Seel, Julie Mulvaney Kemp, Seongeun Jeong, and Fredrich Kahrl.** 2025. “Queued Up: 2025 Edition, Characteristics of Power Plants Seeking Transmission Interconnection As of the End of 2024.” Lawrence Berkeley National Laboratory.
- Ryan, Nicholas.** 2021. “The Competitive Effects of Transmission Infrastructure in the Indian Electricity Market.” *American Economic Journal: Microeconomics*, 13(2): 202–242.
- Ryan, Stephen P.** 2012. “The costs of environmental regulation in a concentrated industry.” *Econometrica*, 80(3): 1019–1061.
- Seel, Joachim, Julie Mulvaney Kemp, Anna Cheyette, Dev Millstein, Will Gorman, Seongeun Jeong, Dana Robson, Rachman Setiawan, and Mark Bolinger.** 2024. “Utility-Scale Solar, 2024 Edition: Empirical Trends in Deployment, Technology, Cost, Performance, PPA Pricing, and Value in the United States.” Lawrence Berkeley National Laboratory.
- Shoemaker, Jason.** 2021. “Interconnection Queue Status Update.” <https://www.pjm.com/-/media/committees-groups/committees/pc/2021/20210831/20210831-item-07-queue-status-update.ashx>.

- Verdier, Valentin, and Carson Reeling.** 2022. “Welfare effects of dynamic matching: An empirical analysis.” *The Review of Economic Studies*, 89(2): 1008–1037.
- Waldinger, Daniel.** 2021. “Targeting in-kind transfers through market design: A revealed preference analysis of public housing allocation.” *American Economic Review*, 111(8): 2660–2696.
- Weintraub, Gabriel Y., C. Lanier Benkard, and Benjamin Van Roy.** 2008. “Markov Perfect Industry Dynamics With Many Firms.” *Econometrica*, 76(6): 1375–1411.
- Weintraub, Gabriel Y, C Lanier Benkard, Przemysław Jeziorski, and Benjamin Van Roy.** 2010. “Nonstationary oblivious equilibrium.” Working Paper.
- Wiser, Ryan H., Dev Millstein, Ben Hoen, Mark Bolinger, Will Gorman, Joseph Rand, Galen L. Barbose, Anna Cheyette, Naïm R. Darghouth, Seongeun Jeong, Julie Mulvaney Kemp, Eric O’Shaughnessy, Bentham Paulos, and Joachim Seel.** 2024. “Land-Based Wind Market Report: 2024 Edition.” Lawrence Berkeley National Laboratory.
- Wolak, Frank A.** 2015. “Measuring the competitiveness benefits of a transmission investment policy: The case of the Alberta electricity market.” *Energy Policy*, 85: 426–444.
- Yang, Chenyu.** 2020. “Vertical structure and innovation: A study of the SoC and smartphone industries.” *The RAND Journal of Economics*, 51(3): 739–785.

A Model Details

We first characterize optimal strategies in Section 5.1 as cutoff rules, derive the law of motion for project masses used in the equilibrium definition in Section 5.3, and prove equilibrium existence.

Notation. We focus on a particular project and suppress the project-specific subscript. Let x denote time-invariant project characteristics, e the entry quarter, c the interconnection cost, and z study information. Let η denote accumulated payoff information: $\eta = \xi^{\text{S1}}$ in Stage 1 and $\eta = \xi^{\text{S1}} + \xi^{\text{S2}}$ in Stage 2, replacing ξ in the arguments of \bar{V} , W^{S1} and W^{S2} in (3), (4) and (5). The exogenous probabilities of exits, $1 - \delta^{\text{S1}}$ and $1 - \delta^{\text{S2}}$, are based on x , and we suppress their i subscript too. We also define the queue statuses $\mathcal{K}_t(e, x)$ as a finite vector of variables that determine study-arrival probabilities and the distribution of the next study's observed state (c, z) , conditional on the current observed state and (x, e) . The queue status does not affect the transition of η : moving from Stage 1 to Stage 2 only adds the new payoff information ξ^{S2} to ξ^{S1} . In the empirical model, $\mathcal{K}_t(e, x)$ consists of the number of queued projects with weakly higher priority, the number of such projects in the same TO, capacity of queued projects in the same TO, and accumulated capacity of each fuel type up to t . Finally, we assume that (x, e, c, z, t) have finite supports, the accumulated payoff state η has continuous support, and the queue-status \mathcal{K} lies in bounded subsets of Euclidean space.

A.1 Cutoff Strategy

Define the *stay surplus* $\mathcal{U}_t^s(x, e, c, z, \eta)$ as the value of waiting in each stage $s \in \{1, 2\}$ (waiting with study 1 or 2), so that the continuation values are $W_t^s(x, e, c, z, \eta) = \max\{0, \mathcal{U}_t^s(x, e, c, z, \eta)\}$. The waiting value in the two stages \mathcal{U}_t^s are

$$\mathcal{U}_t^{\text{S2}}(x, e, c, z, \eta) = -\gamma^{\text{S2}} + \beta\delta^{\text{S2}} \left[\sum_{c'} q^{\text{S2}}(c'|x, e, t, c, z) \bar{V}(x, e, t, c', \eta) + (1 - Q^{\text{S2}}(x, e, t, c, z)) W_{t+1}^{\text{S2}}(x, e, c, z, \eta) \right], \quad (\text{A.1})$$

$$\begin{aligned} \mathcal{U}_t^{\text{S1}}(x, e, c, z, \eta) = & -\gamma^{\text{S1}} + \beta\delta^{\text{S1}} \left[\sum_{c'} q^{\text{S1},f}(c'|x, e, t, c, z) E_{\xi^{\text{S2}}} [\bar{V}(x, e, t, c', \eta + \xi^{\text{S2}})] \right. \\ & + \sum_{c', z'} q^{\text{S1}}(c', z'|x, e, t, c, z) E_{\xi^{\text{S2}}} [W_t^{\text{S2}}(x, e, c', z', \eta + \xi^{\text{S2}})] \\ & \left. + (1 - Q^{\text{S1}}(x, e, t, c, z)) W_{t+1}^{\text{S1}}(x, e, c, z, \eta) \right], \quad (\text{A.2}) \end{aligned}$$

We characterize the project strategies under the following assumptions:

Assumption 1 (Regularity). Waiting costs satisfy $\gamma^{S1}, \gamma^{S2} > 0$. The unobserved heterogeneity ξ^{S1} , ξ^{S2} , and ξ^f have absolutely continuous distributions with full support. The probabilities of surviving exogenous departures are strictly positive, $\delta^s > 0$.

Under this assumption, positive waiting costs are reasonable in our context because projects pay for the costs of site control and study management. We also assume that ξ^{S1} , ξ^{S2} , and ξ^f are normally distributed in the model in Section 5. Empirically, we find that the δ^s values are close to 1. Under these assumptions, we first show that \mathcal{U}_t^s has the following properties:

Lemma 1. For fixed (x, e, t, c, z) , $t < T$, and s , \mathcal{U}_t^s is continuous and strictly increasing in η , and there exists a unique value of η such that $\mathcal{U}_t^s = 0$.

Proof. Backward induction on t : the terminal payoff $\bar{V}(x, e, t, c, \eta) = E_{\xi^f}[\max(\pi_i(t) + \xi^f, 0)]$ is continuous and strictly increasing in η under Assumption 1. In stage 2, $\sum_{c'} q^{S2} \bar{V}$ is a weighted sum of continuous, strictly increasing functions of η with nonnegative weights, and $(1 - Q^{S2})W_{t+1}^{S2}$ is continuous and weakly increasing by induction (where $W_T^{S2} = 0$), which together imply that \mathcal{U}_t^{S2} is continuous and strictly increasing. The same reasoning shows that \mathcal{U}_t^{S1} also has these properties. Then, to show that there exists a unique η for $\mathcal{U}_t^s = 0$ given s , it suffices to find values of η at which \mathcal{U}_t^s is negative and positive, respectively. Note that when $\eta \rightarrow -\infty$, $\bar{V}_t \rightarrow 0$, and by induction, $W_t^{S2} \rightarrow 0$ for any $t < T$, which implies that there must exist a sufficiently negative η such that $\mathcal{U}_t^{S2} < 0$ for positive γ^{S2} . Similar reasoning shows that there must exist a sufficiently large η for $\mathcal{U}_t^{S2} > 0$. The same argument applies for \mathcal{U}_t^{S1} . Strict monotonicity implies the uniqueness of the zero. □

The lemma thus shows that the optimal waiting decision is characterized by a cutoff

$$\eta^{s*}(x, e, t, c, z) = \inf\{\eta : \mathcal{U}_t^s(x, e, c, z, \eta) \geq 0\}, \tag{A.3}$$

where a project continues if $\eta \geq \eta^{s*}$ and withdraws otherwise.

We further note that the project strategies can be simplified to a “bang-bang” solution, where projects either exit right after learning about new information from a study, or do not endogenously exit. This strategy is consistent with the empirical pattern we observe in the data. The following assumption implies such a strategy:

Assumption 2 (Waiting value increases over time). Given η and $s \in \{1, 2\}$, $\mathcal{U}_{t+1}^s(x, e, c, z, \eta) \geq \mathcal{U}_t^s(x, e, c, z, \eta)$.

The condition is more likely to hold when projects have the correct belief that study-arrival probabilities increase over time, which is consistent with improvement of queue positions as they wait longer in equilibrium, and that the dispersions of ξ^{S2} and ξ^f increase with waiting time, raising the option value of remaining.

A.2 State Transitions

In the above, we have described the project strategies given their beliefs, and those beliefs are subject to the restriction in Assumption 2. This section describes a model of how PJM processes studies, which determines a project's state transition probabilities. These probabilities must be consistent with project beliefs in an equilibrium.

A.2.1 Transitions of η

We first describe how the distribution of accumulated payoff information, η , changes over time. To keep the notation tractable, we explicitly use the parametric assumptions on ξ^{S1} and ξ^{S2} in Section 5. The innovation in payoff information is independent of queue statuses and of the observed study-state transition. The only transition in accumulated payoff information occurs when $\eta = \xi^{S1}$ in Stage 1 to $\eta' = \xi^{S1} + \xi^{S2}$ in Stage 2. We assume ξ^{S1} has standard deviation σ^{S1} , and ξ^{S2} has standard deviation $\sigma^{S2} \cdot \tau^{\kappa^{S2}}$, where τ is the waiting time and $\kappa^{S2} > 0$.

After a non-terminal first study in period t , the improper density of $\eta \equiv \xi^{S1}$ among projects who do not withdraw is

$$g_t^{S1}(\eta \mid x, e, c, z) = \frac{1}{\sigma^{S1}} \phi\left(\frac{\eta}{\sigma^{S1}}\right) \mathbf{1}\{\eta \geq \eta^{1*}(x, e, t, c, z)\}, \quad (\text{A.4})$$

where ϕ is the standard normal density. After a non-terminal second study in period t , the improper density of $\eta' = \eta + \xi^{S2}$ among projects who do not withdraw is

$$g_t^{S2}(\eta' \mid \eta, x, e, c', z') = \frac{1}{\sigma^{S2}(t-e)^{\kappa^{S2}}} \phi\left(\frac{\eta' - \eta}{\sigma^{S2}(t-e)^{\kappa^{S2}}}\right) \mathbf{1}\{\eta' \geq \eta^{2*}(x, e, t, c', z')\}. \quad (\text{A.5})$$

The normal density component in (A.5) does not depend on (c, z) , (c', z') , or $\mathcal{K}_t(e, x)$; these variables affect the mass of continuing projects only through the cutoff.

A.2.2 Transitions of c and z and Study Arrival Probabilities

We assume that the probabilities of (1) receiving a new terminal second study with cost c' in Stage 1, (2) receiving a new non-terminal second study with cost c' and updated study information z' in Stage 1, and (3) receiving the third study with cost information c' in Stage 2 are functions of $(x, e, t, c, z, \mathcal{K}_t(e, x))$, and are smooth in $\mathcal{K}_t(e, x)$. Thus Q^{S1} and Q^{S2} depend on the observed state and queue status, but not on η . In practice, we use an ordered-probit model for the transition of costs, and probit models for the transitions of other states (Appendix D).

A.3 Transitions of the Queue

We now describe, given how PJM processes studies and project strategies, how the composition of the queue changes over time. Let $m_t^s(x, e, c, z, \eta)$ denote the mass density of projects in stage $s \in \{1, 2\}$ at the start of quarter t , after the most recent withdrawal decision, where its integral with respect to η produces the mass of projects given (x, e, c, z) . Let $N_e(x)$ denote the exogenous mass of potential entrants in quarter e , and $q_0(c, z | x, e)$ the probability of a non-terminal first study with state (c, z) , so that $\sum_{c,z} q_0 = 1 - q^f$. The entry probability is

$$p^{\text{ent}}(x, e) = \Pr(EV(x, e) > C(x, e)), \quad (\text{A.6})$$

where C has a beta distribution specified in Section 6.3.

The Stage-1 mass of projects after entry is not exogenous: it equals the mass of potential projects multiplied by the entry probability, the probability of a non-terminal first-study state and the density of η for not withdrawing. Thus,

$$m_e^{\text{S1}}(x, e, c, z, \eta) = N_e(x) p^{\text{ent}}(x, e) q_0(c, z | x, e) g_e^{\text{S1}}(\eta | x, e, c, z). \quad (\text{A.7})$$

To describe the changes of the queue mass over time, we require notation on the transition probabilities of (c, z) defined in Appendix A.2.2. For notational simplification, we slightly abuse notation and reuse q and Q from project beliefs but condition explicitly on queue statuses $\mathcal{K}_t(e, x)$.

The Stage-1 mass transition when $t \geq e$ is:

$$m_{t+1}^{\text{S1}}(x, e, c, z, \eta) = \delta^{\text{S1}} [1 - Q^{\text{S1}}(x, e, t, c, z; \mathcal{K}_t(e, x))] m_t^{\text{S1}}(x, e, c, z, \eta). \quad (\text{A.8})$$

The projects leaving the queue include transitions to Stage 2 and exogenous exits at a per-period probability of $1 - \delta^{\text{S1}}$. For the projects receiving a terminal study 2, the completed capacity in a

period is the mass in Stage 1 receiving the terminal study 2 times the respective capacity and the probability of completion.

The Stage-2 mass consists of continuing Stage-2 projects and Stage-1 projects receiving a non-terminal second study:

$$\begin{aligned}
 m_{t+1}^{S2}(x, e, c', z', \eta') &= \delta^{S2} [1 - Q^{S2}(x, e, t, c', z'; \mathcal{K}_t(e, x))] m_t^{S2}(x, e, c', z', \eta') \\
 &\quad + \sum_{c, z} \int \delta^{S1} q^{S1}(c', z' | x, e, t, c, z; \mathcal{K}_t(e, x)) g_t^{S2}(\eta' | \eta, x, e, c', z') m_t^{S1}(x, e, c, z, \eta) d\eta.
 \end{aligned}
 \tag{A.9}$$

The leaving mass includes projects receiving study 3 and exogenous exits at a per-period probability of $1 - \delta^{S2}$. For the projects receiving study 3, the completed capacity in a period is the mass in Stage 2 receiving the third study times the respective capacity and the probability of completion.

A.4 Queue Status and Operating Revenues

We now construct queue status variables based on the mass density functions defined above. The queue position in period t for those entering in period e is the number of queued projects with higher-or-equal priority, i.e., those with entry quarter $\tilde{e} \leq e$:

$$\sum_s \sum_{\tilde{x}} \sum_{\tilde{e} \leq e} \sum_{c, z} \int m_t^s(\tilde{x}, \tilde{e}, c, z, \eta) d\eta,
 \tag{A.10}$$

Other queue statuses used in our empirical model defined in Section 5.3 are computed similarly. For example, the same-TO queue position restricts the sum above to projects in the same TO zone, same-TO queued capacity weights each project by capacity, and accumulated completed capacity sums completion flows by fuel type. We keep the notation focused on queue position because the other components are finite sums of the same mass and completion objects.

The wholesale price in t is determined by the queue status of accumulated capacity of each fuel type up to t . The accumulated completion adds to the supply curve in Appendix B, and its crossing with the exogenous demand yields the new wholesale price. A project's revenue, \tilde{r} , is computed as the discounted sum of wholesale price times the project capacity, adjusted for fuel-type efficiency, over a 25-year service life. We assume that the resulting \tilde{r} is continuous in the queue status.³¹

³¹In the actual implementation in Appendix B, we construct a step function based on the fuel types. For equilibrium existence purposes, the function can be smoothed at the break points to ensure existence. We use the step function directly in equilibrium calculation through an iterative algorithm. We do not find non-existence in practice.

A.5 Equilibrium Existence

A **non-stationary queuing equilibrium** is defined as the collection of cutoff strategies η^{s*} , entry probabilities p^{ent} , queue statuses $\{\mathcal{K}_t(e, x)\}_{t,e,x}$ and revenues \tilde{r} that satisfy Equations (A.3), (A.6) and the conditions in Appendix A.4. Given the queue statuses and the resulting project revenue, backward induction yields the cutoffs and determine entry probabilities. Then, (A.7)–(A.10) produce new queue statuses. Call this mapping Γ . In the arguments below, we show that Γ maps a compact set into itself and is continuous. Existence thus follows from Brouwer’s fixed point theorem.

First, consider the queue-position component. It lies in $[0, \bar{N}]$, where $\bar{N} = \sum_{e,x} N_e(x)$. Other components of \mathcal{K} are also bounded because they are finite sums of project counts, project capacity, or completed capacity over finite supports. Let \bar{K}_j denote a finite upper bound for component j of \mathcal{K} . The domain $\mathcal{D} = \prod_j [0, \bar{K}_j]$ is compact and convex, and Γ maps \mathcal{D} into itself.

Second, value functions are continuous in queue statuses by backward induction over continuous study-arrival probabilities and $\max\{0, \cdot\}$. Entry probabilities are continuous in queue statuses via (A.6) and the continuity of value functions. The project revenue, \tilde{r} in the payoff function, is based on wholesale prices, which continuously depend on \mathcal{K} through accumulated completed capacity, and this function is continuous. As a result, cutoffs are continuous in queue statuses given the continuity in \mathcal{U}_t^s . The primitive transition of η is independent of queue statuses; the post-withdrawal densities in (A.4)–(A.5) are continuous in queue statuses only through the cutoffs. The transition probabilities of (c, z) in Appendix A.2.2 are continuous in queue statuses by assumption. Therefore, the mass transitions (A.7)–(A.9) are continuous in queue statuses. The mapping Γ is thus continuous. Given that Γ is a continuous mapping from a compact set into itself, Brouwer’s fixed point theorem implies the existence of the equilibrium.

B Construction of Revenue from Power Production

This section details how we construct present values of wholesale electricity revenues for projects of different fuel types. For estimation, each year’s revenue per megawatt capacity is the observed wholesale electricity price adjusted for the project’s fuel type efficiency. For prices after 2020, we use the same price as the last quarter of 2020.³² The present value is the sum of revenues in the next 25 years after the in-service date of a project, discounted at the annual rate of 5%.³³

³²In effect, we assume that the projects believe the power demand to be flat as in prior years, which implies that the surge in power demand driven by AI and data centers in later years would be a surprise to projects.

³³We do not have data on capacity market payments or any subsidies specific to fuel types. In the project payoff functions, we include covariates based on fuel types and sizes and estimate their parameters to capture these effects.

For simulation, the mix of in-service projects would change, leading to different wholesale electricity prices. We assume that demand is perfectly inelastic, and we construct supply curves based on the existing generators prior to 2012 (whose exits are held fixed as observed in the data) and new generators that complete in the queuing equilibrium model. Crossing the observed quantity (from the perfectly inelastic demand) with the new equilibrium supply yields new equilibrium prices.

B.1 Supply Curve

We construct hourly supply curves for the PJM Interconnection from 2011 through 2022. The construction follows Cicala (2022) and Hausman (2025), with modifications for PJM-specific data availability.

The supply curve is based on a merit-order representation of competitive project offers. Under competitive bidding, project offers are approximated by marginal costs. We therefore rank dispatchable generators by estimated marginal cost and construct the hourly supply curve from their cumulative available capacity. We use this merit-order approach, rather than an empirical supply curve based on realized net generation, because it allows us to evaluate counterfactual capacity additions and produces quarterly normalized LMPs that closely track actual PJM prices.

The primary data sources are EIA Forms 860, 923, and 906; EIA fuel price and operation and maintenance cost data; EPA Continuous Emissions Monitoring System (CEMS) data and Power Sector Programs Progress Reports; PJM Data Miner data on hourly load and generation; NRC Daily Power Status reports; S&P Global emissions allowance prices; NREL solar radiation data; PRISM county-level weather records; and U.S. Census geocode files.

Throughout this appendix, a “unit” refers to the generating unit that enters the merit-order supply curve. In most cases, this corresponds to an EIA-listed generator. For fossil plants with boiler-level operating or emissions data, boiler-level information is mapped to generators using EIA boiler-to-generator linkages. Plants refer to physical sites that may contain multiple generating units.

B.1.1 Unit-level Marginal Cost

We estimate an hourly marginal cost for each dispatchable unit. For fossil units, marginal cost is the sum of fuel costs, emissions allowance costs, and variable operation and maintenance costs:

$$MC_{it} = FuelCost_{it} + EmissionsCost_{it} + VOM_{it}, \quad (\text{B.11})$$

where $FuelCost_{it}$ is the fuel cost of producing one MWh, $EmissionsCost_{it}$ is the emissions allowance cost per MWh, and VOM_{it} is variable operation and maintenance cost.

Fuel cost combines each unit’s heat rate, fuel mix, and fuel price:

$$FuelCost_{it} = HR_{it} \sum_f \theta_{it}^f P_{it}^f. \tag{B.12}$$

Here f indexes sub-fuel categories, θ_{it}^f is the heat-input share of fuel f , P_{it}^f is the corresponding fuel price, and HR_{it} is the unit’s heat rate. For natural gas and oil units, we use daily Henry Hub and WTI spot prices, adjusted by plant-year markups estimated from EIA fuel receipt data, to capture daily fuel-price variation not observed in the monthly EIA series. Missing plant-level fuel prices are filled using state-, division-, and national-level averages.

Emissions costs equal the unit’s emissions rate per MWh multiplied by the relevant allowance price. Units are assigned to SO₂ and NO_x programs based on location and program rules. For seasonal NO_x markets, emissions costs apply only during the ozone-season window for the unit’s county.

Variable operation and maintenance costs capture non-fuel and non-emissions expenses that vary with generation, including consumables, routine maintenance, and other production-related expenses. We assign each unit a technology-year-specific variable O&M cost in dollars per MWh and add it to marginal cost as a flat per-MWh adder.

Fossil fuel-unit marginal costs are winsorized at the 1st and 99th percentiles within year to reduce the influence of extreme outliers. Constructing these measures requires harmonizing generator, plant, and boiler identifiers across EIA and EPA records; maintaining boiler-to-generator mappings over time; mapping facilities to counties and time zones; and converting all hourly observations to a common time standard before merging with PJM operations data.

For non-fossil units, we make two simplifying assumptions. Renewable resources, including wind, solar, hydro, and geothermal units, are assigned zero marginal cost. Nuclear units are assigned a constant marginal cost of \$17.13/MWh, based on the EIA average operating expense for nuclear generation.

B.1.2 Available Generating Capacity

We next construct hourly available capacity for each unit. For fossil units monitored by CEMS, hourly net generation is calculated as reported gross load multiplied by the unit’s gross-to-net conversion factor. For fossil units without CEMS coverage, monthly net generation from EIA-906

is allocated across hours of the month using the PJM-wide load profile. Each fossil unit’s hourly capacity is constrained by its observed daily maximum, preventing the merit order from dispatching capacity that the unit could not physically have produced on that day.

For non-fossil units, we use resource-specific availability measures. Wind generation is taken directly from PJM at hourly resolution. Solar generation is taken from PJM for 2019 onward and reconstructed for earlier years by allocating monthly EIA-906 solar generation across hours in proportion to satellite-measured global horizontal irradiance at the plant location. Nuclear generation is constructed from daily NRC reactor capacity factors and spread uniformly across hours within each day. Hydroelectric, storage, biomass, and other minor fuels are represented by a synthetic zero-cost unit with capacity equal to PJM’s reported hourly generation from these sources.

B.2 Demand

Hourly electricity demand is measured using PJM-wide metered load. In the market-clearing exercise, demand is treated as perfectly inelastic within each hour. The predicted clearing price is therefore the marginal cost of the unit needed to meet realized load.

B.3 Market-Clearing Price and Validation

For each hour, we sort available dispatchable units in ascending order of marginal cost and accumulate available capacity along the merit-order curve. The predicted market-clearing price, \hat{P}_t , is the marginal cost of the first unit at which cumulative available capacity equals or exceeds PJM-wide metered load.

Figure B.1 compares the quarterly average of \hat{P}_t with the quarterly average of actual PJM real-time hourly LMPs from 2011 through 2022. The predicted series broadly tracks the actual LMP series.

B.4 Using the Supply Curve in the Structural Model

The structural model uses the constructed supply curve to predict how market prices respond to counterfactual capacity additions. The model takes as inputs a discretized representation of the hourly merit-order supply curve, a marginal cost distribution for new fossil-fuel entrants, and existing PJM nameplate capacity by quarter and technology bin.

The timing and amount of new capacity entering the market are determined within the structural model. For each counterfactual capacity vector, the model inserts new capacity into the existing merit-order curve. Renewable additions are assigned zero marginal cost and placed at the bottom of

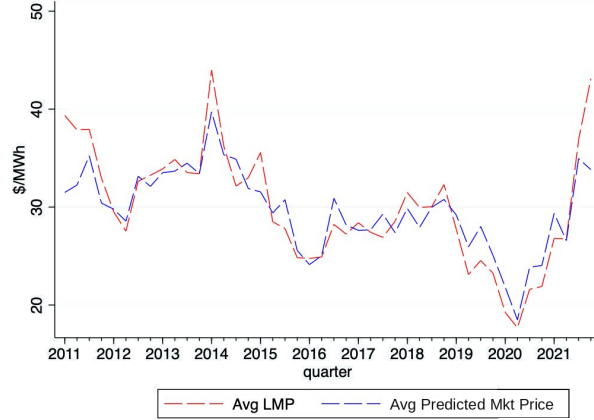


Figure B.1: Predicted and Actual PJM Real-Time LMPs

the merit order. Non-renewable additions are treated as new natural-gas capacity and distributed across ten heat-rate bins using the observed capacity distribution of new natural-gas units built in PJM. The marginal cost of each natural-gas bin is calculated using the bin’s average heat rate, annual natural gas price, emissions cost, and variable operation and maintenance cost.

To make the counterfactual price calculations computationally feasible, we approximate each quarter’s hourly demand distribution using 20 representative hours. Within each quarter, hours with similar net demand are grouped into 20 clusters using k -means clustering. Each cluster is represented by one hour, whose weight equals the share of quarter-hours assigned to that cluster.

After inserting new capacity, the model re-sorts units by marginal cost and identifies the clearing price for each representative hour. The quarterly market price is the weighted average of representative-hour clearing prices:

$$\hat{P}_q = \frac{\sum_{h \in \mathcal{C}_q} \omega_h \hat{P}_h}{\sum_{h \in \mathcal{C}_q} \omega_h}, \quad (\text{B.13})$$

where \mathcal{C}_q is the set of representative hours in quarter q , ω_h is the representative-hour weight, and \hat{P}_h is the predicted clearing price for representative hour h .

Because the structural model endogenizes only the queue projects in the estimation sample, realized PJM capacity may also change because of retirements, projects outside the modeled queue, or other non-modeled additions. To reconcile model-implied capacity with observed PJM capacity, we compute a residual capacity wedge by quarter and technology bin. In counterfactual exercises, this wedge is held fixed, so changes in predicted prices are driven only by changes in model-implied capacity additions.

B.5 From Quarterly Prices to Project-Level Revenue

We convert the predicted quarterly price series into project-level revenue using each project's capacity, completion quarter, and technology-specific capacity factor. For each project, we calculate expected revenue from power production over a 25-year operating horizon and discount future revenue at an annual rate of 5 percent.

For a project of technology r that becomes operational in quarter q_0 , expected discounted revenue per MW is

$$R_{q_0} = \sum_{s=0}^{99} \frac{\text{MWh}_r \cdot \widehat{P}_{q_0+s}}{(1.05)^{s/4}}, \quad (\text{B.14})$$

where \widehat{P}_{q_0+s} is the predicted market price in quarter $q_0 + s$, and MWh_r is expected quarterly generation per MW for technology r . Revenue is expressed in millions of dollars per MW.

The structural model aggregates these project-level revenue measures and uses the resulting present value of revenue in the entry and timing decisions.

C Identification of Project Preferences

Fix project characteristics x and entry quarter e . We show below how to identify the payoff specific to each combination of (x, e) as well as distributions of unobserved heterogeneity and construction shocks. We therefore suppress (x, e) from all arguments in this section.

Notation. After a non-terminal first study with state (t, c, z) , define the probability that a project who waits receives a non-terminal second study with state (c', z') after τ_1 quarters. Thus τ_1 is the elapsed time from this non-terminal first-study state to the next second study, whether the second study is terminal or non-terminal:

$$\Lambda^{\text{S1}}(c', z', \tau_1 | t, c, z) = \left[\prod_{h=0}^{\tau_1-1} \delta^{\text{S1}}(1 - Q^{\text{S1}}(t+h, c, z)) \right] \delta^{\text{S1}} q^{\text{S1}}(c', z' | t + \tau_1, c, z). \quad (\text{C.15})$$

The analogous probability that the second study is terminal with interconnection cost c' is

$$\Lambda^{\text{S1},f}(c', \tau_1 | t, c, z) = \left[\prod_{h=0}^{\tau_1-1} \delta^{\text{S1}}(1 - Q^{\text{S1}}(t+h, c, z)) \right] \delta^{\text{S1}} q^{\text{S1},f}(c' | t + \tau_1, c, z). \quad (\text{C.16})$$

After a non-terminal second study at $\tilde{t} = t + \tau_1$ with state (\tilde{t}, c', z') , define the probability that a project who waits receives a terminal study with interconnection cost c'' after another τ_2 quarters:

$$\Lambda^{\text{S2}}(c'', \tau_2 \mid \tilde{t}, c', z') = \left[\prod_{h=0}^{\tau_2-1} \delta^{\text{S2}}(1 - Q^{\text{S2}}(\tilde{t} + h, c', z')) \right] \delta^{\text{S2}} q^{\text{S2}}(c'' \mid \tilde{t} + \tau_2, c', z'). \quad (\text{C.17})$$

We use the following notation for the distributions: $\xi^{\text{S1}} \sim F^{\text{S1}}(\cdot)$, $\xi^{\text{S2}} \sim F_{\tau_1}^{\text{S2}}(\cdot)$, and $\xi^f \sim G_{\tau}(\cdot)$, where τ is the elapsed time from the current non-terminal study state to the terminal study in the branch being considered. Thus, when the second study is terminal, $\tau = \tau_1$ and the distribution is G_{τ_1} ; when the third study is terminal after a non-terminal second study, $\tau = \tau_2$ and the distribution is G_{τ_2} . We impose the normalizations $E[\xi^{\text{S1}}] = 0$, $E[\xi^{\text{S2}} \mid \tau_1] = 0$, and $E[\xi^f \mid \tau] = 0$. We use a_t to denote the present value of the profit from starting to operate the plant in t less the construction cost, which corresponds with $r_{it} - \omega_{it}$ in Equation (2).

Theorem 1. Under the assumptions that (1) the probabilities defined in (C.15), (C.16), and (C.17), as well as the component transition objects Q^s and δ^s , are known and positive, (2) F^{S1} , $F_{\tau_1}^{\text{S2}}$, and G_{τ} are absolutely continuous with positive densities and have full support on \mathbb{R} , (3) conditional on the lagged observed state and waiting time, each new study-cost realization is independent of the payoff shocks and has full support,³⁴ and (4) the derivative of the relevant cutoff with respect to the realized study cost is nonzero at the points used below, F^{S1} , $F_{\tau_1}^{\text{S2}}$, G_{τ} , γ^{S1} , γ^{S2} and a_t are identified for all dates reached with positive probability.

Proof. All probabilities below condition on the lagged observed state and waiting time. By assumption, varying the newly realized study cost changes the continuation cutoff but not the distribution of the payoff shock at that decision node. Since the Λ 's are known and positive, we work with probabilities normalized by the relevant Λ ; the corresponding unnormalized probabilities are observed in the data.

Step 1: terminal shock. Consider projects that have reached a non-terminal second study with state (\tilde{t}, c', z') . Let $\eta = \xi^{\text{S1}} + \xi^{\text{S2}}$, and let H^{S2} denote the distribution of η at this decision node before the withdrawal decision. By Appendix A, the Stage-2 decision is characterized by a cutoff $\eta^{2*}(\tilde{t}, c', z')$, where projects continue if $\eta \geq \eta^{2*}(\tilde{t}, c', z')$.

³⁴The empirical model in Section 5 assumes that c 's support is finite to simplify the notation for transition probabilities. Our characterization of strategies and equilibrium existence still goes through when c has full support and its conditional distributions are absolutely continuous.

The observed immediate withdrawal probability after this non-terminal second study is

$$D^{\text{S}2}(\tilde{t}, c', z') = H^{\text{S}2}(\eta^{2*}(\tilde{t}, c', z')).$$

Next consider the observed joint probability, from the same non-terminal second-study state, of continuing after the second study, receiving a terminal third study after τ_2 quarters with cost c'' , and withdrawing at the terminal study. This probability is

$$\Omega^{\text{S}2}(\tilde{t}, c', z', c'', \tau_2) = \Lambda^{\text{S}2}(c'', \tau_2 \mid \tilde{t}, c', z') M^{\text{S}2}(\tilde{t}, c', z', c'', \tau_2).$$

Since $\Lambda^{\text{S}2}$ is known and positive, $M^{\text{S}2} = \Omega^{\text{S}2}/\Lambda^{\text{S}2}$ is known from data. It equals

$$M^{\text{S}2}(\tilde{t}, c', z', c'', \tau_2) = \int_{\eta^{2*}(\tilde{t}, c', z')}^{\infty} G_{\tau_2}(c'' - a_{\tilde{t}+\tau_2} - \tilde{\eta}) dH^{\text{S}2}(\tilde{\eta}).$$

Differentiating $D^{\text{S}2}$ and $M^{\text{S}2}$ with respect to c' gives

$$-\frac{\partial M^{\text{S}2}(\tilde{t}, c', z', c'', \tau_2)/\partial c'}{\partial D^{\text{S}2}(\tilde{t}, c', z')/\partial c'} = G_{\tau_2}(c'' - a_{\tilde{t}+\tau_2} - \eta^{2*}(\tilde{t}, c', z')). \quad (\text{C.18})$$

The left-hand side is known from data. As c'' varies over its support, the right-hand side traces the CDF G_{τ_2} with a horizontal shift. The mean-zero normalization of G_{τ_2} identifies both G_{τ_2} and

$$b_{\tau_2}^{\text{S}2}(\tilde{t}, c', z') \equiv a_{\tilde{t}+\tau_2} + \eta^{2*}(\tilde{t}, c', z').$$

Step 2: second-study payoff information. Now consider projects that have reached a non-terminal first study with state (t, c, z) . Let $\eta^{1*}(t, c, z)$ denote the Stage-1 cutoff. The immediate withdrawal probability is

$$D^{\text{S}1}(t, c, z) = F^{\text{S}1}(\eta^{1*}(t, c, z)).$$

Suppose a project that continues receives a non-terminal second study after τ_1 quarters, so that $\tilde{t} = t + \tau_1$ and the new state is (c', z', \tilde{t}) . The normalized joint probability of continuing after the first study and withdrawing immediately after the non-terminal second study is

$$M^{\text{S}1}(t, c, z, c', z', \tau_1) = \int_{\eta^{1*}(t, c, z)}^{\infty} F_{\tau_1}^{\text{S}2}(\eta^{2*}(\tilde{t}, c', z') - \tilde{\xi}^{\text{S}1}) dF^{\text{S}1}(\tilde{\xi}^{\text{S}1}).$$

Differentiating D^{S1} and M^{S1} with respect to the first-study cost c gives

$$-\frac{\partial M^{\text{S1}}(t, c, z, c', z', \tau_1)/\partial c}{\partial D^{\text{S1}}(t, c, z)/\partial c} = F_{\tau_1}^{\text{S2}}(\eta^{2*}(\tilde{t}, c', z') - \eta^{1*}(t, c, z)). \quad (\text{C.19})$$

For any fixed τ_2 with positive probability, rewrite the argument on the right-hand side as

$$\eta^{2*}(\tilde{t}, c', z') - \eta^{1*}(t, c, z) = b_{\tau_2}^{\text{S2}}(\tilde{t}, c', z') - b_{\tau_1, \tau_2}^{\text{S1}}(t, c, z),$$

where

$$b_{\tau_1, \tau_2}^{\text{S1}}(t, c, z) \equiv a_{t+\tau_1+\tau_2} + \eta^{1*}(t, c, z).$$

Since $b_{\tau_2}^{\text{S2}}$ is identified from Step 1 and has full support through variation in c' , (C.19) identifies $F_{\tau_1}^{\text{S2}}$ and the shift $b_{\tau_1, \tau_2}^{\text{S1}}(t, c, z)$, using the mean-zero normalization of $F_{\tau_1}^{\text{S2}}$.

Step 3: payoff levels and cutoffs. Using the identified object $b_{\tau_1, \tau_2}^{\text{S1}}$, the first-study withdrawal probability can be written as

$$D^{\text{S1}}(t, c, z) = F^{\text{S1}}(b_{\tau_1, \tau_2}^{\text{S1}}(t, c, z) - a_{t+\tau_1+\tau_2}). \quad (\text{C.20})$$

Variation in $b_{\tau_1, \tau_2}^{\text{S1}}$ traces out the CDF F^{S1} with a horizontal shift. Because F^{S1} has mean zero, this shift identifies $a_{t+\tau_1+\tau_2}$ and hence F^{S1} . The identified a_t then separately identifies the cutoffs $\eta^{1*}(t, c, z)$ and $\eta^{2*}(\tilde{t}, c', z')$ from the identified shifts b^{S1} and b^{S2} .

Step 4: waiting costs. At the Stage-2 cutoff, the project is indifferent between waiting and withdrawing. Let

$$S^{\text{S2}}(\tau_2 | \tilde{t}, c', z') = \prod_{h=0}^{\tau_2-1} \delta^{\text{S2}}(1 - Q^{\text{S2}}(\tilde{t} + h, c', z'))$$

denote the probability of still waiting τ_2 quarters after the second study, before the next terminal-study arrival. The indifference condition implies

$$0 = A^{\text{S2}}(\tilde{t}, c', z') - \gamma^{\text{S2}} B^{\text{S2}}(\tilde{t}, c', z'),$$

where

$$A^{\text{S2}}(\tilde{t}, c', z') = \sum_{c'', \tau_2} \beta^{\tau_2+1} \Lambda^{\text{S2}}(c'', \tau_2 | \tilde{t}, c', z') \int \max\{a_{\tilde{t}+\tau_2} + \eta^{2*}(\tilde{t}, c', z') + v - c'', 0\} dG_{\tau_2}(v)$$

and

$$B^{S2}(\tilde{t}, c', z') = \sum_{\tau_2} \beta^{\tau_2} S^{S2}(\tau_2 | \tilde{t}, c', z').$$

Both A^{S2} and B^{S2} contain only identified objects, so $\gamma^{S2} = A^{S2}/B^{S2}$ is identified.

Similarly, define

$$S^{S1}(\tau_1 | t, c, z) = \prod_{h=0}^{\tau_1-1} \delta^{S1}(1 - Q^{S1}(t+h, c, z)), \quad B^{S1}(t, c, z) = \sum_{\tau_1} \beta^{\tau_1} S^{S1}(\tau_1 | t, c, z).$$

The indifference condition implies

$$0 = A^{S1}(t, c, z) - \gamma^{S1} B^{S1}(t, c, z),$$

where

$$\begin{aligned} A^{S1}(t, c, z) &= \sum_{c', \tau_1} \beta^{\tau_1+1} \Lambda^{S1,f}(c', \tau_1 | t, c, z) \iint \max\{a_{t+\tau_1} + \eta^{1*}(t, c, z) + u + v - c', 0\} dG_{\tau_1}(v) dF_{\tau_1}^{S2}(u) \\ &+ \sum_{c', z', \tau_1} \beta^{\tau_1+1} \Lambda^{S1}(c', z', \tau_1 | t, c, z) \int W^{S2}(t + \tau_1, c', z', \eta^{1*}(t, c, z) + u) dF_{\tau_1}^{S2}(u). \end{aligned}$$

In the first term, we integrate over the final shock after a project receives a terminal second study (dG_{τ_1}). In the second term, W^{S2} is identified from the Stage-2 problem because a_t , G , γ^{S2} , and Λ^{S2} have already been identified. Thus $\gamma^{S1} = A^{S1}/B^{S1}$ is also identified. \square

D State Transitions, Study 1 State Distribution and Potential Entrants

D.1 Details on Project States in the Empirical Model

We first describe a project's post-entry state transitions. Interconnection costs are measured in millions of dollars per megawatt and discretized into four bins: $[0, 0.01]$, $(0.01, 0.05]$, $(0.05, 0.2]$, $(0.2, \infty)$. Let $\ell \in \{1, 2, 3, 4\}$ denote the latest study's cost level. When a project receives a terminal study of level ℓ , we assume its actual cost is drawn from the empirical distribution of final costs in the corresponding bin. We can express the states as $(s, o, \ell, z^{\text{cluster}}, z^{\text{test}})$, where s denotes which study has been received, o denotes the waiting time, ℓ denotes the cost level, z^{cluster} indicates whether the project is assigned to a cost-sharing cluster, and z^{test} indicates whether a set of engineering tests have been performed. Being part of a cost-sharing cluster means that PJM has identified common

components on the grid that a group of projects in the queue may overload, and the costs of upgrading the components will be shared by projects based on their contributions to the overload. Being in a cost-sharing cluster affects the allocation of network-upgrade costs across projects and may lower the cost assigned to an individual project. For the engineering tests variable, we focus on whether project deliverability, multiple-facility contingency, and short-circuit analyses have been performed. These are key tests that assess whether the project can be interconnected and deliver power without violating constraints. As shown below, our estimates indicate that having completed these tests increases later study-arrival probabilities.

The state transitions are built from five sets of probabilities that are functions of a project's current state and characteristics, including fuel type, size, and location. We use p^A for the probability that a study will arrive next period. Conditional on study arrival and the prior state, we use $p^c, p^{\text{test}}, p^{\text{cluster}}$, and p^f for the probabilities of a new cost level, engineering tests completion conditional on $z^{\text{test}} = 0$, cost-sharing-cluster assignment conditional on $z^{\text{cluster}} = 0$, and the second study being final. Both z^{test} and z^{cluster} are absorbing: once they become 1, they remain 1 in subsequent studies.

D.2 Transition Equations

We now express the transition probabilities in Section 5.1 using the primitive probabilities above. Let $z = (z^{\text{cluster}}, z^{\text{test}})$, let τ denote duration in the queue, and let $s = 1$ denote waiting for the second study and $s = 2$ denote waiting for the final study.

For a project in Stage 1, the probability that the second study arrives and is terminal with new cost level ℓ' is

$$q_i^{\text{S1},f}(\ell' | \ell, t, z) = p_i^A(s = 1, \tau, \ell, z) p_i^c(\ell' | s = 1, \tau, \ell, z) p_i^f(\tau, \ell, z).$$

The probability that a non-terminal second study arrives with updated state (ℓ', z') is

$$\begin{aligned} q_i^{\text{S1}}(\ell', z' | \ell, t, z) &= p_i^A(s = 1, \tau, \ell, z) p_i^c(\ell' | s = 1, \tau, \ell, z) (1 - p_i^f(\tau, \ell, z)) \\ &\quad \times h^{\text{cluster}}(z^{\text{cluster}'} | z^{\text{cluster}}) h^{\text{test}}(z^{\text{test}'} | z^{\text{test}}). \end{aligned}$$

where

$$\begin{aligned} h^{\text{test}}(1 | 1) &= 1, & h^{\text{test}}(1 | 0) &= p^{\text{test}}, & h^{\text{test}}(0 | 1) &= 0, & h^{\text{test}}(0 | 0) &= 1 - p^{\text{test}}, \\ h^{\text{cluster}}(1 | 1) &= 1, & h^{\text{cluster}}(1 | 0) &= p^{\text{cluster}}. \end{aligned}$$

Therefore

$$Q_i^{S1}(\ell, t, z) = \sum_{\ell'} q_i^{S1,f}(\ell' | \ell, t, z) + \sum_{\ell', z'} q_i^{S1}(\ell', z' | \ell, t, z) = p_i^A(s = 1, \tau, \ell, z).$$

For a project in Stage 2, every arriving study is terminal. Thus

$$q_i^{S2}(\ell' | \ell, t, z) = p_i^A(s = 2, \tau, \ell, z) p_i^c(\ell' | s = 2, \tau, \ell, z), \quad Q_i^{S2}(\ell, t, z) = \sum_{\ell'} q_i^{S2}(\ell' | \ell, t, z) = p_i^A(s = 2, \tau, \ell, z).$$

A project exits with 0 payoff when reaching the maximum duration (32 quarters).

D.3 Transition Estimates

Table D.1 reports the parameters used in these transition probabilities. The cost column reports parameters from the ordered-probit index. The other columns are from probit indices. We also report observed and fitted means.

D.4 First Study State Distribution

The first-study state is constructed separately from the later transition probabilities. In the empirical implementation, we use the first-study quarter as the observed entry quarter, consistent with the model timing in which projects receive their first study upon entry. We group projects by entry quarter, transmission owner, fuel type (wind, solar, battery, and other), whether it expands an existing plant, and project size bins with the cutoffs at 10, 20, 50, 100, 200, 500, 1000, 1250 MW. For each structural group, we compute the marginal distributions of each state. Under the assumption that these states are independently distributed, we construct the first study state of cost and study information by multiplying the respective marginals.

D.5 Potential Entrants

We construct the non-entering potential projects from the empirical distribution of observed queue entrants. We group observed entrants by entry year (first study date), TO, fuel type indicators (wind, solar, storage, and other), whether the project expands an existing plant, and a coarse size bin: ≤ 20 MW, 20–100 MW, or > 100 MW. We then compute the maximum number of observed entrants of that group across cohort years. In each cohort year, if the observed number of entrants of a group is below this group-specific maximum (across years), we add potential non-entrants drawn from entrants in that group until the cohort-year count reaches the maximum. For each potential

Table D.1: Transition Function Estimates

	Ordered- probit cost state	Study arrival	In cluster	Has test	Study 2 Final
Cutoff 2	0.807*** (0.037)				
Cutoff 3	1.177*** (0.103)				
Prior cost: (0.01, 0.05]	0.599*** (0.083)				
Prior cost: (0.05, 0.2]	1.211*** (0.079)				
Prior cost: > 0.2	2.117*** (0.094)				
Wind	0.594*** (0.111)	0.023 (0.052)	0.422*** (0.133)	0.909** (0.365)	-0.848*** (0.218)
Solar	0.526*** (0.073)	0.131*** (0.042)	0.671*** (0.090)	1.757*** (0.216)	-1.086*** (0.101)
Battery	0.508*** (0.094)	-0.054 (0.056)	1.169*** (0.132)	1.878*** (0.340)	-1.550*** (0.146)
Capacity increase at existing plant	-0.259*** (0.064)	-0.053 (0.034)	0.218*** (0.082)	0.019 (0.213)	0.374*** (0.091)
10–20 MW		0.054 (0.049)	0.411*** (0.101)	0.746*** (0.234)	-0.413*** (0.096)
20–100 MW		0.022 (0.047)	0.785*** (0.105)	0.845*** (0.229)	-1.300*** (0.118)
> 100 MW		-0.141*** (0.051)	1.077*** (0.119)	1.209*** (0.314)	-1.999*** (0.148)
Has test	0.065 (0.070)	-0.172*** (0.039)			
In cluster	-0.352*** (0.086)	-0.063 (0.046)			
ln(MW in TO Queue)			0.086*** (0.023)		
Observed mean	0.324	0.112	0.697	0.744	0.192
Fitted mean	0.436	0.111	0.698	0.745	0.189
Observations	2648	23627	2002	394	2002

The ordered-probit cost-state column uses four cost categories: $[0, 0.01]$, $(0.01, 0.05]$, $(0.05, 0.2]$, and > 0.2 million dollars per MW. The first cutoff is normalized to zero; Cutoff 2 and Cutoff 3 are the estimated higher cutoffs. Prior cost rows indicate the project’s most recent prior study cost, in million dollars per MW. $\ln(\text{MW in TO Queue})$ is the natural log total MW of projects in the same transmission-owner queue. For the cost-state column, observed and fitted means are shares with new cost above \$0.1 million/MW among study arrivals. Other means average the binary outcome and predicted probability. The study arrival probit model also controls for indicators for the number of periods in the queue and their interactions with whether they are waiting for the third study. Coefficient estimates are reported. Standard errors are in parentheses.

non-entrant, we assign the entry quarter by drawing from the empirical distribution of observed entry quarters within the same entry year.

The full construction creates 10,275 potential non-entrants over 2012-2020. To keep the equilibrium simulation manageable, the baseline estimation uses a random 5 percent subsample of these non-entrants. Therefore the number of sampled potential non-entrants is 514.

D.6 Exogenous Long-Tail Withdrawal

The structural model implies that projects do not endogenously withdraw between studies. We therefore assume the observed exits during these periods to be exogenous, such as due to failed permitting, and estimate the exogenous withdrawal probability with a probit model. The estimation sample consists of project-quarter combinations after the non-terminal first studies until their withdrawals or their non-terminal second study, and the quarters after their second study to their withdrawals until their third study. Table D.2 reports the estimates. The implied probabilities of an exogenous exit are 0.029 in stages 1 and 2.

Table D.2: Exogenous Withdrawal Probability

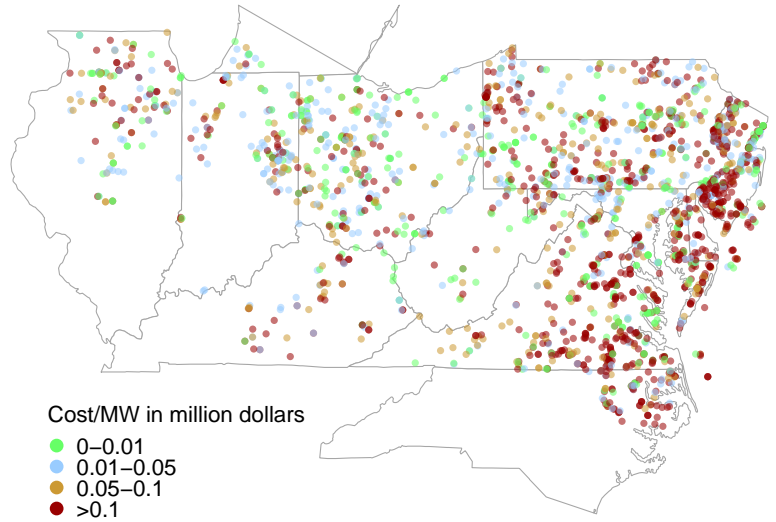
	p^W
Waiting for Study 3	-0.058 (0.040)
Wind	-0.374*** (0.081)
Solar	-0.622*** (0.057)
Storage	-0.524*** (0.069)
Capacity increase at existing plant	-0.391*** (0.050)
ln(MW)	-0.189*** (0.015)
Constant	-0.546*** (0.089)
Observations	18,618
Fitted Mean	0.029

The dependent variable equals one if the project withdraws during the waiting sample. Waiting for Study 3 indicates projects that have received a non-terminal second study and are waiting for the third study. Coefficient estimates are reported. Standard errors are in parentheses.

* $p < 0.10$, ** $p < 0.05$, *** $p < 0.01$.

E Additional Figures and Tables

Figure E.2: Costs by Location



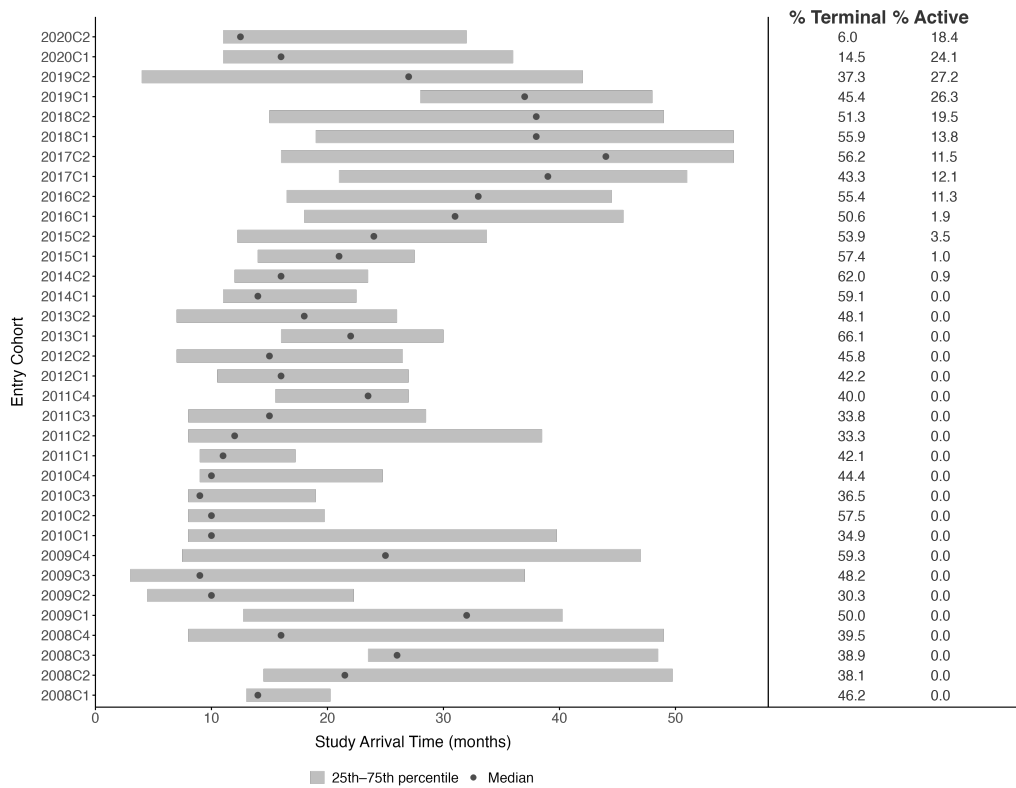
Second study interconnection cost estimates by location. Costs in millions of 2020 dollars per MW.

Table E.3: Top 15 Developers and Selective Completion

Developer	No. of projects	Cohorts with a project	Avg. proj. per cohort	Cohorts, excl. active	Frac. all or 0 completed
Invenergy	83	20	4.2	9	0.78
Community Energy Solar	68	19	3.6	12	0.58
Dominion	63	21	3.0	16	0.81
PSEG	56	18	3.1	18	0.50
LS	47	22	2.1	15	0.80
NextEra	38	12	3.2	6	1.00
Apex	30	14	2.1	6	0.67
EDF	30	12	2.5	7	0.86
SunEnergy1	30	10	3.0	6	0.50
EffiSolar	29	5	5.8	5	0.40
IMG	29	10	2.9	10	0.60
EDP	28	13	2.2	9	0.78
Exelon	27	12	2.3	12	0.92
Urban Grid	27	6	4.5	0	-
AEP	25	12	2.1	11	0.91

Summary statistics for the top 15 developers in our sample by number of projects. Cohorts with a project is the number of queue entry cohorts (out of 34) in which the developer has at least one project. Cohorts, excl. active is the same measure but excludes cohorts where, as of March 2026, at least one of the developer’s projects is still active, i.e., has neither begun operation nor withdrawn. Frac. all or 0 completed is the mean of a developer-cohort indicator for whether either all or none of the projects in that cohort were completed; this mean is taken across cohorts without active projects.

Figure E.3: Study Wait Time (months) by Date of Queue Entry



This figure shows the time to receive the terminal study, measured in months, by entry cohort. The horizontal bar represents the interquartile range (25th-75th percentiles), and the dot indicates the median. “% Terminal” is the share of projects that have received the terminal study among projects entering in a given cohort. “% Active” is the share of projects that are still active among projects in that cohort.

Table E.4: Summary Statistics by Transmission Owner

	Mean	Std. Dev.	25%	75%
<i>Panel A: TO-level totals and shares</i>				
No. of projects	190	191	33	292
Total capacity (GW)	18.5	22.7	3.6	21.1
Avg. capacity per project (MW)	101.9	54.9	60.4	139.1
No. of withdrawals	102	96	20	168
Total withdrawn capacity (GW)	10.20	10.63	2.12	14.56
No. of completions	33	34	4	55
Completed capacity (GW)	2.34	3.13	0.07	3.42
Share renewables	0.69	0.25	0.63	0.88
No. of unique developers	31	26	10	48
<i>Panel B: Within-TO averages</i>				
New projects per year	14.8	14.5	2.5	22.5
Waiting time (mos.)	26.8	4.7	23.9	29.4
Study 1 cost (\$M/MW)	0.14	0.15	0.07	0.16
Time to Study 1 (mos.)	5.3	0.8	4.6	5.4
Study 2 cost (\$M/MW)	0.20	0.17	0.10	0.20
Time to Study 2 (mos.)	14.7	4.4	12.4	15.7
Study 3 cost (\$M/MW)	0.11	0.09	0.05	0.15
Time to Study 3 (mos.)	16.9	4.1	13.6	18.8
Transmission owners	22			

Panel A reports the distribution across TOs of aggregate statistics computed within each TO. Unique developers counts distinct developers within each TO; we are unable to match 2,365 projects (56.7%) in the full project-level sample to a developer that controls the project. Panel B first averages within each TO across its projects, then reports the distribution of those TO-level averages. New projects per year is the total number of projects in a TO divided by the number of years spanned by its queue entries. Waiting time is months from queue entry to completion or withdrawal, excluding projects whose last known status is neither. Study costs (in millions of dollars per MW) and times (in months) are conditional on receiving the respective study. Renewables is solar, wind, and batteries.

Table E.5: New Study Arrival Probit Models With Additional Controls

	(1)	(2)	(3)	(4)	(5)	(6)
	Probit	Probit	Probit	Probit	Probit	Probit
ln(# Higher priority)	-0.028*** (0.004)	-0.017*** (0.005)	-0.019*** (0.008)	-0.015*** (0.005)	-0.018** (0.005)	-0.010 (0.011)
ln(# Higher priority) X Waiting for third study	-0.020*** (0.006)	-0.018** (0.007)	-0.018*** (0.006)	-0.018*** (0.007)	-0.014** (0.006)	-0.020*** (0.007)
ln(# Higher priority in TO)	-0.015*** (0.003)	-0.014*** (0.003)	-0.042*** (0.005)	-0.030*** (0.006)	-0.017*** (0.004)	-0.014*** (0.005)
ln(# Higher priority in TO) X Waiting for third study	-0.013*** (0.005)	-0.020*** (0.006)	-0.011** (0.005)	-0.018*** (0.006)	-0.013*** (0.005)	-0.018*** (0.006)
Waiting for third study	-0.218*** (0.017)	-0.247*** (0.020)	-0.234*** (0.018)	-0.254*** (0.020)	-0.246*** (0.018)	-0.259*** (0.019)
ln(# Withdrawals in TO)			-0.002 (0.001)	-0.003** (0.001)		
ln(# Projects in queue within TO)			0.033*** (0.005)	0.022*** (0.006)		
Wholesale electricity price (\$/MWh)		0.000 (0.000)		0.000 (0.000)		0.000 (0.000)
Ordinance		-0.009* (0.005)		-0.010* (0.005)		0.004 (0.006)
Prior Study Controls	X	X	X	X	X	X
Transmission Owner FE					X	X
Year FE					X	X
Observations	28,917	28,917	28,917	23,869	23,869	23,869
Pseudo R ²	0.177	0.181	0.197	0.167	0.168	0.182

The sample includes projects queued from 2008-2020, observed over time at the quarterly level as they wait in the queue for study arrival. Marginal effects from probit regressions are reported. Standard errors in parentheses, clustered by substation. The dependent variable is an indicator for study arrival (overall mean = 0.11; mean for second study is 0.16 and for third study is 0.06). All specifications control for project size (three bins), fuel type (wind, solar, storage), if the project is a capacity increase at an existing plant, time spent waiting in the queue (measured in quarters), and prior study characteristics, including the project's own cost estimate (three bins) from the prior study (e.g., the first study costs for projects awaiting the second study), indicators for whether the project receives engineering tests and whether it is part of a cost-sharing cluster. Specification (3) and (4) further control for the log size of withdrawn projects waiting for the same or a later study within the same transmission owner over the past two quarters, and the log number of projects in the queue within the same transmission owner. Specifications (2), (4), and (6) additionally control for wholesale electricity prices, defined as the quarterly average of the nearest locational marginal price during peak hours in 2020 (\$/MWh), and ordinance, an indicator for a local ordinance restricting renewable energy development. *** p<0.01, ** p<0.05, * p<0.10.

Table E.6: New Study Arrival Probit Models With Different Time Controls

	(1) None	(2) Linear	(3) Quadratic	(4) Year FE	(5) None
ln(# Higher priority)	-0.028*** (0.004)	-0.024*** (0.005)	-0.020*** (0.008)	-0.018** (0.007)	-0.031*** (0.011)
ln(# Higher priority) X Waiting for third study	-0.020*** (0.006)	-0.021*** (0.006)	-0.020*** (0.006)	-0.016*** (0.006)	0.016 (0.011)
ln(# Higher priority in TO)	-0.015*** (0.003)	-0.015*** (0.003)	-0.015*** (0.003)	-0.015*** (0.003)	-0.025*** (0.005)
ln(# Higher priority in TO) X Waiting for third study	-0.013*** (0.005)	-0.013*** (0.005)	-0.013*** (0.005)	-0.014*** (0.005)	-0.007 (0.008)
Observations	28,917	28,917	28,917	28,917	14,109
R ²	0.177	0.178	0.179	0.189	0.081

The sample includes projects queued from 2008–2020, observed over time at the quarterly level as they wait in the queue for study arrival. Marginal effects from probit regressions are reported. Standard errors are in parentheses and clustered by substation. The dependent variable is an indicator for study arrival (overall mean = 0.11; mean for second study is 0.16 and for third study is 0.06). All specifications control for project size (three bins), fuel type (wind, solar, storage), if the project is a capacity increase at an existing plant, time spent waiting in the queue (measured in quarters), and prior study characteristics, including the project’s own cost estimate (three bins) from the prior study (e.g., the first study costs for projects awaiting the second study), indicators for whether the project receives engineering tests and whether it is part of a cost-sharing cluster. Columns (1)-(4) report estimates with different time controls. Column (5) uses the same time controls as column (1) but restricts the sample to projects with a queue year prior to 2019. *** p<0.01, ** p<0.05, * p<0.10.

Table E.7: Effect of Active Higher-Queued Capacity on Probability of High Interconnection Cost

	10km (1)	20km (2)	Transmission owner (3)	K-means cluster (4)
Panel A: High Total Cost Estimate (mean = 0.37)				
Log Active Higher-Queued MW	-0.034* (0.019)	-0.025 (0.017)	-0.010 (0.010)	0.003 (0.012)
Geographic Region FE	X	X	X	X
Queue Year FE	X	X	X	X
Observations	2,328	2,328	2,328	2,328
R^2	0.518	0.518	0.231	0.230
Panel B: High Network Upgrade Cost Estimate (mean = 0.13)				
Log Active Higher-Queued MW	0.006 (0.015)	0.009 (0.012)	0.004 (0.006)	0.009 (0.007)
Geographic Region FE	X	X	X	X
Queue Year FE	X	X	X	X
Observations	2,328	2,328	2,328	2,328
R^2	0.477	0.477	0.178	0.204

Generators queuing from 2009–2020. Standard errors are in parentheses and clustered by substation. In Panel A, the dependent variable is an indicator for whether the total cost estimate in Study 2 or Study 3 is high, defined as exceeding \$0.1 million per MW. In Panel B, the dependent variable is an indicator for whether the network upgrade cost estimate in Study 2 or Study 3 is high, defined as exceeding \$0.1 million per MW. The regressor of interest is the log of total MW from the focal project and other active projects in the same or earlier interconnection cohort in the local geographic region in the quarter when the focal study is issued. An earlier cohort code indicates higher queue priority. A project is active if it is still waiting in the queue, meaning it has not completed or withdrawn, in the focal study’s issue quarter. Columns vary the geographic definition: 10 km, 20 km, transmission owner, and k-means cluster. All specifications control for project size (three bins), fuel type (wind, solar, storage), whether the project expands an existing plant; whether PJM Regional Transmission Expansion Plan investment was above the 75th percentile of the RTEP distribution within the same transmission owner, measured over a four-year window spanning three years before and one year after the study issue date. The geographic region fixed effects are substation fixed effects in the 10 km and 20 km columns, transmission owner fixed effects in the transmission owner column, and k-means cluster fixed effects in the k-means cluster column. *** $p < 0.01$, ** $p < 0.05$, * $p < 0.10$.

Table E.8: Robustness for Effect of a Costly Prior Interconnection on the Probability of High Total Cost

	Definition of nearby prior interconnection											
	10km		20km			Transmission Owner			K-means cluster			
	(1)	(2)	(3)	(4)	(5)	(6)	(7)	(8)	(9)	(10)	(11)	(12)
<i>A. Total cost > \$1m</i>												
Costly prior	0.104** (0.046)	0.066 (0.052)	0.056 (0.049)	0.117*** (0.034)	-0.004 (0.043)	-0.005 (0.043)	-0.028 (0.025)	-0.010 (0.023)	-0.012 (0.023)	-0.032 (0.025)	-0.036 (0.023)	-0.031 (0.024)
<i>B. Total cost > 90th percentile</i>												
Costly prior	0.124 (0.112)	0.091 (0.071)	0.061 (0.065)	0.076 (0.074)	-0.064 (0.052)	-0.072 (0.059)	-0.030 (0.043)	-0.038 (0.039)	-0.012 (0.039)	-0.065 (0.040)	-0.049 (0.037)	-0.038 (0.037)
<i>C. Cost/MW > \$0.1m</i>												
Costly prior	0.225*** (0.045)	0.010 (0.061)	0.018 (0.063)	0.238*** (0.041)	-0.015 (0.058)	-0.014 (0.061)	0.117*** (0.036)	-0.028 (0.035)	-0.016 (0.034)	0.051 (0.033)	0.043 (0.030)	0.045 (0.030)
<i>D. Cost/MW > 90th percentile</i>												
Costly prior	0.215*** (0.071)	-0.061 (0.106)	-0.027 (0.096)	0.228*** (0.051)	-0.026 (0.067)	-0.010 (0.066)	0.137*** (0.050)	-0.026 (0.050)	-0.035 (0.047)	0.088** (0.041)	0.069* (0.037)	0.071* (0.037)
Geographic Region FE		X	X		X	X		X	X		X	X
Queue Year FE			X			X			X			X

Generators queuing from 2009–2020. Standard errors are in parentheses and clustered by substation. The dependent variable is an indicator for whether the Study 2 or Study 3 cost estimate is high, defined as exceeding \$0.1 million per MW (mean = 0.37). The 90th percentile for the cost of prior interconnection is 9.17, 9.37, 7.54, and 7.64 million dollars for total cost and 0.27, 0.19, 0.16, and 0.15 million dollars for cost per MW, for the 10km, 20km, TO-level, and K-means cluster definitions, respectively. The mean of the key independent variable, costly prior interconnection, is 0.10, 0.02, 0.06, and 0.03 for the 10km specification across Panels A–D; 0.16, 0.04, 0.09, and 0.04 for the 20km specification; 0.29, 0.08, 0.15, and 0.07 for the Transmission Owner level specification; and 0.22, 0.07, 0.11, and 0.07 for the K-means cluster specification. Each estimate corresponds to a separate regression, with rows corresponding to different thresholds for costly prior interconnection and columns corresponding to different definitions of nearby. All specifications control for project size (three bins), fuel type (wind, solar, storage), whether the project expands an existing generator; whether PJM Regional Transmission Expansion Plan investment was above the 75th percentile of the RTEP distribution within the same transmission owner, measured over a four-year window spanning three years before and one year after the study issue date; the log of total entrant capacity (MW) within the previous three years in the local geographic region; and the log capacity of higher-queued projects in the local geographic region. The geographic region fixed effects are substation fixed effects in the 10 km and 20 km columns, transmission owner fixed effects in the transmission owner column, and k-means cluster fixed effects in the k-means cluster column. *** p<0.01, ** p<0.05, * p<0.10.

Table E.9: Predictors of Cost-Share Group Assignment

	<i>Dependent variable: Cost-share group assignment (mean = 0.68)</i>							
	Panel A: Higher-queued capacity				Panel B: Total active capacity			
	10km (1)	20km (2)	Trans. owner (3)	K-means (4)	10km (5)	20km (6)	Trans. owner (7)	K-means (8)
Log Active MW (local region)	0.011 (0.019)	0.010 (0.020)	0.039*** (0.012)	0.016 (0.013)	0.025 (0.018)	0.031* (0.017)	0.046*** (0.011)	0.032** (0.012)
Geographic Region FE	X	X	X	X	X	X	X	X
Queue Year FE	X	X	X	X	X	X	X	X
Observations	1,398	1,398	1,398	1,398	1,398	1,398	1,398	1,398
R^2	0.653	0.653	0.458	0.468	0.654	0.655	0.461	0.471

Projects queuing from 2009–2020 at the second study. The dependent variable is an indicator for whether the project is assigned to a cost-sharing group (sample mean = 0.68); estimates are from linear probability models. Standard errors are in parentheses and clustered by substation. Each column is a separate regression. Panel A (columns 1–4) measures local capacity as the log MW of active higher-queued projects; Panel B (columns 5–8) uses the log total active MW (all cohorts). Active projects are those still waiting in the queue in the study issue quarter. Within each panel, columns vary the geographic definition: 10 km, 20 km, transmission owner, and k-means cluster. All specifications control for project size (three bins), fuel type (wind, solar, storage), whether the project is a capacity expansion to an existing plant; and whether PJM Regional Transmission Expansion Plan investment was above the 75th percentile of the RTEP distribution within the same transmission owner, measured over a four-year window spanning three years before and one year after the study issue date. The geographic region fixed effects are substation fixed effects in the 10 km and 20 km columns, transmission owner fixed effects in the transmission owner column, and k-means cluster fixed effects in the k-means cluster column. *** p<0.01, ** p<0.05, * p<0.10.

Table E.10: Local Queue Scale and Cost-Share Group Assignment: Effect on High Interconnection Cost at Increasing Thresholds

	Total cost				Network upgrade cost			
	>0.10 (1)	>0.15 (2)	>0.20 (3)	>0.25 (4)	>0.10 (5)	>0.15 (6)	>0.20 (7)	>0.25 (8)
Log Active Higher-Priority MW (local)	0.022 (0.014)	0.014 (0.013)	-0.002 (0.011)	-0.006 (0.010)	0.013 (0.008)	0.006 (0.008)	0.004 (0.008)	0.004 (0.007)
In Cost-Share Group	-0.054* (0.032)	-0.110*** (0.028)	-0.090*** (0.024)	-0.072*** (0.021)	-0.055*** (0.015)	-0.034*** (0.011)	-0.029*** (0.011)	-0.026*** (0.009)
Transmission Owner FE	X	X	X	X	X	X	X	X
Queue Year FE	X	X	X	X	X	X	X	X
Mean of dep. var.	0.34	0.23	0.19	0.15	0.11	0.08	0.08	0.07
Observations	3,121	3,121	3,121	3,121	3,121	3,121	3,121	3,121
R^2	0.298	0.295	0.307	0.293	0.150	0.145	0.146	0.146

Cost-transition estimates. Projects queuing from 2009–2020, observed at Study 1 or Study 2 (transitions to the next study). The dependent variable is an indicator for whether the *next* study’s cost per MW exceeds the column threshold, in millions of dollars per MW. Columns 1–4 use total interconnection cost; columns 5–8 use network upgrade cost. Standard errors are in parentheses and clustered by substation. Log Active Higher-Queued MW (local) is the log of total MW of the focal project and other active projects in the same or earlier interconnection cohort within the focal project’s transmission owner. In Cost-Share Group is an indicator for whether the project is assigned to a cost-sharing group. All specifications control for the current study’s cost-category dummies (cutoffs at \$0.01, \$0.05, and \$0.20 per MW, in the same cost type as the outcome), fuel type (wind, solar, storage), whether the project is a capacity expansion at an existing plant, an engineering-test indicator, and a Study 2 indicator. *** p<0.01, ** p<0.05, * p<0.10.

Table E.11: Construction Cost Inputs by Fuel Type

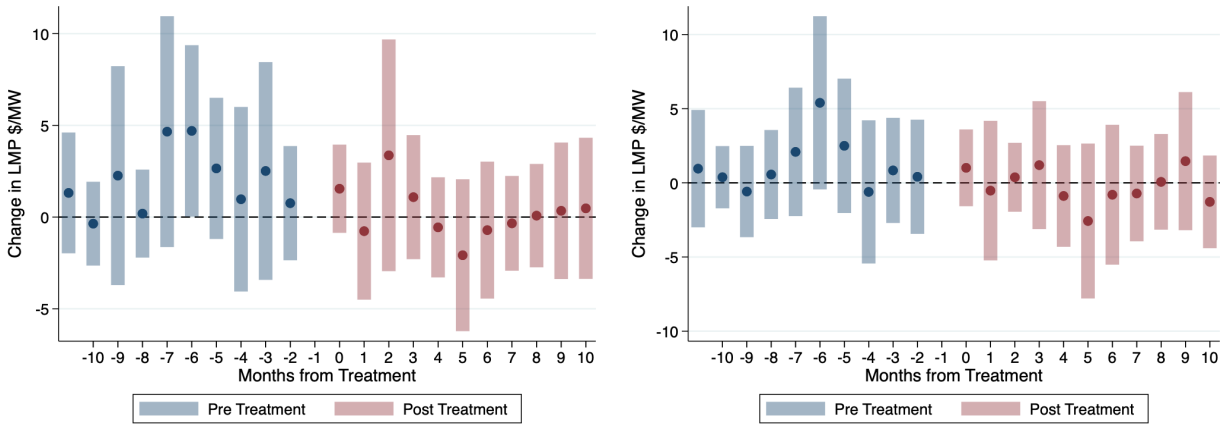
	2012	2013	2014	2015	2016	2017	2018	2019	2020
Gas (combined cycle)	1.017	0.917	0.917	0.917	0.978	0.978	0.978	0.958	0.958
Wind (onshore)	–	2.105	1.918	1.814	1.758	1.739	1.424	1.408	1.498
Solar PV	–	2.408	2.270	1.899	1.391	1.523	1.201	1.167	1.076
Storage (4-hour battery)	1.750	1.489	1.331	1.026	0.849	0.701	0.621	0.572	0.521

The costs are in \$ million/MW. Gas uses EIA natural-gas combined-cycle installation costs. Wind uses EIA onshore-wind construction costs. Solar uses EIA Form 860/923 utility-scale PV installed costs in \$/kWAC, converted to \$ million/MW and multiplied by 0.65 to reflect the investment tax credit. Storage uses BloombergNEF battery pack prices plus NREL ATB-based balance-of-system costs for a 4-hour utility-scale battery, multiplied by 0.55 to reflect the battery subsidy. “–” denotes no observation for that year.

Figure E.4: Effect of Interconnections with Network Upgrade Costs on Local Wholesale Prices

(a) Adding 20 MW New Capacity that Pays Network Upgrade Costs

(b) Adding 100 MW New Capacity that Pays Network Upgrade Costs



Panel (a) plots event-study estimates of the effect of a new generator with capacity of at least 20 MW beginning operation at a substation on local wholesale electricity prices, focusing on substations where the entering generator is responsible for transmission network upgrade costs as part of the interconnection process. Panel (b) uses a 100 MW threshold. Treated observations are substation-months in which a generator above the corresponding capacity threshold begins operation and is responsible for network upgrade costs; control observations are substation-months without such entry and include substation-months with entry of smaller or non-network-upgrade-paying generators. The dependent variable is the monthly average peak-hour locational marginal price at the substation level (mean = \$34.89/MWh), constructed from PJM locational marginal price data over 2008-2020. Estimates are obtained using the Callaway and Sant’Anna (2021) difference-in-differences estimator with doubly robust inverse probability weighting. Standard errors are clustered at the substation level.

F Additional Counterfactual Tables and Figures

Table F.12: By-Size Entry Surplus Changes from Study Speedups

	(1)	(2)	(3)	(4)
	As-is	10%	20%	50%
Renewable	245.6	+17.7	+34.3	+66.3
≤ 20 MW	163.5	+4.1	+7.3	+13.1
20–100 MW	240.4	+12.0	+22.4	+41.6
> 100 MW	259.8	+22.0	+43.0	+83.9
Non-renewable	216.0	+8.1	+14.2	+24.9
≤ 20 MW	291.2	+4.8	+7.8	+13.2
20–100 MW	348.7	+10.4	+18.2	+33.7
> 100 MW	205.5	+8.1	+14.2	+24.8

Columns (2)-(4) report per-MW entry surplus changes relative to as-is in column (1), in \$1,000 per MW. The surplus is defined as $E \max\{0, EV_i - C_i\}$ in \$Bn.

Table F.13: By-Size Entrant Count Changes from Study Speedups

	(1)	(2)	(3)	(4)
	As-is	10%	20%	50%
Renewable	2062	+6	+10	+18
≤ 20 MW	1037	+1	+1	+2
20–100 MW	607	+2	+4	+6
> 100 MW	417	+3	+5	+10
Non-renewable	646	+1	+2	+4
≤ 20 MW	320	+0	+0	+1
20–100 MW	135	+0	+0	+1
> 100 MW	191	+1	+1	+2

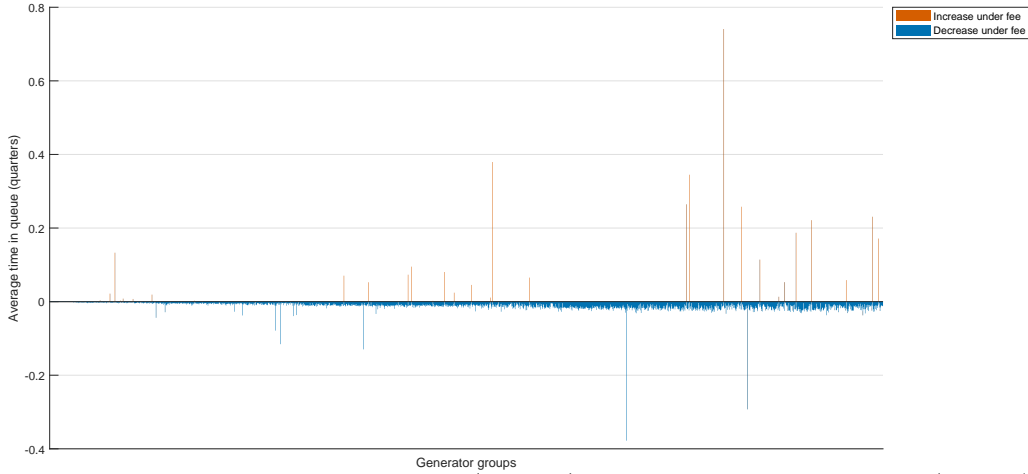
Columns (2)-(4) report the changes relative to column (1), the as-is equilibrium.

Table F.14: By-Size Entry Surplus Changes from Fee Policies: \$50,000/MW and \$500,000 Flat

	(1)	(2)	(3)	(4)	(5)	(6)
	As-is	Per-MW payment: \$50k/MW			Flat payment: \$500k	
		Nonrefundable fee	Deposit	Budget-neutral	Nonrefundable fee	Deposit
Renewable	245.6	-39.8	-32.6	-9.8	-4.1	-3.8
≤ 20 MW	163.5	-40.5	-33.9	-12.8	-27.5	-23.0
20–100 MW	240.4	-40.8	-33.0	-8.8	-5.6	-4.8
> 100 MW	259.8	-39.4	-32.2	-9.7	-0.0	-0.6
Non-renewable	216.0	-37.6	-30.2	-7.1	-0.8	-0.6
≤ 20 MW	291.2	-42.1	-30.8	+4.7	-34.1	-23.9
20–100 MW	348.7	-42.8	-31.8	+2.6	-6.8	-4.9
> 100 MW	205.5	-37.2	-30.1	-8.1	+0.7	+0.4

Columns (2)-(6) report per-MW entry surplus changes relative to as-is in column (1), in \$1,000 per MW. The surplus is defined as $E \max\{0, EV_i - C_i\}$ in \$Bn.

Figure F.5: Change in Time in Queue by Generator Group under a \$20,000/MW Entry Fee



The figure plots the change in time in queue (quarters) after imposing an entry fee of \$20,000/MW, relative to the as-is equilibrium. Each group is defined as a fuel type, TO, entry quarter, and size-bin combination. We group generators into eight size bins with cutoffs at 10, 20, 50, 100, 200, 500, and 1000 MW. There are 1,845 generator groups. For each group, we plot the change in time in queue.

Table F.15: By-Size Entrant Count Changes from Payment Policies

	(1)	(2)	(3)	(4)	(5)	(6)
	As-is	Per-MW payment: \$20k/MW			Flat payment: \$100k	
		Nonrefundable fee	Deposit	Budget-neutral	Nonrefundable fee	Deposit
Renewable	2062	-17	-15	-7	-20	-18
≤ 20 MW	1037	-11	-9	-5	-20	-17
20–100 MW	607	-4	-3	-1	+0	+0
> 100 MW	417	-3	-2	-1	+0	+0
Non-renewable	646	-4	-3	-1	-17	-16
≤ 20 MW	320	-2	-1	+0	-17	-16
20–100 MW	135	-1	+0	+0	+0	+0
> 100 MW	191	-2	-1	+0	+0	+0

Columns (2)-(6) report the changes relative to column (1), the as-is equilibrium.

Table F.16: By-Size Entrant Count Changes from Payment Policies: \$50,000/MW and \$500,000 Flat

	(1)	(2)	(3)	(4)	(5)	(6)
	As-is	Per-MW payment: \$50k/MW			Flat payment: \$500k	
		Nonrefundable fee	Deposit	Budget-neutral	Nonrefundable fee	Deposit
Renewable	2062	-93	-76	-46	-178	-136
≤20 MW	1037	-75	-61	-39	-177	-135
20–100 MW	607	-10	-8	-3	-1	-1
>100 MW	417	-9	-7	-4	+0	+0
Non-renewable	646	-11	-9	-3	-33	-27
≤20 MW	320	-4	-3	+0	-33	-27
20–100 MW	135	-1	-1	+0	+0	+0
>100 MW	191	-5	-4	-2	+0	+0

Columns (2)-(6) report the changes relative to column (1), the as-is equilibrium.

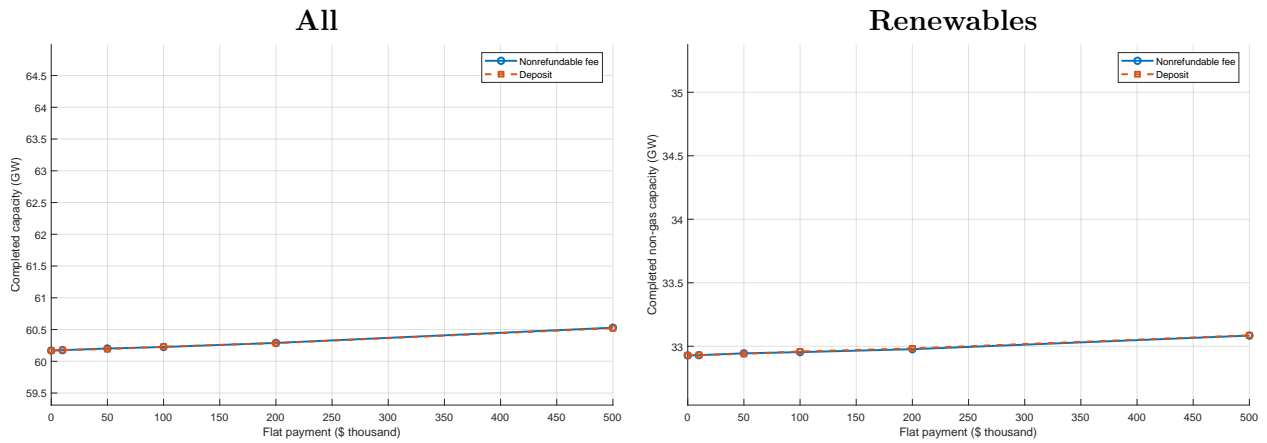


Figure F.6: Completed GW vs. Flat Fee Level

Each point is an equilibrium simulation. Two series: nonrefundable fee (solid) and deposit (dashed).

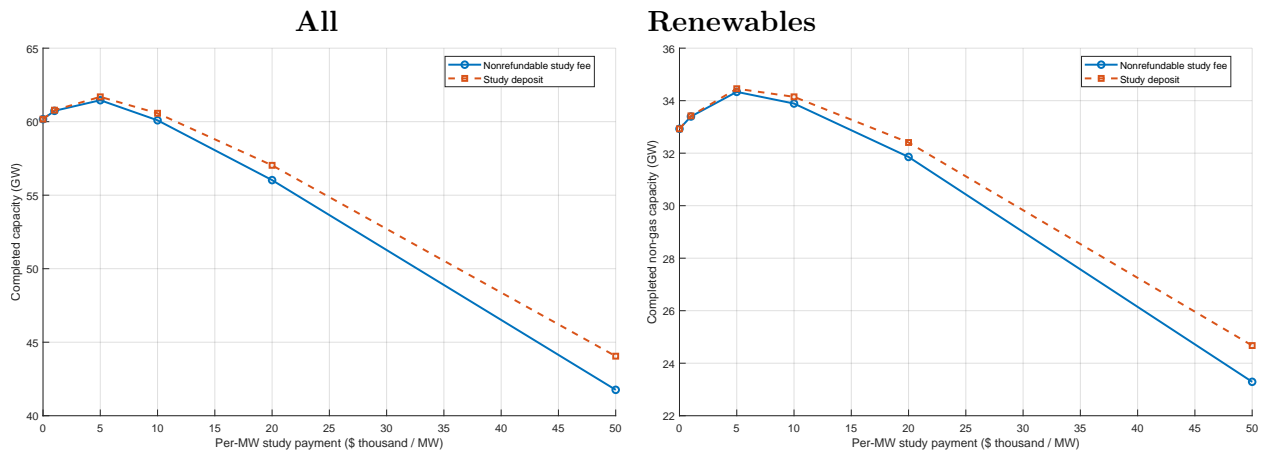


Figure F.7: Completed GW vs. Per-MW Study Fee Level

Each point is an equilibrium simulation. Two series: nonrefundable fee (solid) and deposits (dashed).